Mineral Res. Expl. Bull., 118, 1-7, 1996

UPPER CRETACEOUS/PALEOCENE TRANSITION RELATIONS IN THE GÜRÜN AUTOCHTHON, EAST TAURIDES-SW SİVAS (TURKEY)

Eşref ATABEY*

ABSTRACT.- The aim of this study is to determine the upper Cretaceous/Paleocene relation in the Akdere Basin (Gürün-SW Sivas) of eastern Taurids. The upper Cretaceous/Paleocene boundary in the studied is well observed. Microbreccia levels with intraformational conglomerate/breccia and biogenic limestone occurrences exist in places along the upper Cretaceous/Paleocene boundary. The rocks in the microbrecciated character show a texture of biolithclast packstone-grainstone and their depositional environment grades from slope to the basin. Most of the intraformational conglomerate/breccias on the upper Cretaceous/Paleocene boundary indicate possible movements of the sea floor controlled by tectonism during this time. On the uplifted blocks of the faults, syngenetic with the sedimentation, an environment which is vulnerable for some reef-building organisms, such as algae-corals and Bryozoa, was developed and biogenic limestones were deposited. Intraformational conglomerate/breccias were accumulated as resedimented rocks on the slopes and steeps of the fault fronts. As a result of these activities, sedimentary fissures (Neptunian dykes) were formed due to the crackings on the sea floor. This basin movement on the upper Cretaceous/Paleocene boundary gave also rise to the development of local uncorformities (hiatus).

INTRODUCTION

Based on the fossil data, a number of 15 extinction events has been determined through the geological times. Of these, the ones is upper Permian and upper Cretaceous were used to determine the boundaries between Paleozoic, Mesozoic, and Cenozoic systems. Although the biologic crisis on the Permo-Triassic boundary can be easily explained by the plate tectonics, the biologic crisis on the upper Cretaceous/Paleocene boundary with the sediment variations observed on the C/T boundary are attributed to different matters. Alvarez et al. (1980) and Officer and Drake (1983; 1985) explained the biologic crisis and the variations in sediments with a impact of meteorite and volcanism hypotheses, respectively.

Erosion caused by the submarine cold water currents, hiatus observed on the boundary in most places, widespread clay occurrences, increase in the carbonate dissolution, and the fluctuations in the sea level associated with tectonism are some of changes observed in the sediments on the Upper Cretaceous/Paleocene boundary. The reasons of the changes were studied by various workers. Moore et al. (1978), Keller and Barron (1983) and Keller et al. (1987) tested the presence of deep sea hiatus in Paleogene and described them as mechanical and chemical erosion surfaces on which no sedimentation takes place. According to these workers, condensation of oxygene-18, an increase or decrease in the number of planktonic foraminifer species, dissolution of carbonates, and a drop in the sea level are the main factors affecting the sedimentation. Accordi and Carbone (1992) and Lucic et al. (1993) determined the hiatus in Adriatic and attributed them to the planktonic foraminifers, nannoplanktones, and lithostratigraphy. The presence of clays was observed in various C/T boundaries by Officer and Drake (1985), in Spain, Denmark, and New Zealand by Schmitz (1988), and in Montana C/T boundary by Fastovsky et al. (1989). The biologic crisis on the C/T boundary and the change in the sediment character are attributed to a drop in the sea level by Ekdale and Bromley (1984), an increase in temperature by Emiliani (1980), and calcite dissolution due to surficial water by Officer and Drake (1983). Raup and Sepkoski (1984) stated that the biologic crisis is periodical and that it is repeated in every 26 million years. Hsu et al. (1982), however, point out that catastrophic environmental change in the beginning of Paleocene gave rise to the biologic crisis and affected the accumulation of sedi-

ments. Arthur et al. (1977) examined the upper Cretaceous/Paleocene sequence in Gabbio, Italy, in lithostratigraphic-sedimentologic-magnetostratigraphic and biostratigraphic ways. Butler et al. (1977) studied the *C/T* boundary of San Juan Basin, New Mexico, in a magnetostratigraphic way. Surlyk (1980) discussed the evolution of C/T boundary.

The main objective of this study is to determine whether microbreccia levels with intraformational conglomerate/breccia and biogenic limestone occurrences observed on the *C/T* boundary of the study area were formed as a result of one or more causes representing the changes in the sediment character that are stated above. It will be also explained that there is break in sedimentation and if there is any, this is whether due to a submarine erosion, carbonate dissolution, cooling of the sea water, or tectonics.

In some studies carried out in Turkey, upper Cretaceous/Paleocene relation is based on biostratigraphic and mineralogic data (Ünalan et al., 1976; Sirel et al., 1986; Yalçın and İnan, 1992).

Considering the objective of this study, columnar sections of lateral direction in close distances were measured in Akdere village, 30 km West of Gürün (Figure 1A), to the north Kahvepınarı place, north of Abdalpınarı village, and between Ziyaret Hill and Arpaçukuru village (Fig. 1B). Sedimentary petrography, electron (SEM), and paleontological studies were conducted on the samples collected. The possible events on the upper Cretaceous/Paleocene boundary are explained by combining the results obtained from these studies with the field observations.

THE LITHOFACIES DESCRIPTION OF THE UPPER CRETACEOUS/PALEOCENE BOUNDARY

The upper Cretaceous/Paleocene boundary in the study area is located south of the Akdere foreland-intermountain basin which was developed on the Gürün autochthon (Atabey, 1993b) (Fig. 1B). It is traced about 20 km in between the Kahvepınarı place and the Arpaçukuru village (Fig. 1B) Lithostratigraphic criteria descriptive for the *C/T* boundary in this place are brecciation, changes in the thickness of bed, lateral unconformities, and lateral facies changes. A number of four facies types was differentiated on the *C/T* boundary with the aid of field and laboratory data obtained from the columnar sections taken in close distances along the boundary. These are; conglomerate/breccia facies (Facies-1), reef-biogenic limestone facies (Facies-2), bio-intra-lithoclast packstone-grainstone facies (Facies-3), and pelagic mudstone-wackestone facies (Facies-4). These facies are not characterized with together but locally with only a few them.

Facies-1: Conglomerate/breccia facies

It is seen in dark gray, yellowish, and brown colors in the field. It is exposed in the Ziyaret hill 500 m north of Abdalpınarı. The facies with massive and thick bedded character has a thickness of 7 m in the Ziyaret hill. The unit, cropping out on the upper Cretaceous pelagics again. The steepness of a fault trending along the E-W direction on the Ziyaret hill forms a topographic mound (Fig. 2). Conglomerate/breccia facies sets above the pelagic mudstone-wackestone (Akdere. Fm.) of upper Cretaceous age (upper Campanian-Maestrichtian) at the basement. It is overlian by the reef-biogenic limestone.

This facies with a intraformational conglomerate/breccia character is composed of angular, subangular, and subrounded pebbles with a grain size of 5-30 cm. 85 % of the pebbles carbonates (Yanıktepe Fm.) comprising the basement. Grains are tightly bounded by a carbonate cement. This facies type is only seen at the Ziyaret hill along C/T boundary (Fig. 1B, section no 2).

Facies-2: Reef-biogenic limestone facies

Like the Facies-1, this facies type is also located at the Ziyaret hill. It is distinguished from the conglomerate facies with its light gray, whitish color (Figure 3). Its typical exposure is at the Ziyaret hill. It is completely massive and displays a thickness between 1 and 5 m. The unit, laterally cropping out along a distance of 0.5-1 km, is pinched out by the pelagic rocks. The facies is laterally transitional with the informational conglomerate/breccias at the basement and is covered by the pelagics above.

It shows a boundstone texture under microscope. Most of its constituents are red algae *(Lithot-*

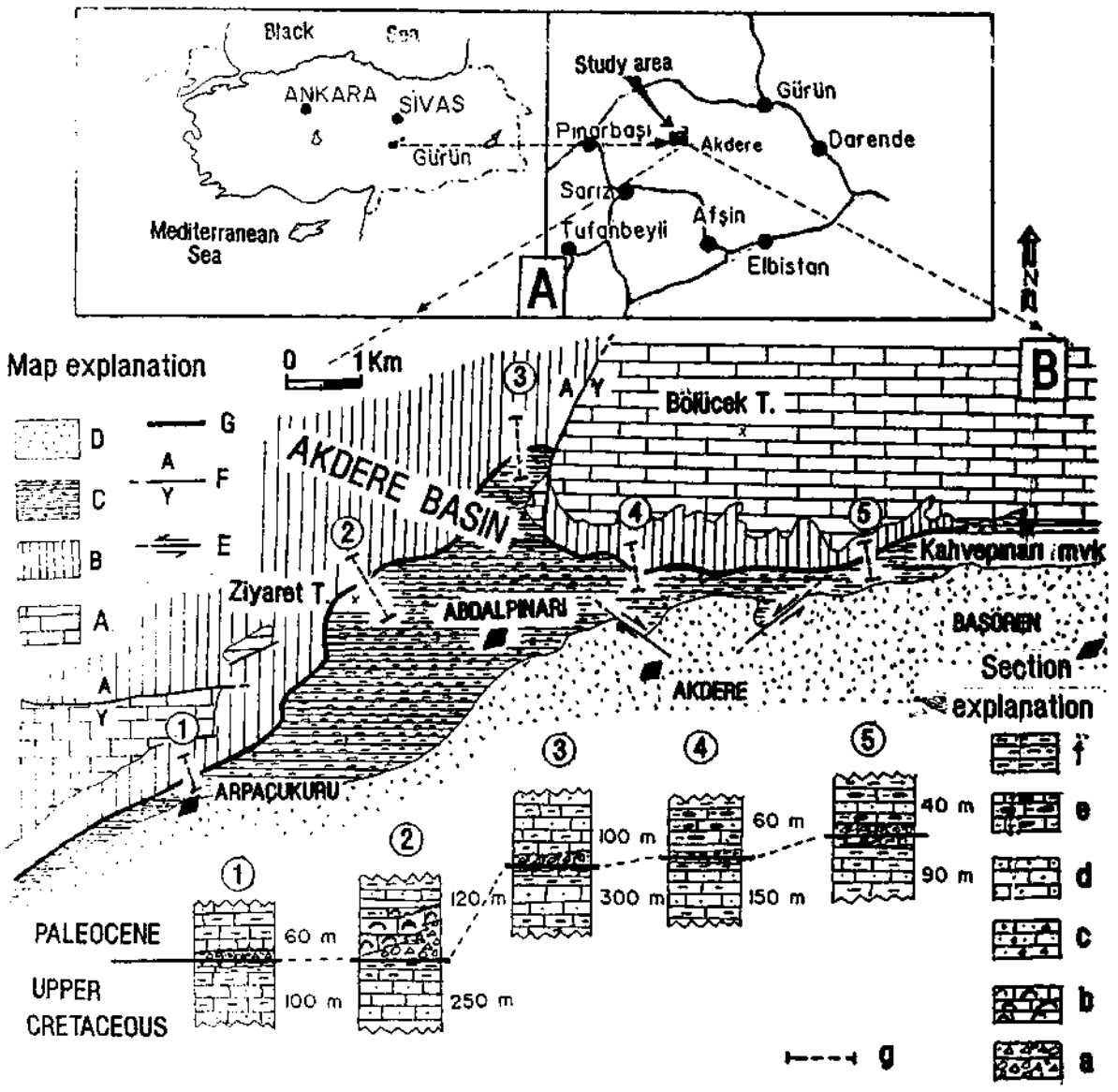

Figure 1. (A)-Location map, (B)-Geological map upper Cretaceous/Paleocene boundary: Map Explanations: A-Upper Santonian-Campanian (Yanıktepe Fm.), B-Upper Campanian-Maestrichtian (Akdere Fm.), C-Paleocene (Abdalpman Fm.), D-Lutetian unit, E-Strike slip fault, F-slip fault, G-C/T boundary, Section Explanations: a-Conglomerate/breccia, b-Algae limestone, c-Breccia/calcarenite, d-Calcarenite, e-Nodular chert bearing clayey limestone, f-Marl, g-Section locations.

hamnium sp., *Archeaolithothamnium* sp., *Mesophyllum* sp., *Coralline* sp., *Lithophyllum* sp.), *coral, Broyozoa* sp., Miliolidae, echinoid, and some benthic foraminiferas. Fragments of pelagic mudstone-wackestone (belonging to upper Cretaceous) and mud pellets with intraclasts are also contained in the rock. The pores of Broyozoa and the braches of the corals are filled with a calcite cement giving a roofstone texture (Embry and Klovan, 1971) to the rock.

Facies-3: Bio-intra-lithoclast packstone-grainstone facies

It is shown along the C/T boundary in the sections no 1, 3, and 5 (Fig. 1). The facies shows a microbrecciform character as an interlayer between the pelagic rocks (Fig. 4). The bed thickness is between 20-30 cm in section no 1, 10-20 cm in section no 3, and 20-30 cm in section no 5.In all these three locations, the facies laterally continues along a length of 200-300 m.

These microbreccias display a bio-intra-lithoclast packstone-grainstone texture under microscope (Dunham, 1962). Some lithoclasts belong to the shallow water carbonates (Yanıktepe Fm.: upper Santonian-Campanian) and some belong to the pelagic mudstone-wackestones (Akdere Fm.: upper Campanian-Maestrichtian). Intraclasts, however, belong to rock units of Paleocene age (Abdalpınarı Fm.) (Atabey, 1993a). Fissure-fracture and scour structures are developed in the rock. The boundaries of fissure and fractures have the traces of in-situ breaking (Fig. 5 and 6). Fissure and fractures are filled with shallow marine benthcis, algae, miliolids, echinoids, and lime mud (Fig. 5, 6 and 8). The structures formed by these type fractures and filling of them with the sediments is known as Neptunian dykes which indicate a submarine erosion (Pavlow, 1896, Bates and Jackson, 1980). Syntaxial cement developed in the echinoids within the fractures indicates a pheratic marine conditions. It also points out that the character of the environment was changed from deep to shallow marine condition (Fig. 7). The presence of dissolution pores or scours in calcites was also observed in the electron microscope photographs (Fig. 9). This dissolution process is accomplished by cold water currents. Mud lithoclasts forming the rock comprise foraminifera and nannoplanktons of upper Campanian-Maestrichtian age while syngenetic intraclasts comprise foraminiferas of Paleocene age and abundant amounts of nannoplanktons (Atabey, 1995). The names of the fossils are given in Facies-4.

Facies-4: Pelagic mudstone-wackestone facies

This facies takes place as an interlevel below both conglomerate/breccia facies and microbreccias and also above the microbreccias. The ones below the Facies-1 and Facies-3 are the pelagic levels belonging to upper Cretaceous while the ones above these facies are the pelagic levels belonging to Paleocene. These rocks presents in both levels completely show a pelagic mudstone-wackestone texture. These thin bedded pelagics can be laterally traced. Most of the constituents of lime muds belonging to both upper Cretaceous and Paleocene are composed of foraminifers and nannoplanktons. The foraminiferas of upper Campanian-Maestrichtian are: *Globotruncana linneiana, Globotruncana cf. area, Globotruncana subspinosa, Globotruncana falsostuarti, Globotruncana stuarti, Globotruncana conica.* The nannoplanktons are: *Predicosphaera cretacea, Eiffellithus turriserffelli, Quadrum trifidum, Calcuqutes obscurus, Arkhangelskella cymbiormis, Microrhabdulus decoratus.* The foraminifers of Paleocene are: *Morozovella cf. pseudobulloides, Planorotalites cf. compressa, Globoratalia cf. velascoensis, Globoratalia stuarti, Opertorbitolites sp. The nannoplanktons are: Discoaster multiradiatus, Ericsonia cava, Ericsonia ovalis, Cocolithus eopelaqcus, Ellipsolithus macellus, Sphenolithus primus.*

DISCUSSION

The upper Cretaceous/Paleocene boundary in the study area is partly differentiated with the pelagic limestones of brecciform character. In addition, the local reef developments and biogenic, clastic limestone levels are the other facies assemblages of this boundary. The lateral and vertical relations on the C/T boundary, which reflects a shallow marine depositional environment, are the product of syngenetic faulting previaled in the basin at that time. Another feature supporting for the movement of the sea floor is the development of sedimentary fractures (Neptunian dykes). The filling of these fractures, wholly observed in the pelagic levels, with the shallow marine bioclastics is an indicative of the current movements effective on the sea floor. Syngenetic faultings were dominant during the C/T stage and, hence, some rising sites were locally developed. The typical example of this at the Ziyaret hill. Intraformational conglomerate/breccias (Facies-1). Were accumulated as resedimented rocks on the slopes and steeps of the faults syngenetic with the sedimentation. A shallow marine environment was prevailed on the uplifted blocks of the faults and conditions vulnerable for the deposition of

algae-coral-bryozoa bearing reef limestones were developed at these sites (Facies-2). Along all the C/T boundary, in places, where the syngenetic faultings were not effective or the strike was not large, deep marine conditions were prevailed. Consequently, while local shallow environments were developing along the boundary (as in the case of Ziyaret hill), basin-slope environment conditions were also dominated in places (section locations no 1, 3, 4, and 5). Continuous faulting of the basin slope affected the sediment character. The movement on the sea floor gave rise to fracturings in the basement sediments and these fractures were filled with the pelagic muds, pelagic foraminifers, and some organisms dragged from the platform margin with submarine current. Neptunian dykes were formed in this way and the rock had a microbrecciform character (Facies-3). Lehner (1991) stated that Neptunian dykes could be formed as a result of the movement of syngenetic faults developing along the platform margin-basin slope. In the electron microscopy studies conducted on the microbreccias, dissolutions on the fossil shells, sweeping out of carbonates by the current motion, and some breaks in the sedimentation were observed. The dissolution of carbonates on the C/T boundary negatively affected the carbonate accumulation and, therefore, local hiatus were developed. Syntaxial cement development detected in the echinoids indicates that the deepening in the environment was not continuous. This type of cement also indicates that in some cases, the environment was getting shallower and was subjected to the fresh water occupation.

The breaks in the sedimentation together with the sea floor movements on the C/T boundary and sea floor erosions are the indicative of the presence of submarine unconformaties (hiatus).

It is concluded that at that time, there were rises and drops in the sea level on the C/T boundary, dissolution of carbonates depending on the depth thus affecting the accumulation of sediments, development of shallow marine facies depending on the sea level rising, development on neptunian dykes due on the sediments of the sea floor caused by syngenetic faults, and this activity also gave rise to some local unconformities (hiatus).

ACKNOWLEDGEMENTS

I would like to express my gratitude to Prof. Dr. Baki Varol, University of Ankara, for his critiques and reviewing the manuscript. Thanks go to Nevbahar Atabey, Erdoğan İnal, Ayşe Ayaroğlu, Afet Kallioğlu, Aynur Hakyemez, and Emir N. Erkan of General Directorate of Mineral Research and Exploration of Turkey (MTA) for making determination of fossil species.

Manuscript Received January 27, 1995

REFERENCES

Accordi, G. ve Carbone, F., 1992, Lithofacies map of the Hellenide Pre-Apulian zone (Ionian Islands, Greece), Centra dı studio Per la Geol. Dell. Italia centrale: Spec. Publ. 27 s.

Alvarez, L.W., Alvarez, W., Asaro, F. ve Michel, H.V., 1980, Extraterrestrial cause for the Cretaceous-Tertiary extinction: Science, 208, 1095-110.

Alvarez, W., Kaufmann, E.G, Surlyk, F., Alvarez, L.W., Asaro, F. ve Michel, H.V., 1984, Impact theory of mass extinctions and the invertebrate fossil record: Science, 223, 1135-1141.

Arthur, M.A., Fischer, A.G., Silva, I.P., Lowrie, W., Alvarez, W., Roggenthen, W. M.ve Napoleone, G., 1977, Upper Cretaceous-Paleocene magnetic stratigraphy Gubbio, Italy: Geol. Soc. of Amer. Bull., 88, 367-389.

Atabey, E., 1993a, Gürün Otoktonunun stratigrafisi (Gürün-Sarız arası), Doğu Toroslar-GB Sivas, Türkiye Jeol. Bült., 36/2, 99-113.

———, 1993b, Akdere Basin: An example for the foreland intermontane basin, eastern Tauride Carbonate Platform, Gürün, SW Sivas-Turkey, Geological Romana, 29, 401-409.

....., 1995, Gürün Otoktonu'nun sedimentolojisi ve jeolojik evrimi, Ankara Univ. Fen Bil. Enst. Doktora Tezi, 224s.

Barron, J.A. ve Keller, G., 1982, Widespread Miocene deep-sea hiatuses: coincidence with periods of global cooling: Geology, 10, 577-581.

Bates, R.L. ve Jackson, J.A., 1980, Glossary of Geology, Am. Geol. Inst, Falls Church, Va., 749 ss.

Butler, R.F., Lindsay, E.H., Jacobs, L.L. ve Johnson, N.M., 1977, Magnetostratigraphy of the Cretaceous-Tertiary boundary in the San Juan Basin, New Mexico: Nature, 267, 319-321.

Dunham, R.L., 1962, Classification of carbonate rock according to depositional texture. In: Classification of carbonate rocks (Ed. W. G. Ham): Mem. Am. Assoc. Petrol. Geol. 1, 108-121.

Ekdale, A.A. ve Bromley, R.G., 1984, Sedimentology and Ichnology of the Cretaceous Tertiary boundary in Denmark: Implications for the causes of the Terminal Cretaceous extinction: Jour. Sed. Petrology, 54, 681-703.

Emiliani, C., 1980, Death and Renovation at the end of the Mesozoic: 61, 505-507.

Embry, A.F. ve Klovan, J.E., 1971, A late Devonian reef tract on northeastern banks Island, N.W.T.: Bull. Can. Soc. Petrol. Geol., 19, 730-781.

Fastovsky, D. McSweeney, K. ve Norton, L.D., 1989, Pedogenic development at the Cretaceous-Tertiary boundary, Garfield county, Montana. Jour.Sed. Petrology, 50, 758-767.

Hsü.K.J., He, Q., Mc Kenzie, J.A., Weissert, H., Perch-Nielsen, K., Oberhansli, H., Kelts, K., La Brecque, J., Tauxe, L., Krahenbuhl, U., Percival, S.F., Jr., Wright, R., Karpoff, A. M., Petersen, N., Tucker, P., Poore, R.Z., Gombos, A.m., Pisciotto, K., Carman, M.F., Jr, ve Schreiber, E., 1982, Mass mortality and its environmental and evolutionary consequences: Science, 216, 249-256.

Keller, G. ve Barron, J.A., 1983, Paleoceanograbhic implications of Miocene deep-sea hiatuses: Geol. Soc. of Amer. Bull., 94, 590-613.

———, Herbert, T., Dorsey, R., D'Hondst, S., Johnsson, M. ve Chi, W.R., 1987, Global distribution of late Paleogene hiatuses: Geology, 15, 199-203.

Lehner, B.L., 1991, Neptunian dykes along a drowned carbonate platform margin: an indication for recurrent extensional tectonic activity?, Terra Nova, 3, 593-602

Lucic, D, Benic, J., Stankovic, D. ve Miletic, D., 1993, Cretaceous/Tertiary boundary from the Koraljka-1 off-shore well (SW of Zadar, Adriatic Sea): Geol. Croat., 46, 41-61.

Moore, T.C., Jr., van Andel, Tj. H., Sancetta, C. ve Prias, N., 1978, Cenozoic hiatuses in marine sediments. Micropaleontology, 24, 113-138.

Officer, C.B. ve Drake, C.L., 1983, The Cretaceous-Tertiary transition: Science, 219, 1383-1390.

....., ..., 1985, Terminal Cretaceous environmental events: Science, 227, 1161-1166.

Pavlow., A.W., 1896, On dikes of Oligocene sandstone in Neocomian clays of the district of Alatyr in Russia. Geol. Magazine, 4,3, 49-53.

Raup, D.M., ve Sepkoski, J.J., 1984, Periodicity of extinctions in the geologic past: Proc. Natl. Acad. Sci. USA., 81, 801-805.

Schmitz, B., 1988, Origin of microlayering in worldwide distributed Ir-rich marine Cretaceous/Tertiary boundary clays: Geology, 116, 1068-1072.

Sirel, E., Dager, Z. ve Sözeri, B., 1986, Some biostratigraphic and paleogeographic observations on the Cretaceous/Tertiary boundary in the Haymana-Polatlı region (central Turkey): Lecture notes in global Bio-events, Ed. By O. Walliser, Springer- Verlag, Berlin, Heidelberg.

Smith, J. ve Hertogen, J., 1980, An extraterrestrial event at the Cretaceous-Tertiary boundary: Nature, 285, 199.

Surlyk, F., 1980, The Cretaceous-Tertiary boundary event: Nature, 285, 187-189.

Ünalan, G., Yüksel, V., Tekeli, T., Gönenç, D., Seyirt, Z. ve Hüseyin, S., 1976, Haymana-Polatlı yöresi Üst Kretase-Alt Kretase sedimentlerinin stratigrafisi ve paleocoğrafik evrimi: Türkiye Jeol. Kur. Bull, 19, 159-176.

Yalçın, H. ve İnan, N., 1992, Tecer Formasyonunda (Sivas) Kretase-Tersiyer geçişine paleontolojik, mineralojik ve jeokimyasal yaklaşımlar, Türkiye Jeol. Bült., 35, 95-102.

PLATE

PLATE -I

Fig. 2. Conglomerate/breccia level (Facies-1) at the basement of Paleocene, 1 km north of the Abdalpınarı village, Ziyaret hill.

Fig. 3. Biogenic limestone facies (Facies-2). Algae-Coralla-Broyozoa bearing reef limestone occurrences. 1 km north of the Abdalpınarı village, Ziyaret hill.

Fig. 4. Microbreccia levels observed on the upper Cretaceos/Paleocene boundary, 1 km north of the Akdere village, site of Section no 5.

Fig. 5. Fissures developed in the pelagic mudstones indicate the fracturing of the sea floor. These are filled with the carbonate grains derived from them. A calcite cement develops in other spaces (white areas). Pelecypod (P), Red algae (A), Mud clast (K), x63.

Fig.6. Sedimentary fractures developed within the pelagic mudstone-wackestone. Red algae filling the fractures (A), Lime mud clasts (K), and lime mud (Kg), x63.

Fig. 7. Syntaxial cement detected in echinoids (S), echinoid (E) characterize the pheratic marine environment. The sample examined belongs to the microbreccia levels (Facies-3), x63.

Fig. 8. Biogenic scours developed in the pelagic mudstones. Scour pores are filled with the lithoclast (L), milliolid (M), and algae (A). White part stand for calcite cemented areas, x63.

Fig. 9. SEM image of dissolution pores (B) observed in the biogenic grains within the lime mud (x2000).

Fig.2

Fig.3

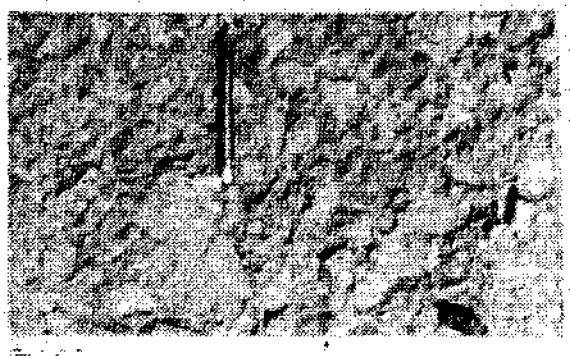

Fig.4

Fig.5

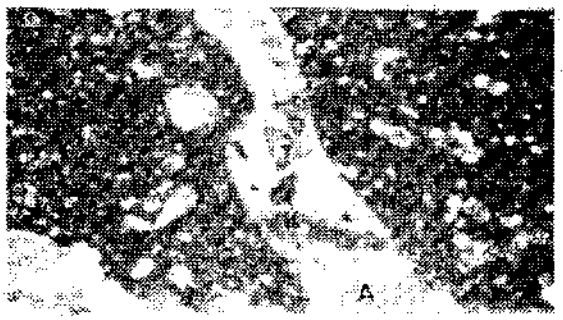

Fig.6

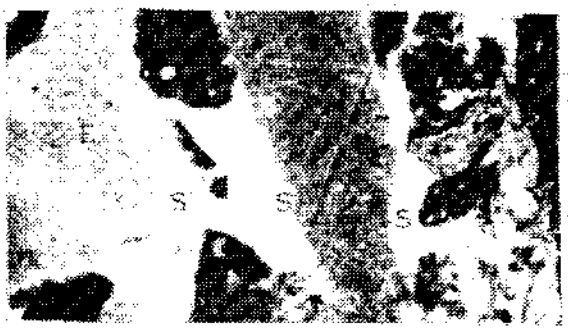

Fig.7

Fig.8

Fig.9

MICROPALEONTOLOGICAL INVESTIGATION AND ENVIRONMENTAL INTERPRETATION (OSTRACODA) OF THE PLIOCENE SEQUENCE OF BURDUR BASIN

Cemal TUNOĞLU* and Emel BAYHAN*

ABSTRACT.- In this study, micropaleontological studies based on ostracods are carried out on units belonging to Pliocene aged sedimentary units in Burdur basin in SW Anatolia and environmental assesments are made through other macro and micro level data (lithostratigraphic and mineralogic). As a result of investigations ten different ostracoda species are determined in 4 different ostracoda genus belonging to fresh water environment and these fauna are found in 8 samples from 5 measured stratigraphic sections. Existing of Heterocypris, Candona, Ilyocypris and Limnocythere species and their known living environments conform with the volcanic, sedimentologic, tectonic and hydrothermal processes in that period and support each other. Clay mineralogy, geochemistry and ostracoda fauna of this environment reflect all characteristics of lake facies which are fed from the continent. It has been demonstrated that, the present Burdur lake gained its actuel setting through a regressive sedimentation towards NW, and the ostracoda findings show a regular increase on the fresh water characteristics.

Mineral Res. Expl. Bull., 118, 9-14, 1996

INNER PLATFORM SEDIMENTS WITH Praebullalveolina afyonica SIREL and ACAR AROUND ELAZIĞ REGION (E. Turkey)

Niyazi AVŞAR*

ABSTRACT.- The presence of the Alveolinidae, Peneroplidae and Miliolidae families, which represent the inner platform sediments of Eocene has been rarely reported in the Mediterranean countries and Turkey up to now. The following fossil assemblage *Praebullalveolina afyonica* Sirel & Acar, *Praerhapydionina huberi* Henson,Peneroplis *damesini* Henson, *Peneroplis* aff. *laevigatus* d'Orbingy, *Spirolina* aff. *cylindracea* Lamarck, *Nummulites striatus* (Bruguiere), *Gyroidinella magna* (Le Calvez), *Asterigerina rotula* (Kaufmann), *Halkyardia minima* (Liebus) and Miliolidae have described from the Upper Eocene inner platform sediments around Alatarla, NW Elazığ, E. Turkey. Systematic description and picture of the Anatolian form and the unique alveolinid, *Praebullalveolina afyonica.* Sirel & Acar, of Upper Eocene sediments and also, some pictures of the species, which are only characterized by the Middle-Upper Eocene sequence, have been given.

INTRODUCTION

The porcelaneous foraminifers such as Alveolinidae, Peneroplidae and Miliolidae families which represent inner platform Eocene deposits, have all been recorded in the Mediterranean countries. The same forms of porcelaneous foraminifers of Upper Eocene limestones in the petroleum wells in Iran and Iraq (Henson, 1950); Middle Eocene limestones with *Borelis vonderschimitti* of Vicenza (N. Italy) (Schweighauser, 1951); Middle Eocene limestone with Peneroplidae of Pyrenees (N. Spain) (Caus, 1974); Middle Eocene limestone with *Rhapydionina malatyaensis* Sirel, Miliolidae and Peneroplidae of Malatya (E. Turkey) (Sirel, 1976); Upper Eocene limestones with *Praebullalveolina afyonica* Sirel & Acar, 1982); Middle Eocene limestone containing *Malatyna drobnae* Sirel & Acar, Miliolidae and Peneroplidae in Malatya (E. Turkey) (Sirel & Acar, 1993) have only documented by the authors in the areas mentioned above. In addition, Henson (1950) reported the presence of the Peneroplidae and Miliolidae forms of Upper Eocene from the core samples taken from the petroleum wells in Iran and Iraq. The sequence containing *Praebullalveolina afyonica* Sirel & Acar, Peneroplidae and Milliolidae, which constutite the subject of the study, are observed around Alatarla village, NW Elazığ (Fig. 1).

The aim of the study is to represent the presence. of the new sequence of Upper Eocene inner shelf carbonates with Alveolinidae, Peneoplidae and Miliolidae forms and particularly the unique form of Anatolian *Praebullalveolina afyonica* Sirel & Acar, which is rarely seen in the Mediteranean countries and Turkey, found second time around Elazıg region.

Due to the hardness of the rock samples, it is not possible to obtain free individuals. For this reason, the present study is only based on selected random and oriented thin sections. All the thin sections are kept in numbers A1 -20 and A1 -21.

STRATIGRAPHY

The following lithostratigraphic units of the Paleozoic, Mesozoic, Eocene and Miocene ages crop out around the investigated area. In this study, lithostratigraphic and biostratigraphic features of Eocene sequence (Fig. 2), around Alatarla village, have been given in detail.

Paleozoic

Paleozoic rock units are represented by metamorphic rock such as crystallized limestones, calcschits, schist, marble and amphibolites around Elazığ region. However, this sequence is characterized by white jointly and fractured marbles in the study area. The unit is accepted to be allochthonous because of the active tectonic events occurred during late Cretaceous. Contact relationship of the

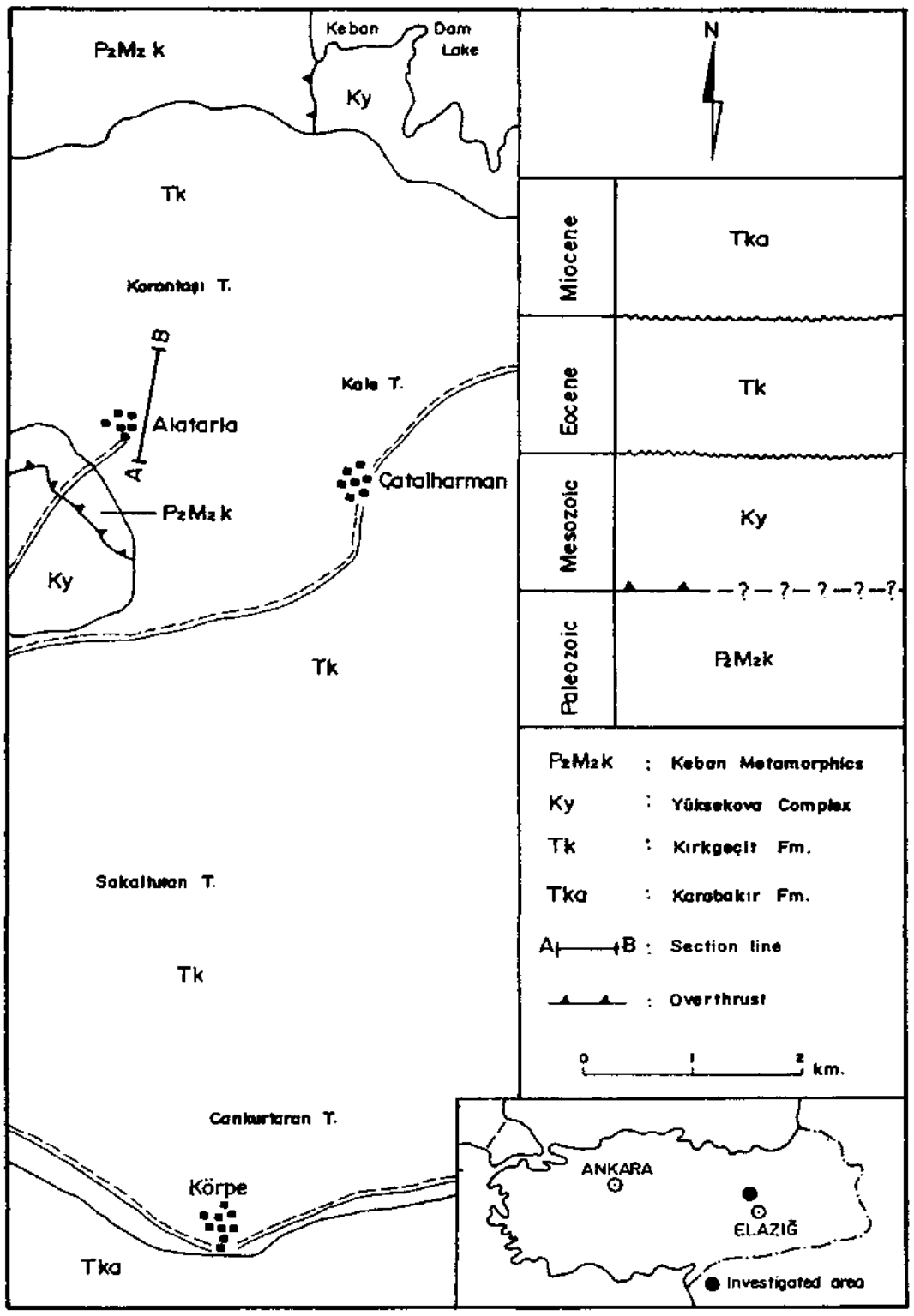

Fig. 1- Geological map of investigated area.

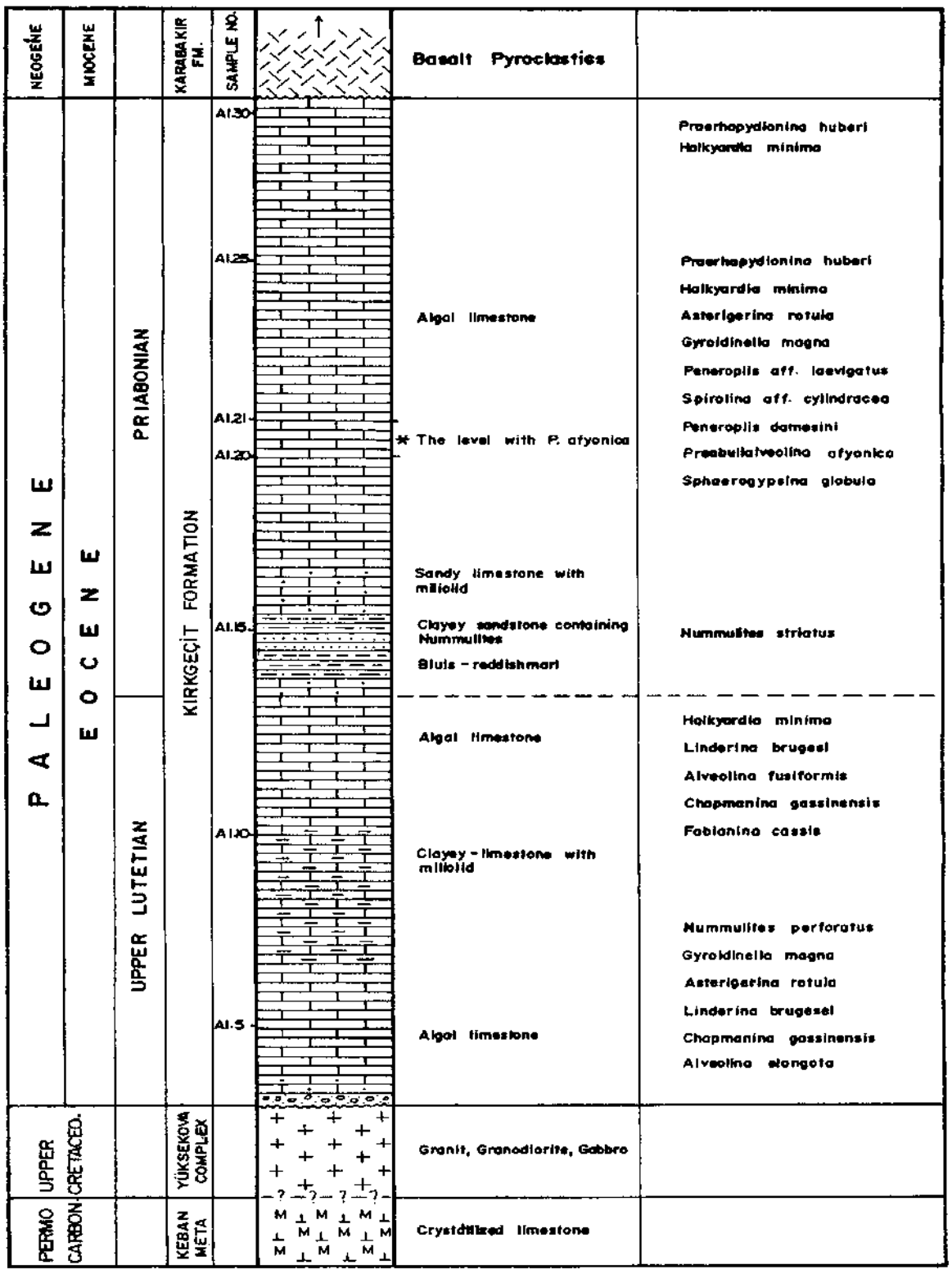

Fig. 2- Columnar section of Eocene sequence around Alatarla village, NW Elazığ.

Paleozoic rocks with Mesozic units are various, however, it is observed that the contact relationship is only tectonic in the study area.

Mesozoic

The unit is mainly represented by gabbro, diorite, granodiorite, granite, diabase, basalt, andesite, pyroclastic rocks and mudstones around the region. However, the main lithology of the investigated area are represented by granite, granodiorite, basalt, andesite and pyroclastics. This magmatic bulk is unconformably covered by younger sedimentary deposits and valcano-clastic rocks.

Eocene

This sequence starts with polygenic heterogeneous, variously colored and medium to thick bedded basal conglomerates, and shows lateral and vertical facies changes. The pebbles of the conglomerates are mainly derived from Paleozoic and Mesozoic aged rock units. This passes upward into clayey-sandy limestones, sandstone, clay and limestones that are all in beige color, fossiliferous and regularly bedded. In the Elazığ region, the following foraminifers were identified, characterizing upper part of the Middle Eocene and Upper Eocene, the result of the paleontologic investigations carried out on Eocene sequence. These are *Nummulites perforates* (Mondfort), *Assilina exponens* (Sowerby), *Alveolina fusiformis* Sowerby, *Alveolina elongata* d'Orbingy, *Sphaerogypsina globula* (Reuss), *Silvestriella tetraedra* (Gümbel), *Maslinella* aff. chapmani Galesner & Wade, *Asterigerina rotula* (Kaufmann), *Chapmanina gassinensis* (Silvestri), *Linderina brugesi* Schlumberger, *Fabiania cassis* (Oppenheim), *Halkyardia minima* (Liebus), *Gyroidinella magna* (Le Calvez), *Nummulites fabianii* (Prever), *Nummulites* ex gr. fabianii, *Nummulites striatus* (Bruguiere), *Praerhapydionina huberi Henson, Peneroplis damesini* Henson, *Praebullalveolina afyonica* Sirel & Acar, *Spirolina* aff. *cylindracea* Lamarck, *Peneroplis* aff. *laevigatus* d'Orbingy, *Peneroplis dusenburyi* Henson, *Heterostegina* sp., *Asterocyclina* sp., *Operculina* sp., *Orbitolites sp., Discocyclina* sp., *Peneroplis sp.,* Miiolidae and Algae.

Similar sequence, that is seen around Alatarla village (NW Elazığ), is composed of clayey limestones which consist of algae and miliolid at the base of the unit. Also the following fosil assemblages were described from this unit; *Nummulites perforates* (Montfort), *Alveolina elongata* d'Orbingy, *Alveolina fusiformis* Sowerby, *Fabiania cassis* (Oppenheim), *Halkyardia minima* (Liebus), *Gyroidinella magna* (Le Calvez), *Asterigerina rotula* (Kaufmann), *Linderina brugesi* Schlumberger and *Chapmanina gassinensis* (Silvestri). According to these fossils, Upper Lutetian age was given to unit. Some workers such as Bieda (1963), Bombita & Moisescu (1968), Blondeau (1972), Rahaghi & Schaub (1976) and Schaub (1981) also express the age of the *Nummulites perforates* (Montfort) as Upper Lutetian. Moreover, the age of *Alveolina elongata* d'Orbingy and *Alveolina fusiformis* Sowerby are reported to be Upper Lutetian. Moreover, the age of Alveolina elongata d'Orbigny and Alveolina fusiformis Sowerby are reported to be Upper Lutetian by Hottinger (1960), Adams (1962) and Dizer (1965). The uppert part of the section includes nummulitic clayey limestone, sandy limestones containing miliolid and algal limestones that comprise *Nummulites striatus* (Bruguiere) *Asterigerina rotula* (Kaufmann), *Sphaerogypsina globula* (Reuss), *Gyroidinella magna* (Le Calvez), *Halkyardia minima* (Liebus), *Praerhapydionina huberi* (Henson), *Peneroplis* aff. *laevigatus* d'Orbigny, *Peneroplis damesini Henson, Spirolina* aff. *cylindracea* Lamarck, *Praebullalveolina afyonica* Sirel & Acar. In accordance with these foraminifer, this part of the sequence is Upper Eocene in age. *Nummulites striatus* (Bruguiere) is characteric form of the Upper Eocene age according to Nemkov (1967), Ferrer (1971), Blondeau (1972) and Schaub (1981). However, in the type locality of *Praebullalveolina afyonica* Sirel & Acar, Sirel and Acar (1982) record the age of the section as Upper Eocene according to the fossil assemblages; *Nummulites fabianii* (Prever), *Nummulites fabianii retiates* (Roveda), *Gyroidinella magna* (Le Calvez), *Halkyardia minima* (Liebus), *Chapmanina gassinensis* (Silvestri), *Peneroplis* aff. *glynnjonesi* Henson, *Peneroplis* aff. damesini Henson.

Miocene

This unit generally consists of basalts, tuffs, agglomerates, limestones and sandstones. Also, the unit unconformably rest on the limestones of the Upper Eocene and the older rock units.

SYSTEMATIC DESCRIPTION

Order : Foraminiferida Eichwald, 1830

Suborder : Miliolina Delage & Herouard, 1986

Superfamily : Miliolacea Ehrenberg, 1839

Family : Alveolinidae Ehrenberg, 1839

Genus : Praebullalveolina Sirel & Acar

Type species : Praebullalveolina afyonica Sirel & Acar

Description

The observed test is small, porcelaneous, slightly natuloid or ovoid in shape (Plate I, figs. 6 8). In general, the diameter of spherical forms varies between 0.498-1.07 mm. Index of elongation (Axial diameter / Equatorial diameter) is 1-1.05. The number of whorls in a 1.07 mm diameter is 7. The first chamber is very small and can not be measured. The apertural face bear both one row of main aperture and one row of secondary aperture. Main apertures provide the relation of two chambers (Plate I, figs. 1 -4, 9-11); the secondary apertures combine one row alveole to preseptal passage of previous chamber (Plate I, figs. 1,3,4,9 and 10).

This alveolinid, found in Elazığ region, was pointed in the genus *Praebullalveolina* Sirel & Acar, because of two rows apertures being seen in their equatorial sections (Plate I, figs. 1,4,9,10). Our species is similar to *Praebullalveolina afyonica* Sirel & Acar with small, spherical, slightly ovoid and natuloid in shape. Therefore, the Elazığ forms, that particularly constitute the main'subject, are named as *"Praebullalveolina afyonica* Sirel & Acar".

DICCUSSION AND RESULTS

In all the Mediterranean countries, porcelaneous foraminifers which characterized the Upper Eocene age inner platform sediments have not been reported earlier except with few researches. So far, the presence of the Upper Eocene inner platform facies have not been reported in Turkey apart from Sirel and Acar (1982). The sequence which observed around Alatarla village (NW Elazığ) is an excellent example for both Turkey and Mediterranean countries with its foraminifer assemblage. The sequence, that is completely composed of algal limestones containing *Nummulites perforatus* (Montfort), *Alveolina elongata* d'Orbigny, *Alveolina fusiformis* Sowerby, conformably rest on top of the late Lutetian (Fig. 2). The same sequence is also characterized by *Nummulites striatus* (Bruguiere), *Praebullalveolina afyonica* Sirel & Acar and *Peneroplis damesini* Henson of late Eocene.

The unique Anatolian alveolinid form of the Upper Eocene, *Praebullalveolina afyonica* Sirel & Acar, has been secondly reported and distinguished in Elazığ area apart from its own type locality. The algal limestones, that *Praebullalveolina afyonica* Sirel & Acar was found in Elazığ area, show great similarity with the sequence characteristics, stratigraphy, foraminifer assemblage and *Praebullalveolina afyonica* Sirel & Acar form of Upper Eocene in Afyon area (Sirel & Acar, 1982).

ACKNOWLEDGEMENT

The author is grateful to Dr. Ercüment SIREL for reviewing the manuscript and for helpful suggestions.

Manuscript received May 5, 1995

REFERENCES

Adams, C.G. (1962). Alveolina from the Eocene of England. Micropal. 8/1, p. 45-54.

Bieda, F. (1963). Larger foraminifera from the Tatra Eocene. Prac. Inst. Geol. I, vol. 37. P. 1-215.

Blondeau, A. (1972). Les Nummulites. Soc. de la Terra, Lib. Vuibert, p.1-254. .

Bombita, G. and Moisescu, V. (1968). Donnees actuelles sur le Nummulitique de Transylvanie. Mem. Bur. Rech. Geol. Min. 58. 693-729.

Caus, E. (1974). Biostratigraphia del Eoceno Medio y Superior del Prepirineo catalan.-Rev, espan. Micropaleont. 7/2, 297-316.

Dizer, A. (1965). Sur quelques Alveolines de Turquie. Rev. Micropaleont. 7, 4, p. 265-279.

Ferrer, J. (1971). El Paleoceno y Eoceno del borde sur-oriental de la depresion del Ebro (Cataluna). Mem. Suisses Paleont. 90, 1-70.

Henson, F.R.S. (1950). Middle Eastern Tertiary Peneroplidae (foraminifera) with remarks on the phylogeny and taxonomy of the family-Thesis, Leiden (Wakefield), p.1-70.

Hottinger, L. (1960). Recherches sur les Alveoles du Paleocene et de l'Eocene. Mem. Suisses Paleont. 75/76, 243 p.

Nemkow. G.I. (1967). Nummulitidis of the Soviet Union and their biostratigraphic significance. Nauca, Moscow, 16/20, 317 p.

Rahaghi, A. and Schaub, H. (1976). Nummulites et Assilines du NE de l'Iran. Eclogae geol. Helv. 69, 765-782.

Schaub, H. (1981). Nummulites et Assilines de la Tethys Paleogene; Taxinofnie, phylogenese et biostratigraphie. Schweizerische Palaontologische Abhandlungen Mem. Suisses de Paleont. 104.

Schweighauser, J. (1951). Ein Vorkommen von Neoalveolina aus dem vicentinischen Obereocaen. Eclogae geol. Helv. 44/2, 465-469.

Sirel, E. (1976). Description of the species of Rhapydionina liburnica Stache, Rhapydionina malatyaensis n. Sp. and new observations on the genus of Rhapydionina Stache.-Bull. Of Min. Res. And Expl. Inst. of Turkey. 86, 101-110.

....., and Acar, S. (1982). Praebullalveolina, a new foraminiferal genus from the Upper Eocene of the Afyon and Çanakkale region (west of Turkey).-Eclogea geol. Helv. 75/3, 821-839.

....., --....., and Acar, S. (1993). Malatyna, a new foraminiferal genus from the Lutetian of Malatya Region (East Turkey), Geol. Croatica, 46/2, 181-188.

PLATES

PLATE -I

Praebullalveolina afyonica Sirel & Acar

Fig. 1 Equatorial section (A1-20/2), X84.

Fig. 2 Oblique section, nearly equatorial (A1-20/6), X52.

Fig. 3 Equatorial section, nearly centered (A1-20/9), X50.

Fig. 4 Equatorial section, (A1-21/2), X90.

Fig. 5 Subequatorial section (A1-6), X63.

Fig. 6 Tangential section (A1-20/5), X47.

Fig. 7 Axial section, (A1-20/3), X41.

Fig. 8 Axial section, (A1-21/1), X61.

Fig. 9 Equatorial section, nearly centered (A1-20/1), X62.

Fig 10 Equatorial section (A1-20/4), X52.

Fig. 11 Equatorial section (A1-20/10), X61.

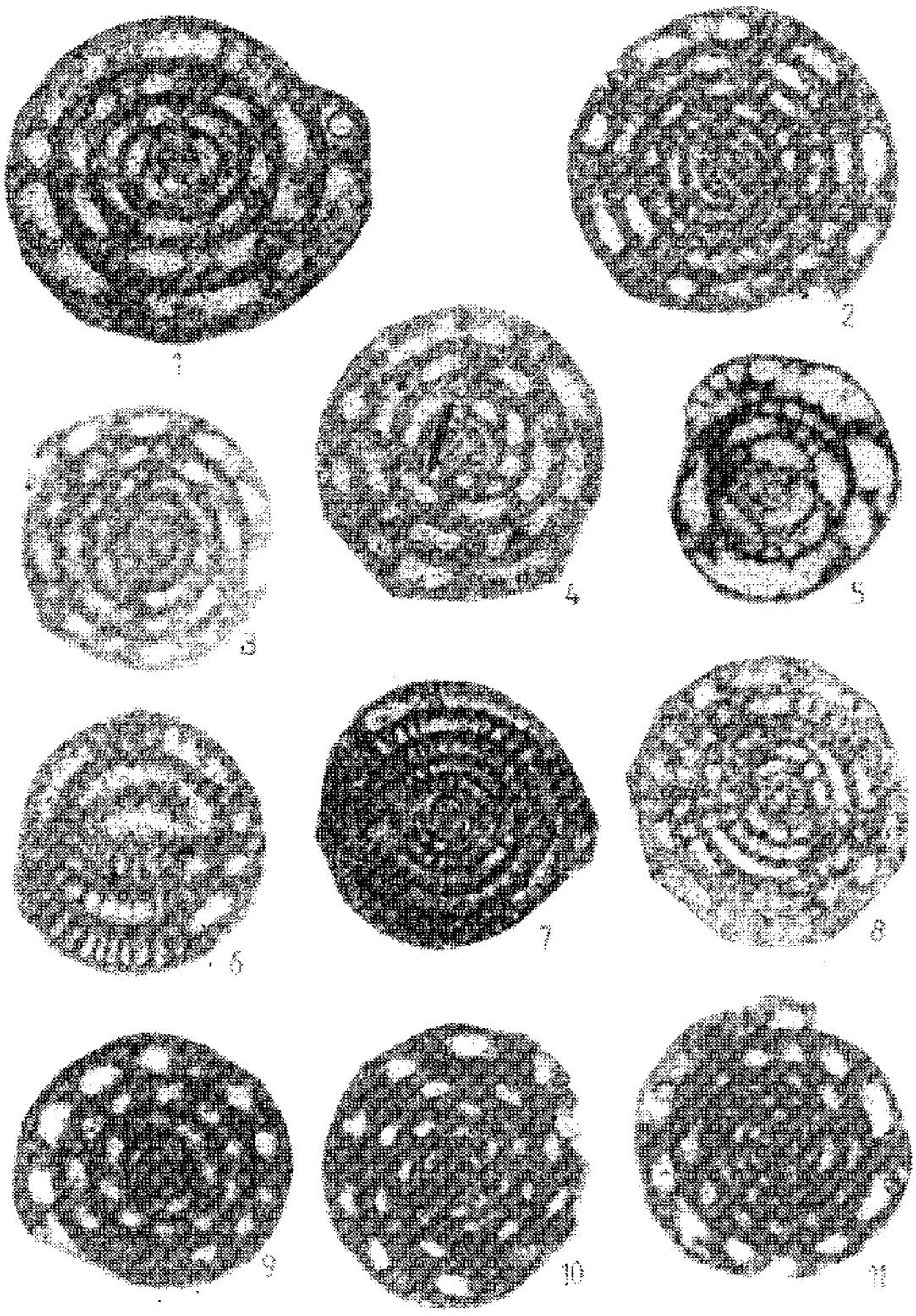

PLATE -II

Nummulites perforatus (Montfort)

Fig. 1 Equatorial section, microspheric form (A1-9/1), X2

Fig. 2 Axial section, microspheric form (A1-9/2), X2

Fig. 3 Equatorial section, microspheric form (A1-9/3), X2

Nummulites striatus (Bruguiere)

Fig. 4 Surface view, macrospheric form (K4-2/1), X6

Fig. 5 Equatorial section, macrospheric form (K4-2/3), X9

Fig. 6 Equatorial section, macrospheric form (K4-2), X10

Praerhapydionina huberi Henson

Fig. 7 Transversal section, slightly oblique (A1-21/10), X52.

Fig. 8 Tangential section (A1-21/8), X44

Fig. 9 Vertical section (A1-21/6), X48

Fig. 10 Vertical section (A1-21/12), X38

Fig. 11 Tangential section (A1-21/7), X38

Alveolina fusiformis Sowerby

Fig. 12 Axial section, macrospheric form (A1-5), X20

Fig. 13 Subaxial section, macrospheric form (A1-12), X20

Fig. 14 Axial section, macrospheric form (Üç-3), X17

Alveolina elongata d'Orbingy

Fig. 15 Axial section, macrospheric form (Üç-1/4), X24

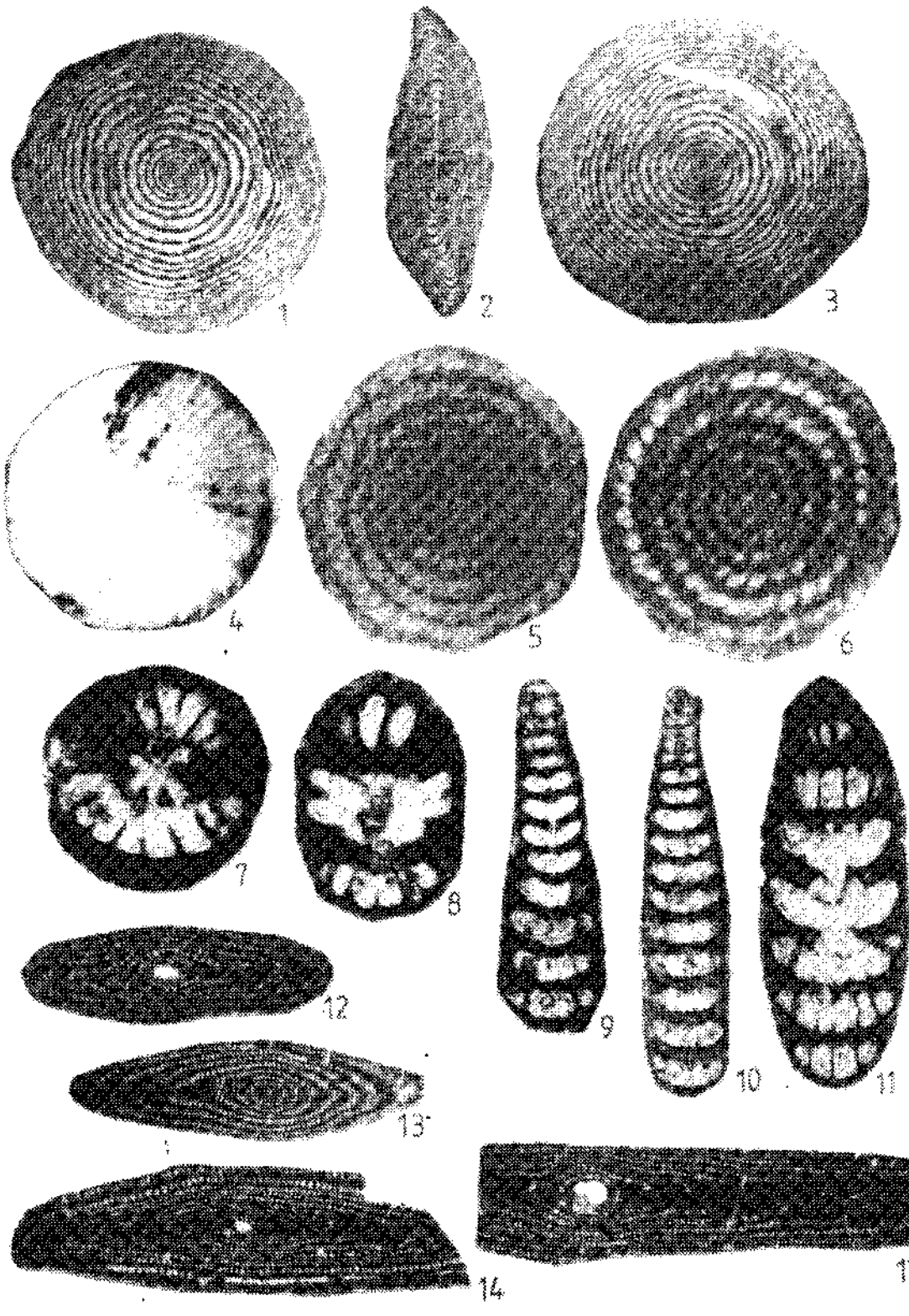
1
2
3
4
5
6
7
8
9
10
11
12
13
14
15

Mineral Res. Expl. Bull., 118, 15-24, 1996

DESCRIPTION AND INTERNAL STRUCTURE OF THE CONDENSATE SERIES: AN EXAMPLE FROM THE BEYŞEHİR-HOYRAN NAPPE

Baki VAROL* and Gürkan TUNAY**

ABSTRACT.- The condensate sequence exposed around Üzümlü-Huğlu, about 30 km SW of Beyşehir, whose typical section is located in the Boyalı Tepe, is one of the best examples of these kind of occurrences in the Beyşehir-Hoyran nappes. This pelagic sequence with a total thickness of 25-30 m overlies the platform type limestones and presents a continuous sedimentation between Early Jurassic and Late Cretaceous. This condensate sequence, formed by a minimum sedimentation in a wide time interval, is composed of 3 parts from bottom to top: 1- Ammonite bearing with red-nodules (Jurassic: total thickness is 7-9 m); 2- White, reddish, and multi-colored, radiolarite interbedded, Calpionella sp. and Globigerina sp. bearing limestones (Lower Cretaceous: total thickness is 3-4 m); and 3- Reddish colored, silica banded or noduled, Globotruncana sp. limestones (Upper Cretaceous: total thickness is 15-17 m).

The condense character of this pelagic sequence described, is determined by the criteria given below:

a- Repetetive deep sea erosional surfaces or hardgrounds. These erosional surfaces are characterized by iron microcrusts and dense filament accumulations which were derived from pelagic lamellibranches (probably Bositra sp.), particularly in Jurassic samples.

b- Deep see fractures and the fractures filled with internal sediments.

c- The abundance of nanno-organism in the pelagic matrix; but their poor preservation due to early diagenesis.

d- The activities of deep sea and micro-endolithic organisms. Especially, active borings of micro-endolithic organisms in the Globotruncana sp. sections,

e- Excess hardness due to early diagenesis and compression and stilolite in the following diagenetic stages.

INTRODUCTION

Condensed sequences are formed either as a result of extreme slows down or stagnant sedimentation. Moreover, submarine erosions are another important factor. These sequences, in spite of having a negligible thickness, precipitated in a wide time interval.

After studying the Swiss Alpine, Heim (1934) concluded that in condensed sequences fossils of different age might be in the same layers and these layers might have settled down slowly in a very long period of time. He also indicated that reworking was the major factor for development of this sequences.

Rod (1946) defined the stratigraphic condensation based on the following features: 1- Enrichment of well-preserved fossils and fossil fragments. 2- Fauna mixing. 3- Widespread distribution and negligible thickness. Rod (1946) also added that reworking was envisaged as a process acting on condansation, but it was not the main reason for its development. Heim (1958) and Wendt (1970) proposed faunal mixing *as* a criterion of stratigraphic condensation. Mensik (1960), when referring of condensed sequences in the Spanish Jura, pointed out the presence of confusion over the terminology and concluded that there was a need for a new definition to overcome this confusion. Jenknyn (1970; 1971) suggested that in an environment where most of the sediments is swept away before it has the chance to settle, the term "reworking" is hardly acceptable and this cannot be considered as a reliable criterion in defining condensation. Holmann (1964) who studied the condensed sequences in the Jurassic red limestones of North Italy, suggested that the role of currents had been considerable although extensive mechanical reworking had not taken place. Flügel (1967) expressed similar opinions on the genesis of the Austrian Stenmühl-Kalke. Some radiolarite and limestone sequences in the Alps have been interpreted as starved basin deposits (Garrison and Fischer, 1971). The maximum floddy surfaces with lowest sedimentation current have arised condensed sequences (Schlager, 1992). The close relationship between sequences and current activities can be explained by occurrence of hard-

grounds. The hardground of Western Sicillian Jurassic represents a most typical example for these occurrences (Wendt, 1963, 1970; Jeynkyns, 1961). Some hardgrounds and stratigraphic condensed sequences in Turkey are observed in red coloured Jurassic ammonite- bearing limestones (Ammonitico Rosso). Their descriptions related to internal structure have been described by Varol and Gökten (1994) and Akkaya (1994) in the vicinity of Ankara and Jurassic Amasya sequences, respectively. The condensed sequences of these regions are mainly Lias and Dogger in age. On the other hand, the condensed sequences studied in this paper are located in Beyşehir-Hoyran Nappe of Taurus tectonic units including pelagic limestones and deep-sea sediments. Detailed stratigraphic studies on this nappe and the definition of condense sequence of Lower Jurassic-Upper Cretaceous age have been made by Gutnic and Monod (1970), Özgül (1971, 1976). Brunn and et al. (1971), and Monod (1977). Moreover, a preliminary sedimentologic study on this nappe has been summarized by Varol and Tunay (1994). This paper is based on a study of mode of occurrences and genesis of internal structure of condensed sequence within the Boyalıtepe section of the Beyşehir-Hoyran nappe. Sedimentologic, petrographic and electron microscopy studies of samples taken from this section were performed in detail.

Geological and Stratigraphic Setting

The condensed sequence in the Beyşehir-Hoyran Nappe is situated about 30 km SW of Beyşehir, around Üzümlü-Huğlu (Fig. 1). The Boyalıtepe Triassic-Lower Jurassic limestone is found at the bottom. This unit is overlain by a condensed sequence with a thickness of 25-30 m (Fig. 2). Moreover, the condensed sequence is also overlain by volcanite, volcanic sandstone, volcanic breccia, lavas and silicified radiolaria bands. The unit, named as volcanic series by Monod (1977), contains large limestone block in places originated from the platform type Boyalıtepe limestones, which forms the basement of condensed sequence.

The platform-type limestones forming the basement of condensed sequences are dolomitic in character. The non-dolomitic series consists of oolitic rocks, algae and foraminiferous mudstones. Some Involute sp. observed in this section are Upper Triassic-Lower Liassic in age (Monod, 1977). The upper most section (about 10 m) of the platform-type massive limestones consists of reddish, thin layered limestones characterizing Megalodont-bearing wackstones and packestones. At Boyalıtepe, the condensed sequences with 25-30 m thickness overlying the limestones are diveded into the three sections as shown below (Plate 1, Fig. 1).

1- Red nodules and ammonite-bearing, marl (Jurassic, total 7-9 m. in thickness), 2- White and red coloured radiolarite interbeded and Calpionella sp. and Tricinella sp.-bearing limestones (Lower Cretaceous, total 3-4 m. in thickness), 3- Red coloured, silica interbedded and banded, globotruncana-bearing stilolitic limestones (Upper Cretaceous, total 15-17 m in thickness).

1-Jurassic: The Jurassic limestones comprising the first of condensed sequences that lie over the platform-type limestones, show characteristic red coloured, nodules and breccia textures and their layer surface show bumpy character (Plate 1; Fig. 2, 3). In these surfaces, ammonites represent syndepositional and post-depositional dissolution of the original aragonitic shell material which makes up irregular surfaces on the bedding surface. The presence of these textures due to the submarine surface erosion and dissolved shell-fragments which charecterize the hardgrounds (Garrision and Fisher, 1971). Morever, micritic grains and ammonite shell fragments originated from chipped surfaces, as internal sediments filling the dissolution voids also indicate the submarine erosion.

The majority of Jurassic condensed sequences are breccia in character. These breccia show maily grain to grain lesser clay filled stilolitic texture; sporadic stilo-breccia texture are also observed. Besides clay mineral, as a laminar (from a few mm to a few cm) hematite and limonite shells within the "Jurassic condensed sequences are quite widespread. Iron shells are also frequently observed, around ammonite shell traces at nearby of internal sediment filled microcracks (sedimentcrack) and on the corrosion surface developed parallel to the layer.

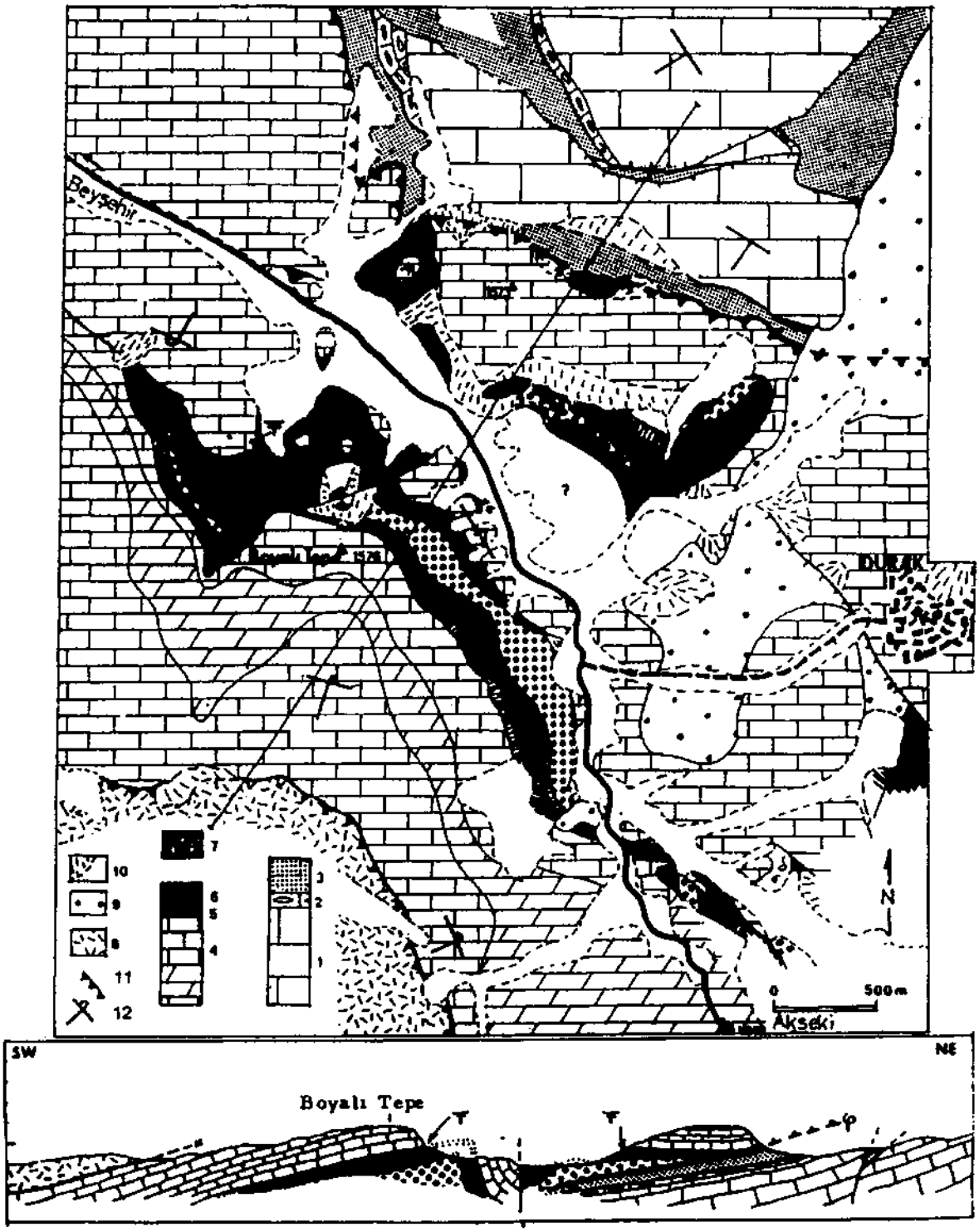

Fig. 1- Geological map and cross section of the Boyalı Tepe condensed sequence (From Monod, 1977). 1- Autochthonous Mesozoic limestones, 2- Nummulitic limestones, 3- Eocene flysch, 4- Boyalı Tepe limestone, 5- Condensed sequence (Liassic-Senonian), 6- Ridiolaria and breccia, 7- Wild flysch, 8- Huğlu tuffites, 9- Neogene deposits, 10- Quaternary, 11- Trust, 12- Overturned bedding.

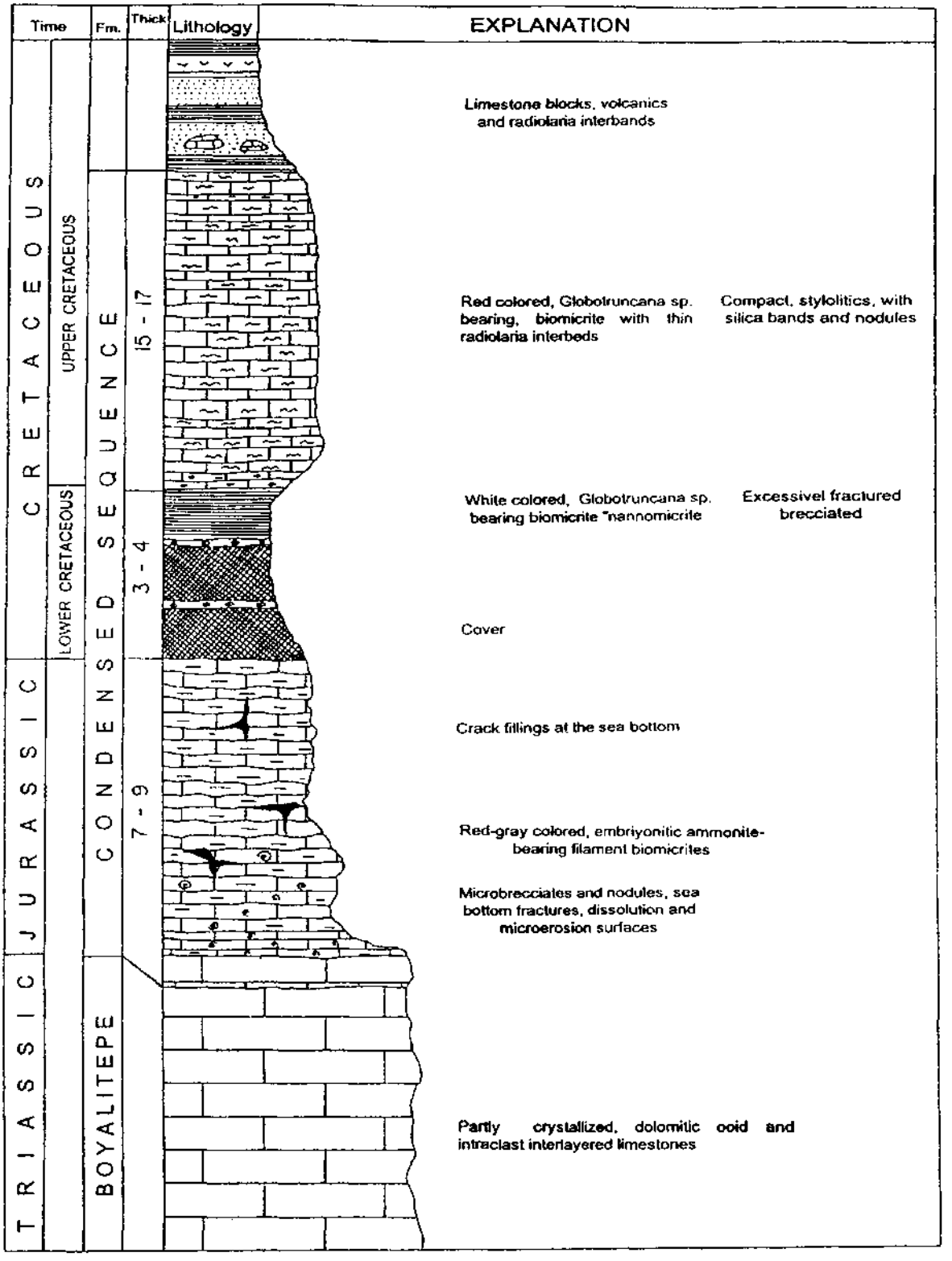

Fig. 2: Stratigraphic columnar section of the Boyalı Tepe.

2- Lower Cretaceous: Due to a probable fault, boundary definition between Jurassic and Lower Cretaceous units is not clear, but Lower Cretaceous-Upper Cretaceous boundary is well observed: The white coloured, clayey limestone section (40-50 in thickness) of Lower Cretaceous is overlain by thin bedded limestone section of Upper Cretaceous (Plate 1, Fig. 4). In some part of the Boyalıtepe cross-section, Jurassic/Lower Cretaceous transition is (from bottom to top) is given below: Nodular Jurassic Limestone (a few m in thickness) and poorly-bedded radiolarites, white and grey coloured, quite hard, massive and thin-bedded Lower Cretaceous limestoes. In places, a microconglomeratic series observed at the upper most section of the radiolarites consist of limestones pebbles of Lower Cretaceous.

3- Upper Cretaceous: The upper most section of Upper Cretaceous aged condensed sequences is represented with red coloured, rather hard and stylolitic-type plaket limestone with interbedded silica layers or irregular nodules of silica (Plate. 1, Fig 5). Around these nodules, in place, manganese and iron coatings are observed. Regularly, stylolite occurs along the layers and follows the layer boundaries. In some sections of the unit, it is difficult to distinguish the real bedding planes from the stylolitic surfaces. Some microlaminations, irregular cracks, and breccia occurrences are also clearly observed within the unit.

MICROFACIES

The microfacies present within the Lower Triassic-Upper Cretaceous condensed sequence are given below; Jurassic, represents two main microfacieses, filaman-type and ammonite bearing limestones. Generally, the definition of the boundaries between two microfacies is quite difficult. Nevertheless, the ammonite bearing limestone is rather hard, light-grey coloured partly brecciated and have nodules textures, whereas, filaman-bearing limestones is red colored, sandy, soft and has a matrix appearance (Plate'1, Fig. 6). At the beginning of sequences of condensed unit, wackestone-packestone-bearing filaman limestone microfacies is dominant. The filamans as massive files have been deposited along the layers (Plate. 1, Fig. 7-8). To the top, the ammonite-bearing limestones and nodular sequences. Moreover, these filaments also fill the micro cracks surrounded by iron and manganese. No paleontologic description has been done yet on these filaments, but some similar forms have been defined as shell fragments of Bositra species by Jenkyns (1971). The ammonites which characterize the Jurassic microfacies, occur in wackestones of 10-20 % and are entirely embrionic in character. The aragonite composition of ammonite shells has been mainly have transformed to calcite and lesser amount has been dissolved. The secondary sparry calcite cementation along with the micritic internal sediments were observed within these dissolved section. The specimens taken from the condensed micritic limestones of Jurassic, indicated that no nanno-organism or their relict are present. Electron micrographs of the specimens show that recrystallized biogenic fragments have given rise to this micritic matrix (Plate I, Fig. 9). Lower Cretaceous section of condensed sequences which is mainly limestone facies in character, consist of Globigerina sp. and Ticinella sp. bearing mudstone-wackestones. Within the this microfacies, the ammonite of micritic-clays fairly high in comparision to other condensed limestone sequences (10-15%). Moreover, amount of nanno-organism is also higher than that of limestones, and well-preserved (Plate I, Fig. 10). In some globigerina chambers, occasionally glauconite mineralisation has occurred in the form of green occurrences. Fe and Mn shells occurrences have not been observed here, but within the Jurassic specimens these shells are abundant. Moreover, similar to this microfacies, a completely calpionella species-bearing and brecciated another microfacies has separated Lower Cretaceous from Jurassic and exposed in a small area. The lateral extension of this microfacies has been restricted by a probable fault.

In Upper Cretaceous, alternation of three microfacies; as red pelagic micrits, radiolarite-bearing micrits and radiolarite levels have been observed. At the bottom and medium level of sequences, the red pelagic micrits are dominant. To the top, they have been replaced by the radiolarite-bearing micrits and radiolarite microfacies. The red pelagic jmicrits microfacies has been represented by the Globotruncana and Globigerina-bearing mudstone and wackestone. Particularly, microlamines formed

by Globotruncana accumulation are widespread (Plate II, Fig. 1). The stilolites are very abundant and most of than are filled by iron. In radiolarite-bearing micritic microfacies, in places micritic cements has been replaced by silica. The remainings of the planktonic foraminiferous (Globotruncana and Globigerina species) have been observed within irregular silica patches. The amount of radiolarites has increased around these fossil remainings. Radiolarite microfacies is pure, but occasionally comprises a various amount of remainings of silicified micritic limestone. These specimens appear red and white in colour.

The most abundant nanno-organism has been observed within the electron micrographs taken from the micritic matrix of pelagic limestone levels. But, these are not well-preserved and most of them are broken and intensly are recrystallized (Plate II, Fig. 2).

DEFINITION PROPERTIES OF CONDENSED SEQUENCE

The condensation of the condensed sequence is controlled by various parameters. The most important is stratigraphic and erosional (reworking) condensation. Since nanno-organisms are not still developed completely in Jurassic, the carbonate production within the pelagic facies has been restricted, eventually it has given rise to stratigraphic condensation (Jenkyns, 1971). In addition, the flow movements on the seamounds causes erosion and sweeping as well as dissolution of carbonate which is controlled by depth (carbonate compensation depth) (Garrison and Fisher, 1971). The condensation factors of the Boyalı Tepe condense are determined and explained below.

Submarine Erosions: The submarine erosions of the condense sequence of the study area is developed dominantly in ammonitic Limestone, microfacieses of Jurassic. The erosion surfaces are covered by microbreccia grain and flaman limestones (plate II, Fig. 3). Milimetric and centimetric scaled iron and manganese crusts are common on the erosion surfaces. In this type submarine erosion samples, sudden lithology changes in the vertical direction, microbreccia grain mixed with filament, the orientation and imbrication are common (Plate II, Fig. 4).

At the same time, the upper part of the biogenic grains is affected by the submarine errosion. Typically ammonite crusts could be seen in samples of Plate II, Figure 5. The upper sections of the ammonite shells situated on the surface of these submarine erosions surfaces which separated ammonite-bearing limestones from flamant limestones as a microdiscordans, are eroded in various scales. In our specimens, this kind of erosion surfaces indicated a hardground occurrence.

The submarine surfaces are also observed within the Lower and Upper Cretaceous section of condenced sequences. The breccia grains with Calpionella sp. and Ticinella sp. of Lower Cretaceous present within the limestones almost in some age and lithology explained that the sea floor erosion has developed during deposition or just after. No microbreccias have been observed in pelagic micrites of Upper Cretaceous. The submarine erosions are very small but widespread. On these surface oriented and micrograted pelagic microorganism shells are common. Late diagenetic stiolilization commonly present within the Upper Cretaceous limestones, mostly prefered the surface of interbedded layers which was developed by micro erosion surfaces.

Neptunian Dykes: This structure is actively seen in Jurassic age sequences. These are lateral and obliques cracks which are developed in the layers. They are different in size, and they are mostly thined and diaspeared ant the width of them vary from a few centimeter and decimeter. The cracks dominantly developed in ammonitic limestones are filled with filament limestones (Plate II, Fig. 6). These could be seen in breccia and nodular structured Jurassic condensed sequences. No atmosphere condition and meteoric diagenesis have been seen near and around the crack system. All the cracks are filled with marine sediments, therefore it shows that cracks were developed at the sea bottom.

Dissolution Voids: Different size or dissolution void effects could be seen in all condense levels. The dissolution voids are present in micritic matrix (mainly in ammonit shells). They are developed as a dissolution mold or irregular voids. The inner side is filled with crystal silt and drusty cement. Very

small (in micron size) voids are also very common. Mainly in Jurassic samples, they developed both on organism shells and micritic matrix (Plate II, Fig. 7). These are similar to the holes of the endolitic organisms. Absence of organism marks in the environment, it supposes to the biogenic genesis. Most of the dissolution voids are open. But SEM analyses showed that the wall of the voids are cemented with very fine grained marine materials.

Early Cementation: The most widespread hardground occurrences within condensed sequence are present mainly in Jurassic, and partly in Cretaceous. The recrystallised micrit crystals, clay, iron, manganase minerals and activity of endolitic organisims clearly showed an early cementation. The matrix is made up of irregular shaped crystals, 4-7 micron in size; party they are come together in heaps. These features showed that the genesis was biogenic (Fisher at al; 1967). The crystals originating from aragonite shells Jurassic specimens are common. Most of them were transferred to calcite. In Upper Cretaceous specimens, the micritic matrix presenting early cementation was made of magnesium-calcite. The micritic crystals originated from nanno organism shell walls were partly or completely crystallized. When the recrystallization was not strong enough, the nanno organisms were partly protected. The micrit matrixes (nanno micritic) in all specimens, have been intensely hollowed by the micro organism hollowing hardground. This clearly indicated a hardground occurrence.

Early diagenetic mineralization is another indication for hardground occurrence in condensed sequence. All clays, which are illite in character, crystallized either in dissolution surfaces or in dissolution voids (Plate II, Fig. 8). Iron mineralization is represented by mainly hematite and limonite stains. They are mainly seen as thin films on the surfaces of erosional hardground or on the microcrack walls and in the microcracks. Ot the other hand, in brecciated Jurassic hardgrounds, they surrounded all brecciated grains as a thin film. When the sedimentation rate was minimal or zero, it brecciated that the iron mineralization concentrated on the hardgrounds was in relation with the oxidation of sea floor (micrit matrix) effected by sea water in a long time (Jenkyns, 1970). In addition, the presence of breccias which accompany with this mineralization, also explains a dissolution and erosion on the early hardground (Hollman, 1962 and 1964).

Bioerosion: The maximum activity of endolites has been observed within the Upper Cretaceous aged pelagic micrites. The tubes varying from a new microns to tens microns, as indicated above, have caused intense burrowing of both micritic cement and biogenic grains. These microorganisms are composed of a few types. Coloni-type microorganisms have various type branchies and sinusoidal structures. These mainly cause burrowing of micritic cements (Plate II, Figs 9,10). Up to date, these endolitic fossils occurring in the deep sea have not been mentioned yet. The fossils within the Boyalı Tepe specimens are probably the first fossils defined. In respect to appearance, these are smilar to the types, which caused the microbiologic alteration described in the Bahama recent deep sea carbonates. They were described as mushroom-type endolitics living at 210-1450 m. depths below the light zone (Marjone and Perkins, 1979).

DISCUSSION AND RESULTS

With maximum 25-30 m thickness, conformably development of the Lower Jurassic-Upper Cretaceous aged pelagic limestones interbedded with radiolarites within the Beyşehir-Hoyran nappe, clearly indicated a condensed sequences occurrence. Generally, sedimentation in lesser amount occurs in the condensed sequences, but similar sequences show much thicker sedimentation within the same geological time (Jenkyns, 1971). Here, the rate of sedimentation is too slow, namely, the thickness of the unit is 25-30 cm in a million year. The development of microerosion and microunconformity surfaces have indicated a sea floor erosion and removal of sediment. This may give rise a condensation. However, a sedimentation deficiency in the form of sediment removal, may not be resulted in the Boyalı Tepe condensed sequences alone. Such sea floor erosions have been mainly observed in the Jurassic-Lower Cretaceous periods.

In the Boyalı Tepe columnar section, the lack of the Calpionella-bearing series of Lower Cretaceous age and as its being intracalated, indicated that these thin condensed Calpionella-bearing units

might have been removed during sea floor erosion, wheras, along Upper Cretaceous in Globotruncana the sequence of traces of the sea floor erosion have been observed in minor amount. This observation explained that the condensed sequences of the Boyalı Tepe have been occurred by both stratigraphic and erosional (reworking) condensation due to undeveloped nanno-organism (Jenkyns, 1971). Lack of nanno-organism has been observed in the electron micrographs of the Jurassic samples. Studied condensed sequences indicated that only Upper Cretaceous pelagic limestones are rich in nanno-organism that their matrix are nanno-micritics in character. The globotruncana-bearing micrites of Upper Cretaceous also comprise essential amount of nanno-organism. But these are poorly preserved due to intense recrystallization in the Boyalı Tepe Column section. This clearly explains that the condensation within the Lower Upper Cretaceous sequences has developed after the nanno-organism deposition. Wheras this phenomena has not been observed within the Jurassic sequences has not been explained using by electron microscopy. It is quite difficult to say that these closely interlocked subhedral and anhedral crystals (4-5 micron in size) have been originated by chemical processes. However their irregular crystal shapes and partially accumulation forms support their organic origin. Besides, presence of highly altered and dissolved macroshells, development of many caves in micritic matrix at the ammonite-bearing sequences of Jurassic and filling of them by large and small micrites, emphasizes mobility of carbonate materials related to sea floor dissolutions and erosion.

The main point of this study is to define events giving rise to condensation and environmental development. Although the evidences obtained up to date, are not sufficient to explain these events, but some vital clues have been obtained. From the literature, it is evident that some different opinions are present on genesis and depths of condensed sequences. These have formed on the seamounts with a few meters in depth (Jenkyns, 1971) or formed within the bathyal abyssal environment (Garrison and Fisher, 1971). The stromatolies formed within the condensed sequences support the first opinion, silica and radiolarite alternation which is associate with pelagic mudstone supports. the second opinion. At the Boyalı Tepe condensed sequence, the lack of stromatolites defines a depth below a light zone (max. 200-300 m). On the other hand, from the studied condensed sequence, it is believed that the beginning parth of the sequence (Lower Jurassic) is not very deep. Because the beginning parth of condensed sequence (red micrites), as seen in Fig. 2, was developed on the platform-type limestones as coating. Lack of algaes within the these sequences, most probably due to stable environment and current action rather than environment depth. The development of condensed sequence on the drowned platform straight away is most probable. Abundant sedimentary cracks on (neptunion dykes) occurred in Jurassic, explain strain tectonic regime formed on the deepening platform. The floor currents arisen from fast deepening, have prevented sedimentation, sea floor carbonate sweeping and erosion are the main features for the Jurassic-Lower Cretaceous condensation. Within the these sequences, abundant embrionic ammonite-bearing micrite intraclasting and their mixing with laminated filaman limestones support a current action. Moreover, large amount of iron mineralization indicates a slow sedimentation caused by these current and presence of aerobic conditions at the sea floor. Before hematite mineralization, abundant carbonate dissolution formed on the floor, particularly on hardgrounds is another importants points. These dissolution surfaces and/or voids have been covered by a thin hematite layer or filings. Besides, Illite-type clays have been observed in the some dissolution voids. All these occurrences are the simple examples of mineralization on the sea floor, at carbonate sedimentation stages partly slowing down and breaking in some cases. After Jurassic, the radiolarite sequences with few meter thickness within the condensed sequence, passed from carbonate deposition to silica deposition. As proposed by Garrision and Fisher (1971), this might be below the carbonate equilibrium level depth (CCD). This depth varies from 4100 to 4500 m for actual oceans. At the Boyalı Tepe condensed sequence, by end of Jurassic, environment depth should have reached these depths. At the beginning of Lower Cretaceous, reworking of carbonate deposition and starting of the intense nanno-micrite deposition have clearly indicated shallow environment for a while. Particularly, the lack of Calpionella-bearing

unit within this sequence most probably due to erosion during this shallowing phase. Moreover, there is no evidence that this shallowing phase developed as a terrestrial cycling and later eroded. Unfortunately, here these evidences can not explain this absence. As well as fault actions controlling basin, deepening and shallowing and causing the submarine erosions by sedimentation are quite possible.

Upper Cretaceous is represented completely by globotruncana-bearing mudstones and interbedded radiolarites. This suggests that sea floor depth would reach the CCD level and is instable of equilibrium. In this way, passing from carbonate to siliceous sediments and radiolarites may attribute to variation of sea floor depth and also sea floor current actions of CCD and temperature variations.

According to above given information, it is concluded that the Boyalı Tepe condensed sequence is represented by the abundant amount of pelagic limestone and radiolarite-bearing deep sea sediments forming on the platform-type limestone. From the present study on the limestone facies, it is evident that the environment has deepened continuously, but became shallow for a while Particularly, in Upper Cretaceous, variations of the CCD level have mostly controlled the condensations. The current actions giving rise to forming of condensed may be directly resulted from this rapid deepening. Many works have confirmed this idea. This action, improved by the control of a probable fault, has deepened the environment from platform-type limestones to the distance (4500-500 m.) in which.

Manuscript received June 15, 1995

REFERENCES

Akay, E., 1981, Beyşehir yöresinde (Orta Toroslar) olası Alt Kimmeriyen dağ oluşum izleri: Türkiye Jeol. Kur. Bull. 26/2, 26-29.

Alkaya, A.,1994, Amasya kuzeyi Sinemuriyen-Alt Pliyensbahiyen (Alt Jura) "Ammonitici rosso" istifi, erken çimentolanma, hardground ve stratigrafik kondansasyon: Sert zeminler ve Kondanse istifler Simp. Bildiri Özleri, Ankara.

Blumenthal, M., 1946, Seydişehir-Beyşehir hindenlandındaki Toros Dağları'nın Jeolojisi: MTA yay., seri D, no. 2, Ankara.

Brunn, J.H., Dumont, J.H.; Graciansky, P. ch. de; Gutnic, M.; Juteau, Th.; Marcoux, J.; Monod, O. and Poisson, A., 1971, Outline of the geology of western Taurids. Geology and History of Turkey: Petroleum exploration Society of Libya, Tripoli, 225-255.

Fischer, A.G. and Garrison, R.E., 1967, Carbonate lithification on the sea floor: J. Geol., 75, 488-496.

.....; Honjo, S. and Garrison, R.E., 1967, Electron micrographs of limestone and their nannofossils: Monographs in Geology and Paleontology (A.G. Fischer, Editor), 1, Princeton University Press, 141 pp.

Flügel, H.W., 1967, Die Lithogenese der Steinmuhlkalke des Arracher Steinburches (Jura, Österreich): Sedimentol, 9, 23-53.

Garrison, R.E., 1967, Pelagic limestone of the Oberalm Beds (Upper Jurassic-Lower Cretaceous), Austrian Alps: Bull. Can. Petrol. Geol., 15, 21-49.

.....—; and Fisher, A.G., 1971, Deep-water limestone and radiolarites of the Alpine Jurassic. In: G.M. Friedman [Editor], Depositional Environments in Carbonate Rocks; a symposium. Soc. Econ.Paleont. Miner. Spec. Publ. 14, 20-56.

Gutnic, M. and Monod, O., 1970, Un serie Mesozoique condansee dans les nappes du Taurus occidental, la serie du Boyalı Tepe: C.R., somm., soc. Geol. 75, 166-167.

Heim, A., 1934, Stratigraphische Kondansation: Eclog. Geol. Helv. 27, 372-383.

.....--; 1958, Oceanic sedimentation and submarine discontinuities: Eclog. Geol. Helv. 51, 642-649.

. . . . . .--; and Seitz, O., 1934, Die mittlere Kreide in den helvetischen Alpe von Rheintal und Voralberg und das problem der Kondensation: Denkscher. Schweiz. Naturf. Ges. 69, 185-310.

Hollman, R., 1962, Ülber subsolution und die 'Knollenkalke' des Calcare Ammonitico rosso Superiore im Monte Baldo: Neues Jb. Geol. Palaont., Mh. 1962, 163-179.

Hollman, R., 1964, Subsolitions-Fragmente (Zur Biostratinomie der Ammonoidea im Malm des Monte Baldo/Norditalien: Neues Jb. Geol. Palaont., Abh, 119, 22-82.

Jenkyns, H.C., 1970, Fossils manganese nodules from the west Sicilian Jurassic: Eclog. Geol. Helv. 63, 741-774.

————; 1971, The genesis of condensed sequences in the Tethyan Jurassic: Lethaia, 4, 327-352.

Ketin, I. 1966, Anadolu'nun tektonik birlikleri: MTA Derg., 66., 20-31 Ankara,

Marjorie, Z. ve Perkins, R., 1979, Microbial alteration of Bahamian deep-sea carbonates: Carbonate diagenesis Reprint series volum 1 of the Internation Association of Sedimentologist eds. By Maunice E. Tucker and Robin G.C. Bathurst, 50-51.

Mensink, H., 1960, Bespiel fur die stratigrapische Kondensation, Schichtlucke und den Leitwert von Ammomniten aus dem Jura Spaniens: Geol. Rdsch. 49,70-82.

Monod, O., 1977, Recherches geologique dans le Taurus occidental au sud de Beyşehir (Turquie): These Univ. Paris-Sud Orsay, 442 s.

Özgül, N., 1971, Orta Torosların kuzey kesiminin yapısal gelişiminde blok hareketlerin önemi: Türkiye Jeol. Kur. Bült., 14, 75-87.

————; 1976, Toroslar'ın bazı temel jeoloji özellikleri: Türkiye Jeol. Kur. Bült., 19, 65-78.

Öztürk, E.M., Dalkılıç, H., Ergin, A. and Avşar, Ö.P., 1987, Sultandağı Güneydoğusu ile Anamasdağı Dolayının Jeolojisi: MTA Raporu, 8191, Ankara.

Rod, E., 1946, Ülber'ein Fossillager im oberan Malm der Melchtaleralpen: Eclog. Geol. Helv. 39, 177-198.

Schaub, H.P., 1948, Über Aufarbeitung und Kondensation: Eclog. Geol. Helv. 41, 89-94.

Schlager, W., 1992, Sedimontology and sequence stratigraphy of reefts and carbonate platforms: Published by American Association of Petroleum Geologist, Tulsa Oklahoma U.S.A., 1-67,

Simpson, J., 1985, Stylolite- controlled layering in an homogeneous limestone: pseudo-bedding produced by burial diagenesis: Reprint series volum 1 of the Internation Association of Sedimentologist. edited by Maurice E. Tucker and Robin G.C. Bathurst, 293-308.

Varol, B. and Gökten, E. 1994, The facies properties and depositional environments of nodular limestones and red marly limestones (Ammonitico rosso) in the Ankara Jurassic sequence, central Turkey: Terra Nova, 6, 64-71.

—-. . . . .; and Tunay, G., 1994, Kondense tanımı ve iç yapısı: Beyşehir-Hoyran napından örnekler: Sert Zeminler ve Kondanse istifler Simp. Bildiri Özleri, Ankara.

Wendt, J., 1963, Stratigraphisch-palontologische Untersuchungen im Dogger, Westsiziliens: Bull. Soc. Paleont. Ital., 2, 57-145.

. . . . . —-; 1970, Stratigraphische Kondensation in tridischen und Jurassischen Cephalopodenkalken der Tethys: Neus Jb. Geol. Palaont., Mh. 1970, 433-448.

PLATES

PLATE-I

Fig. 1: General view of the Boyalı Tepe condensed, sequence; a- Platform limestones, b- Condensed sequence. Sequence has an overturned structure.

Fig. 2,3: Jurassic condensed limestone levels; brecciated and nodular character is typical. Iron coating, clay and phosphate minerals are typical in dark colored parts, indicated by arrows.

Fig. 4: Lower-Upper Cretaceous transition in the condensed sequence; the thickness of this part of sequence is 1 m; a- Radiolarite brecciated limestone bands; b- Pelagic limestones (Lower) with a white clayey appearance; c- Red colored, compact and silica banded pelagic limestones (Upper Cretaceous)

Fig. 5: Close pan view condansede Upper Cretaceous red pelagic limestones. Stilolizations along microfolding and beddings are typical.

Fig. 6: Reddish levels showing red-white color differentiation in the Jurassic condansede sequence. White (light colored) parts are ammonite limestone, red (dark colored) partsare flaman limestone. Flaman limestone are observed as matrix and matrix and microfissure fillings.

Fig. 7,8: Jurassic flaman limestones; intense packings formed by flamans represent the microshells deposited on hardgrounds in the condensede sequence. Due to the sea floor-currents, these are generally oriented.

Fig. 9: Nanno-organism well preserved in the Lower Cretaceous pelagic micrites. All the micrite matrix are probably derived from the nanno-organisims "nannomicrite".

Fig. 10: Electron microscope image of highly recrystallized micritic matrix in the Jurassic condensede sequence. Irregular grain size distribution probably supports the biogenic origin.


1


2

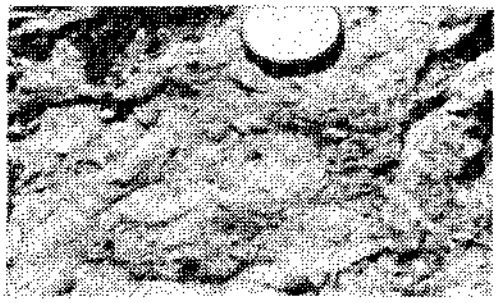
3


4

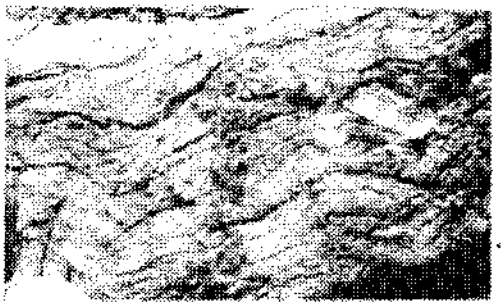
5


6


7


8


9


10

PLATE-II

Fig. 1: Microorganism laminations in the Upper Cretaceous pelagic limestones. They are formed by sweeping and election from the micritic matrix.

Fig. 2: Electron microscope view of micritic matrix of Upper Cretaceous red pelagic limestones. Highly recrystallization causes nanno-organisms being poorly preserved.

Fig. 3: Compact and irregular transition between flaman limestones (a) and ammonite limestones (b) indicates a sub-marine microerosion surface.

Fig. 4,5: Flaman limestones are either transported into the ammonite limestone fragments (hard sea floor erosion) (4) or fill in their microfissures (sea floor cracking) (5).

Fig. 6: Dissolution on the hardgrounds representing the Jurassic condensed sequence. Micro dissolution voids, internal sediment fillings anderosional surfaces in the dissolving part of the hardgrounds are typical (a). Ammonite shells in these sections are also partially dissolved and fractured.

Fig. 7: Electron microscope view of a sample from the Jurassic condensed sequence. Many microspaces (sieve texture) on the biogenic grains are the indicative of active carbonate dissolution on the hardgrounds.

Fig. 8: Clay mineralizations in the micritic levels of the condensed sequences. Filling of microspaces in the limestones by the illite type clay minerals may indicate that day mineralization was developed after the carbonate dissolution.

Fig. 9,10: Tupes micro burrowing organism colonized on the Upper Cretaceous red micrites of the condensed sequence (9). The fact that they burrow micrite matrix and nanno-organisms (10) next to them is an important for the formation of early sea floor hardening (hardground).

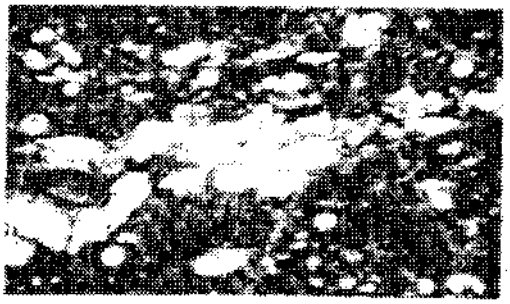

1

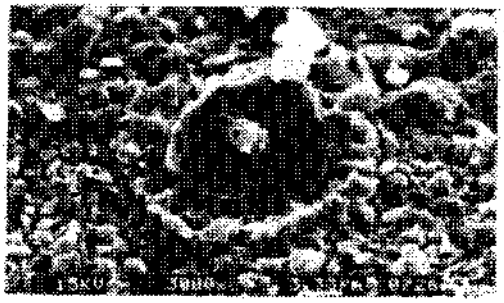

2

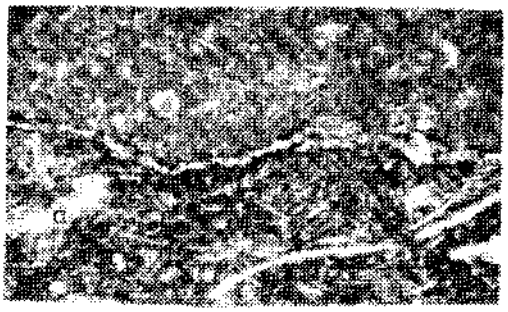

3

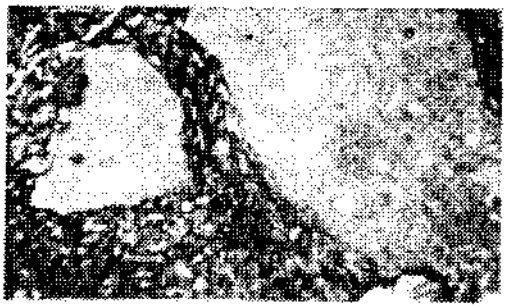

4

5

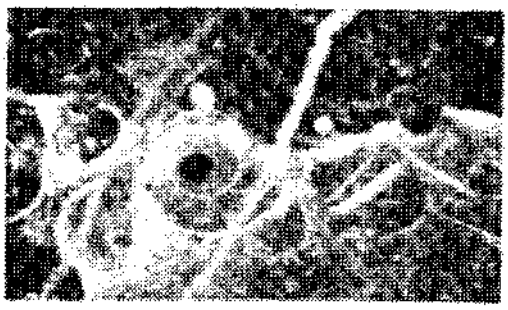

6

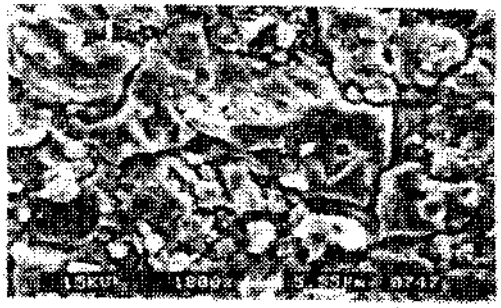

7

8

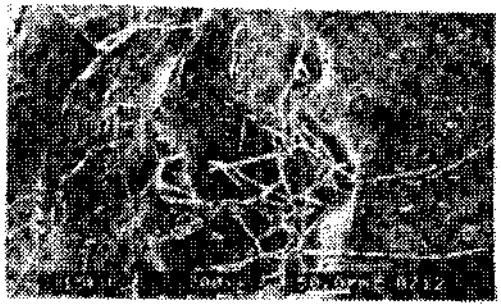

9

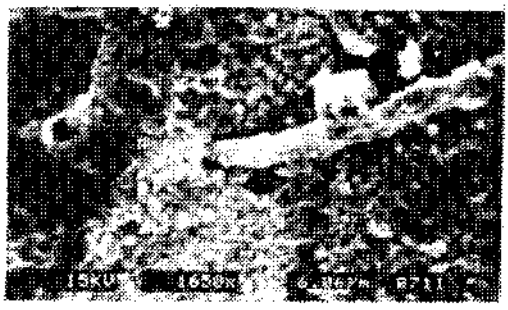

10

MINERALOGY AND GENESIS OF THE ZINC-LEAD DEPOTISTS OF THE YAHYALI (KAYSERİ)-DEMİRKAZIK (NiĞDE-ÇAMARDI) REGION

İbrahim ÇOPUROĞLU**

ABSTRACT.- The area under study is situated in region, north east of Middle Toros, where faults, thrust faults, fracture zones are commanly present. Many zinc-lead deposits, small-big occurrences in the form of vein, lode, fault and karst fillings along the Yahyalı-Demirkazık region, were deposited in the vanious carbonate rocks of Permian-Jurassic age. Ore minerals of the deposits are sphalerite, galena, smitsonite, anglesite and cerussite. The primary mineral parageneses are composed of pyrite, chalcopyrite, arsenopyrite, pyrhotite, magnetite, molibdenite, bravoite, fahlore (tetraedrite, freibergite), nativ Ag, argentite and nativ gold ore. While gothite, lepidocrosite, malachite, azurite, covelline, hemimorphite and hidrozincite from the secondary minerals, the gangue minerals are made up calcite, dolomite, quartz and barite. These minerals assemblage parageneses, indicate high temperature formations. In addition to this, sphalerite and galene contain Fe, Cu, Mn, Al, Mg, ni, V, W, Co, Cd, Ir, Ge, Ag, and Au moreover, the content or Sr is 2,13 %, a very high value. All these proofs point out that the orebodies are probably hydrothermal. According to the plate tectonic model calc alkali magma splits in to two grats due to gravitation before intrusion. One part of these, calc alkali magma, formed granitoid rocks which along Bolkar mountains and the other areas under investigation, the other has no significant mineralizations part of magma was rich in metal ions both parts were in placed in the weak zones of limestones, fractures and faults. Karstification process is continuing even today. The effect of the atmospheric conditions and underground hot water allows the ore in the area to remobilize, and provides it for sedimentation.

MORPHOLOGICAL FEATURES, AGES AND NEOTECTONIC SIGNIFICANCE OF PAMUKKALE TRAVERTINES

Erhan ALTUNEL***

ABSTRACT.- The Pamukkale travertines in the northern margin of the Denizli basin can be classified into five categories based on their morphology. These are: (1) terraced-mound travertines, (2) fissure-ridge travertines, (3) range-front travertines, (4) self-built channel travertines, and (5) eroded-sheet travertines. Three of these classes, range-front travertines, self-built channel travertines and fissure-ridge travertines are of special tectonic significance because they contain syndepositional and postdepositional tectonic structures. Uranyum series dating method has been applied to the Pamukkale travertines and showed that travertine deposition has continued for at least the last 400 000 in different localities. Extensional fissures, that supply water to the travertines, have been dilating at average rates between 0.02 and 0.1 mm/yr, and propagating laterally at about 20 mm/yr. The time averaged rates of extension of the plateau as a whole having been between 0.23 and 0.6 mm/yr during the last 200 000 years.

Mineral Res. Expl. Bull., 118, 25-50, 1996

DISCUSSION ON THE ORIGIN OF OTLUKİLİSE IRON DEPOSIT GÜRÜN-SİVAS

Dönmez ÇiFTÇİ* Taner ÜNLÜ, and İ. Sönmez SAYILI*

ABSTRACT.- In this study, the geological aspects of Otlukilise iron deposit near Gürün (Sivas, Turkey) is investigated and possible mechanicms responsible for the formation of that deposit are discussed.

Otlukilise iron occurrences are located in volcanosedimentary levels in Yanıktepe and Akdere formations which are age of Upper Cretaceous and Paleocene, respectively.

The occurrence of Otlukilise iron formations is belived to have taken place as enrichments by secondary processes from siderite ores volcanosedimentary origin in relation with volcanic intercalations. Studies carried out on iron rich massive ores indicate an old formation in a sedimentary basin that represented by cumulative supplements of iron and associated elements which are directly on indirectly leached from serpentinites by submarine volcanites spreading out into an environment of carbonate deposition and hydrothermal exhalative fluxes and associated silicate phases formed by intensive silica rich fluids of hydrothermal origin and sulphide phases resulted from reactions of seewater and the same submarine volcanites.

Sequential conjugateness observed especially among quartz and siderite, clay and/or clay bearing siderite layers in iron poor conglomerate breccia ore samples and estimations realized by certain mathematical rules indicate a sedimentary relationship prior to deformation. Both massive ores and fragments are deposited by the processes during formation of an ore horizon intercalated by clay and quartz rich levels and/or just after the movements at the bottom of the basin. Thus, Otlukilise iron deposits represent an other sample of Lahn-Dill type syn-sedimentary volcanogenic or exhalative-sedimentary type ore formation as Deveci Iron Deposits (Hekimhan-Malatya, Turkey) do.

INTRODUCTION

Otlukilise iron deposit located near Gökçeyazı village of Konakpınar country of Gürün town of Sivas, which takes place in Elbistan K38 b4 sheet, will be evaluated in this study.

Lithological units of the studied area and its vicinity belong to Geyikdağ unit (Özgül, 1976) in Eastern Tauride Platform consisting of sedimentary rocks of Gürün autoctone and young sediments and volcanites of Pliocene - Quaternary age (Atabey, 1993 *b)*.

The main regional geological studies are carried out by Akkuş, 1971, Kurtman, 1978; Aziz et al. 1981; Özer et al. 1984; Alkan and Turkmen, 1987; Kozlu et al. 1990 and Atabey, 1993 a, b, c. Stratigraphic correlation columns, created by the studies of various authors in the investigated area is illustrated in Fig. 1. The names of the formations are different according to different authors. Çiftçi, (1994) is referred to more detailed information.

Mining geological studies are carried out since 1960 at Otlukilise Iron Deposit and its surrounding. In all these studies, it has been announced that the deposits and mineralizations are located at the cracks and open spaces of limestones but the genesis of ore has not been well established (Gülibrahimoğlu, 1979).

Although no available data is present for the genetical interpretations in the given studies, due to relationship of mineralizations in the region, all authors has come to the consequence of a metasomatic type of formation. However, discussions of various opinions have raised different syntheses about the sources of ore - bearing rock. Some authors suppose submarine volcanics as host rocks of ores (Gümüş, 1962, 1964), while others advocate epigenetic character of ore formation occurred by the effect between plutonic rocks and the same volcanites which include ore solutions and limestones (Kormalı, 1972). Other authors suppose that iron is derived from leaching of iron bearing sedimentary rocks (Barosh, 1971).

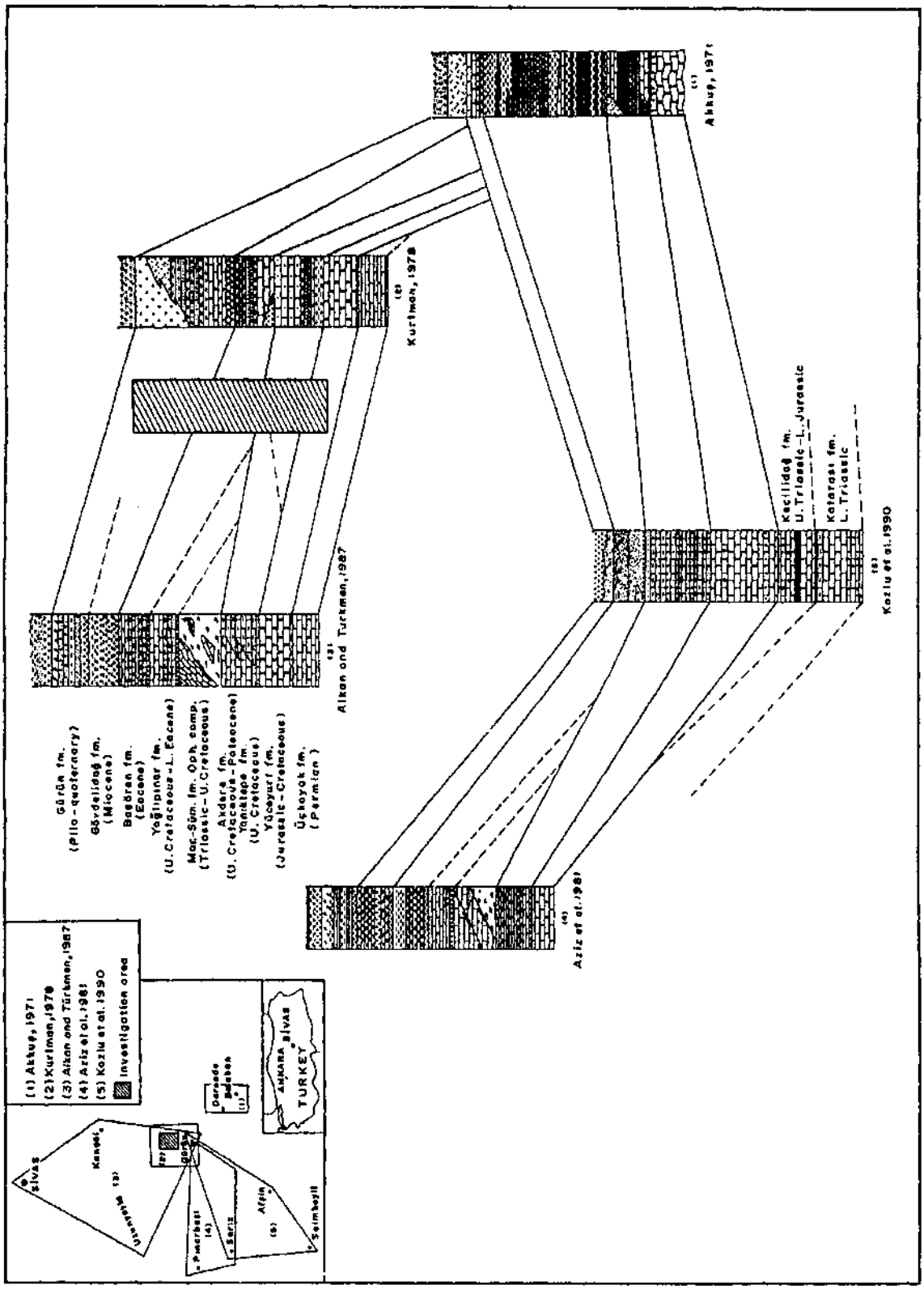

Fig. 1- Nonscaled stratigraphic sequences (investigated area is shown by striped lines). Ophiolitic overlying at NE-Se direction and unconformity between Yüceyurt and Akdere formations out of Gürün vicinity (Kurtman, 1978) is supported by these correlations.

Epigenesis or syngenesis of Otlukilise Iron Deposit creates the focus of genetical discussions of the mineralizations. This study aims to bring a new aspect for genetical discussions by means of mineralogical, petrographical and geochemical studies carried out mainly on massive and conglomeratic - breccious ore samples.

GEOLOGY OF STUDY AREA

Units cropping out in the studied area and its vicinity are represented by Yüceyurt formation, Yanıktepe formation, Akdere formation, Başören formation, Gövdelidağ formation, Gürün formation and young volcanites from older to younger, respectively (Fig. 2).

200 hand specimens collected from the lithologies of above mentioned formations are mineralogically and petrographically investigated. The details of these studies are presented below.

Yüceyurt Formation (Jky)

This formation consists of completely recrystallized and spatially dolomitized limestones while they are platy at the bottom becoming more and more massive to the top and at the uppermost part fossil shells bearing highly fractured and brecciated. Two types of limestones with micritic and sparitic matrix are recognized.

Micritic limestones consist of fine grained, equigranular calcites and some dolomite crystals in addition to recrystallized fossil shells, cherts and rarely opaque minerals. Larger calcites and iron oxide and hydroxide stainings are observed at the calcites. All of these data suppose that carbonates are transported in the some basin and are cemented partly by own components and partly by the material into which they are transported.

Sparry limestones are sligthly rounded and generally formed by angular micritic and sparry limestones fragments which are cemented by sparry matrix. Calcite fragments are associated by some dolomites and rarely chalcedony and opaque minerals. Two different deformation have been determined at the fragments of rocks. First deformation is caused brecciation and the second one another brecciation and penetration of ironoxide and hydroxide bearing fluids into the fractures and cracks of others.

Basing on the paleontological studies carried out on the collected samples from the investigated area (Çiftçi, 1994), the age of Yüceyurt formation is determined as early Upper Cretaceous (Coniacian - Santonian). Depending on the previous studies (Aziz and Erakman, 1980; Aziz et al. 1981; Alkan and Turkmen, 1987; Kozlu et al. 1990), the age of formation is Jurassic-Cretaceous.

Although the bottom of Yüceyurt formation can not be observed in the studied area, this formation uncomformably overlies the limestones of the formations of Keçilidağ (Kozlu et al. 1990) of Upper Triassic - Lower Jurassic age at the east of Saimbeyli, Katarası (Aziz et al. 1981) of lower Triassic age at the east of the Tufanbeyli and Üçoyak (Kurtman, 1978; Alkan and Türkmen, 1987) of Permian age at the nortwest of Gürün. Yüceyurt formation is uncomformably overlained by Yanıktepe formation which can be clearly seen at the investigated area.

Jurassic - Cretaceous limestones with similar characteristic are named as Köroğlu Tepe formation due to previous studies (Demirtaşlı, 1967; Metin, 1982; Metin et al. 1987; Alkan and Turkmen, 1987). But above mentioned formation does not crop out typically at the region of Köroğlu Tepe. Afterwards, Yüceyurt Tepe and its vicinity located norteast of Sarız, is accepted as typical location and so mentioned formation name has been changed as Yüceyurt formation (Kozlu et al. 1990).

Yanıktepe Formation (Ky)

Yanıktepe formation begins with rudist bearing limestones and continuies with shale, marl and sandstone alternations.

Volcanic rock fragments are also abundant in the alternating rocks of this formation.

Rudist bearing limestones appear to be as conglomerates and consist of spatially dolomitized limestone fragments of sparrite and micrite character, fina grained quartz and chert particles, fossil

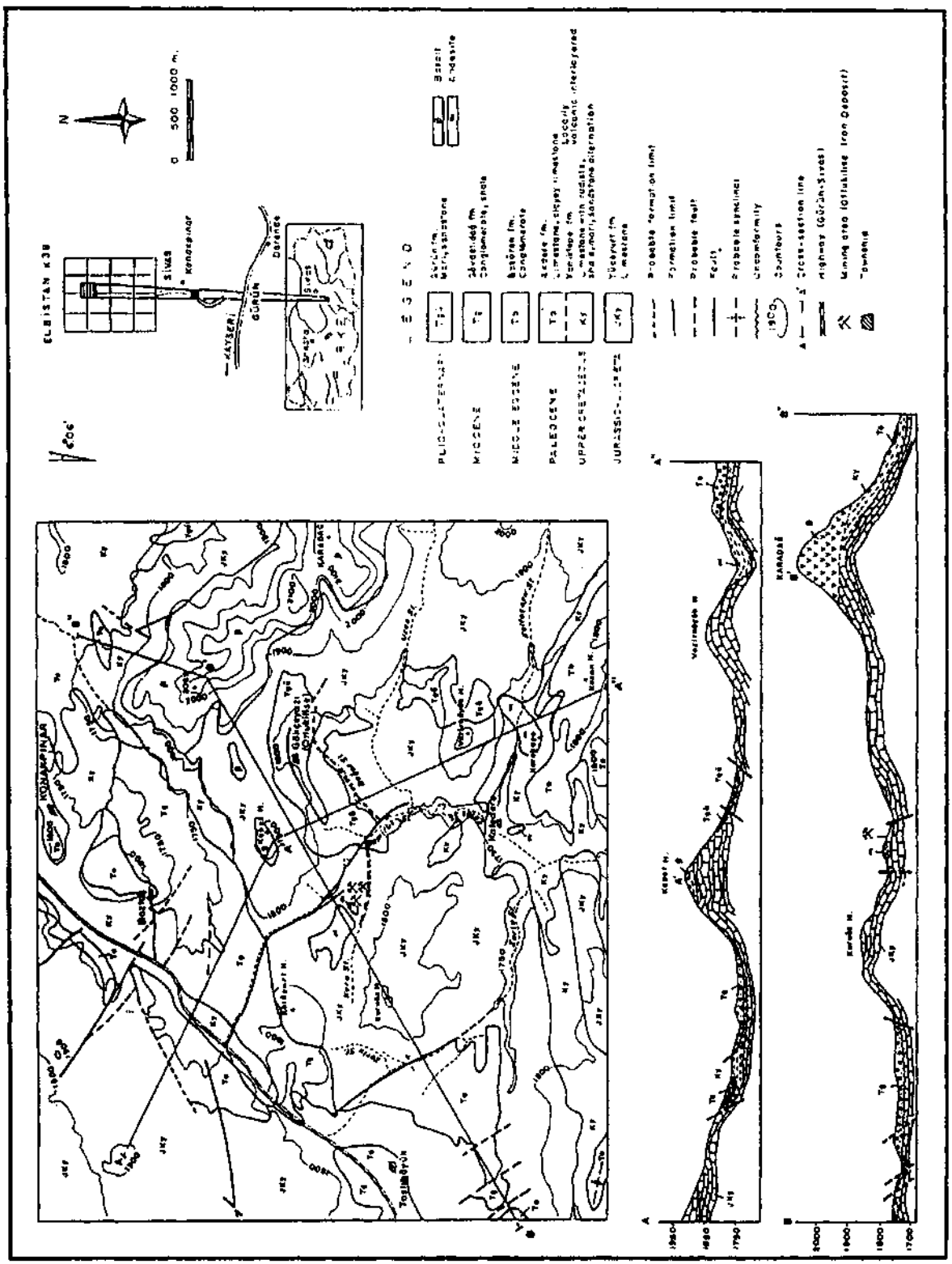

Figure 2- Geological map of Otlukilise iron deposit and its surrounding (compiled after Çiftçi, 1994).

fragments (algs and rudist shells) and micritic and sparritic cemented some volcanic rock fragments. Strongly deformed parts of these limestones grained breccia character. Secondary calcite fillings, siderite occurrences and dolomitized parts and stainings by ironoxide and hydroxides are observed at the cracks and fractures.

The sizes of volcanic rock fragments reach up to 1.5 mm and above. Fragments are usually rounded though some angular. Recognizable minerals which are plagioclase laths and altered mafic minerals which are partially replaced by opaque minerals (Plate 1, Figure 1). In addition, some serpentinite type rock fragments are also observed in some samples. Chromite particles exhibit locally streched an torn apart structures.

Sandstones of shale, marl, sandstone alternations include micritic and sparitic rock fragments, intensively packed fossil shell fragments, chalcedony, quartize, opaque minerals and abundant volcanic rock fragments. On the other hand, volcanic rock fragments consist of quartz, some chert and opaque minerals.

Based on planctonic studies carried out on shales and marls (Çiftçi, 1994) and fossil findings, the age of Yanıktepe formation, representing a shallow marine character, is Late Cretaceous (Campanian - Maastrichtian).

Yanıktepe formation overlies unconformably Yüceyurt formation and is conformably overlained by Akdere formation in the studied area.

Yanıktepe formation is originally named after Özgül et al. (1973) at south of Gürün out of investigated area where its thickness up to 300 m, and aged as Upper Cretaceous by same authors.

Akdere Formation

Gray, light gray, cream and spatially yellowish, reddish colored limestones with are amount of volcanic rock fragments, marly limestones and breccious limestones form the rock of Akdere formation, which is observed in some localities of the studied area.

Limestones and marly limestones consist of especially micritic rock fragments which grade into coarser grains by recrystallization. These rock include small amount of dolomite, fossil shells and fragments, quartz, chalcedony and rarely volcanic rock particles.

Coarse grained, angular rock fragments scattered within a fine grained micritic carbonate matrix are observed in the samples of breccious apperance. Secondary calcites and locally dolomit and siderite and stainings of ironoxide and hydroxide are the main components in the cracks and fractures. In addition, rounded and locally coarser volcanic rock fragments are abundant in the investigated samples (Plate I; Fig. 2). Plagioclase laths, mafic minerals replaced by opaque minerals, spatially chloritizations and carbonatizations are the main characteristics of volcanic rock fragments.

According to the fossil findings (Çiftçi, 1994), the age of Akdere formation is supposed to be younger than Maastrichtian.

Lower contact of Akdere formation is transitional to by Yanıktepe, but upper contact shows unconformatable relations to Başören formation of Mid Eocene age and Gövdelidağ formation of Miocene age.

Outside of the investigated area, around Sarız, the age of the succession reach up to Early Eocene represented by calcarenite, brecciated limestone, marly limestone and locally micritic limestone lying over rudist bearing limestones of Mesozoic carbonate platform (Kozlu et al. 1990). Sequence of deep basin sediments with the thickness of 100 m. (Atabey, 1993a, 1993b), cropping out related with rudist bearing limestones in the region and studied area is called as Akdere Formation (Aziz et al. 1981).

Başören Formation (Tb)

Sequence commencing with red cream colored, rounded basal conglomerate in the study area continuies up to upper levels of the sequence with light gray colored shale, marl, marly limestones and limestone with abundant nummulites at the outside of investigated area.

Conglomerates are formed by micritic and sparitic rock fragments, dolomitic and at the same time ironoxide stained rock fragments, quartz, chalcedony and volcanic rock fragments which all are cemented by generally sparitic and locally, micritic material. These conglomerates also include rock fragments of Yüceyurt, Yanıktepe and Akdere formations.

The age of this formation is supposed to be Mid Eocene (Upper Lutetian) due to previous studies (Aziz et al. 1981; Alkan and Türkmen, 1987). The name of the formation comes from Başören village (Azizetal. 1981).

Başören formation overlies unconformably Akdere formation and is again unconformably overlained by Gürün formation.

Gövdelidağ Formation (Tg)

The formation commences by conglomerates at the bottom and continuies with sandstone and marl alternations which exhibit lateral transitions with conglomerates to the top. Clay rich levels increase in conglomerates so they gradually amount of the rock fragments of ophiolites. Lithologies of this formation have limestones, cherts and small amount of the rock fragments of ophiolites. Lithologies of this formation have light yellow, greenish yellow and reddish colors and very soft character and are rich in clay. Gövdelidağ formation exhibits lateral and vertical fades changes with repetition short intervals.

The matrix of coglomerates are in sparitic and their gravels consist of iron rich ring like textured carbonates, fossils shells and particles in which sparries are penetrated, locally brecciated, micritic and sparitic carbonate particles and fein grained quartz, chert and very small amount of volcanic rock fragments.

Because matrix of any accurate fossil findings could not been found in the investigated lithologies, no age could be evaluated for Gövdelidağ formation. Only conclusion for it is that its deposition indicate a very shallow marinal with high energy or continental environment. The age of formation is Miocene due to Aziz et al. (1981) which is an accepted age in this study or Upper Miocene according to Alkan and Turkmen, (1987).

Gövdelidağ formation overlies unconformably Yücetepe, Yanıktepe and Akdere formations.

Gürün Formation (Tgü)

Light yellow, greenish yellow colored thin layered fresh water limestone, shale, marl and locally tuffs levels of this formation crop out outside of the study area, while it is represented by marl-sandstone alternation in the investigated area. Rock fragments of older lithologies are observed in sandstones.

No paleontological data has been found in Gürün formation. Due to the stratigraphic level and using the data previous authors (Kurtman, 1978; Alkan and Türkmen, 1987) the age has been accepted Plio - Quaternary.

This formation cover unconformably Yüceyurt and Yanıktepe formations in the studied area.

The name of the formation is given after the vicinity of Gürün by Kurtman, (1978), where it is most clearly and widespread observed.

Volcanites

Volcanites of the studied area represented by Karakaya andesites and Karadağ basalts.

Karakaya andesites (a)

The andesites are grayish white colored and fractured.

Phenocrystals of andesites consist of coarse grains of plagioclase and greenish brown amphiboles and locally partly martitized magnetites, ilmenomagnetites and limenites. These minerals are surrounded by a matrix of fine grained plagioclase and amphibole microlits opaque minerals and volcanic glass. This matrix is partly kaolinized and stained by iron oxides and hydroxides. Hyalopilitic texture is very clear in the rocks.

Besides andesites, often agglomerates, tuffs and volcanic breccia are the other rock types. With increasing amount of volcanic glass, tuffs are

evolved from andesites. Andesites and tuffs gain an apperance of breccia where strongly fractured. These fragments are healed by ironoxide and hydroxide fillings.

The age of volcanites, depending upon filed relations and previous studies (Kurtman, 1978; Alkan and Türkmen, 1987) is supposed to be Pliocene.

Karadağ Basalt (B)

The basalts are brown, gray and black colored and furnished by cracks.

Phenocrystals of basalts consist of labradoriteite type of the plagioclase, pyroxenes with euhedral to subhedral crystalls which are amphibolized and partly replaced by opaque minerals, iddignsitized olivines and thin long ilmenite crystals. Matrix is mostly made up of plagioclase microlites, besides volcanic glass. Flow, hyalopilitic and pilotaxitic texture are clearly observed in basalts.

BASIN EVOLUTION MODEL

Basing on the lithologies presented above, the following basin evolution model can be suggested (Fig. 3).

First depositions, opened over the basement, Yüceyurt formation (I) consist of shale, marl, sandstone alternation (II). This sequence associated with marinal and continental (?) volcanic activity is called as Yanıktepe formation. Pelagic sediments of Akdere formation (III) indicating the sinking of the basin, include volcanic intercalations. This sequence of transgressive character, described in II. And III. Stages, evolved to a presumably subaerial environment at Lower Eocene changing later marinal environment and so the sediments of Başören formation deposited (IV). It is assumed that folding and fracture dynamic probably prevailed at subaerial environment stage. Gövdelidağ formation of aerial character unconformably overlies the previous units and Gürün formation again unconformably covers the underlying units.

MINING GEOLOGY

The access to the Otlukilise iron Deposit is by means of mine road of 3.5 km long seperated to east from the 25 km of Gürün - Sivas main road.

Otlukilise iron Deposit located in the study area has been mined with concession number of 55/334 by Demir Export Ltd. company since 1961. Five occurrences in concession area and one outside are located in the region (Fig. 4). Except occurrence Nr. 2 called a main ore deposit (Otlukilise iron Deposit), Taşlıhöyük Occurrence (Nr. 5) with economic resource, operated earlier and currently abandoned.

Two types mineralization occur at Otlukilise iron deposit. First type is represented by massive ore which consist of mainly hematite and some goethite. Extention of this type is limited by limestones at east, west and south, and by conglomeratic breccia ore at north. Second type is formed by low grade conglomeratic breccia ores comprised from ore fragments of predominantly hematite components, sand or coarse sized geothite fragments, iron bearing sandstone fragments, ophiolitic rock fragments, siderite gravels, detritic grains in clay size. This type of one in the field is surrounded by limestones at east and west. Ore deposit cut by NE-SW trending faults and ore is also controlled by these faults. Evidences are abundant about the development of faults during and/or after mineralization. Faults mentioned above caused for ores to crop out.

Because of mineable feature and similarities with probable other occurrences, Otlukilise iron deposit will be investigated detail and the results obtained from this deposit will eventually help for evaluation of other occurrences.

PETROGRAPHY OF DRILL - CORE SAMPLES

200 core samples, compiled systematically from five drills at Otlukilise iron Deposit opened during 1977 - 1978 period by MTA General Directorate have been petrographically investigated. They show that there are different between the first 70 metres and the rest of the drill.

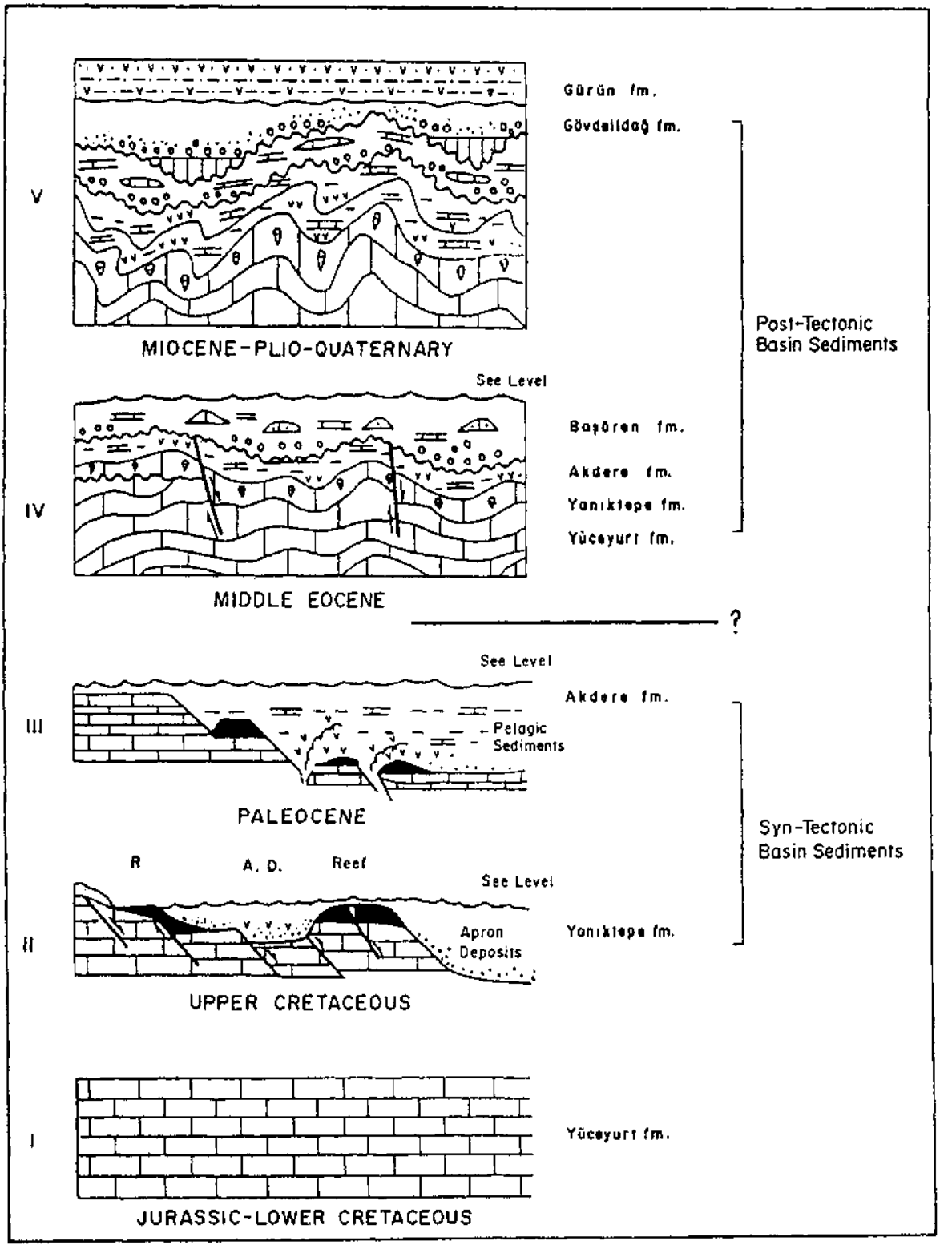

Figure 3- Generalized basin evolution model of the investigated area.

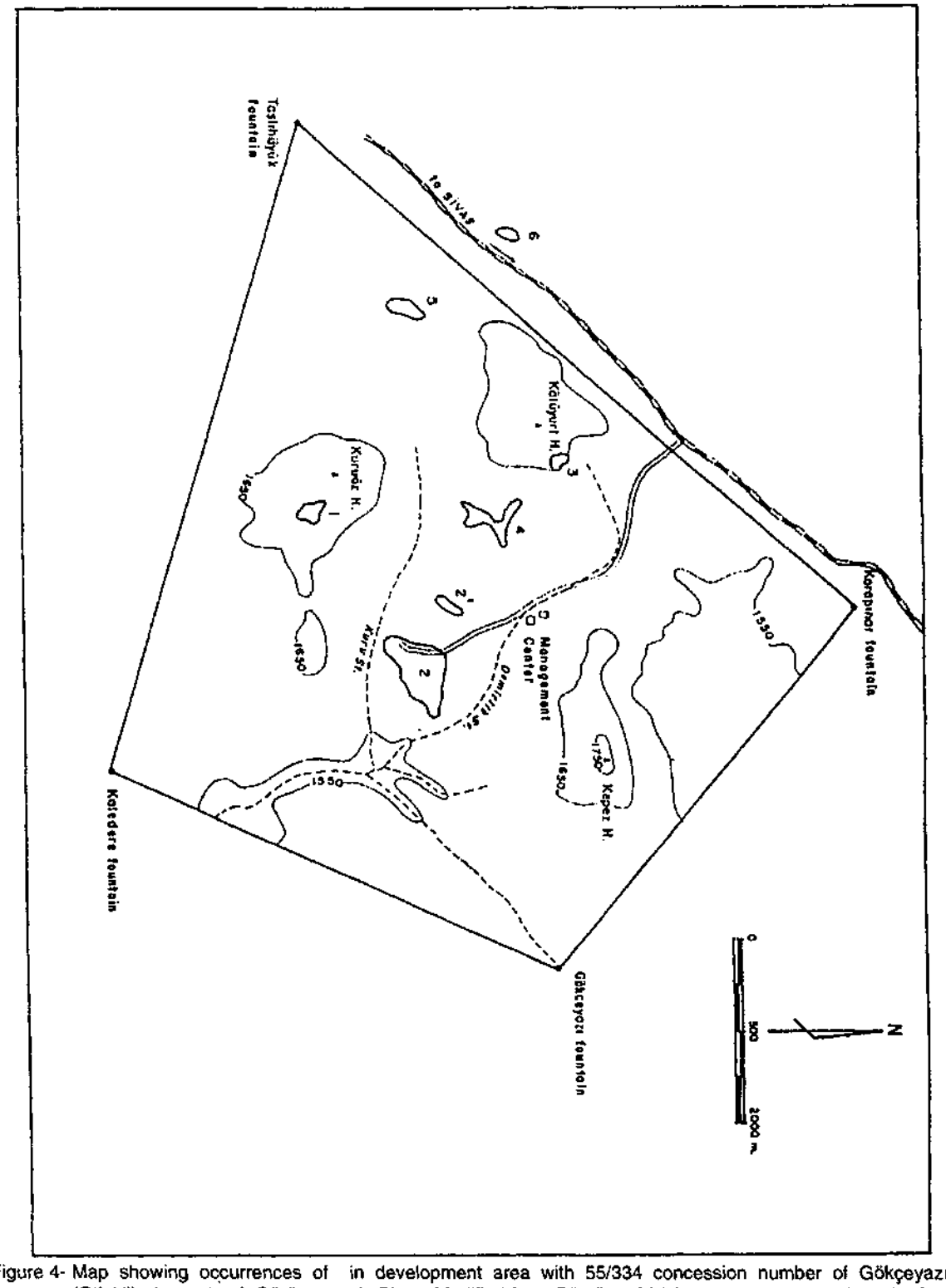

Figure 4- Map showing occurrences of in development area with 55/334 concession number of Gökçeyazı (Otlukilise) county of Gürün town is Sivas. Modified from Gümüş, 1964 (occurrence are numbered 1,2,... 6 and occurrence number 2 indicate "Main Deposit".

Section of volcanic rocks

Andesites, andesitic tuffs and pyroclastic and locally thin carbonate fragments cemented by ironoxides are observed at the core samples from surface to 70 metres. Light yellowish rocks, stained by ironoxides and hydroxides are cemented toughly.

Sizes of rock fragments reach up to 2 cm. Rounded locally angular grains are surrounded by ironoxides and hydroxides. Plagioclases with magnetite inclusions, brown hornblende and trace amount of opaque minerals form phenocrystals of volcanic rock fragments. Matrix consist of volcanic glass in which some plagioclase microlites and fine grained magnetites occur. Angular carbonate rock fragments are also found this section.

Section of ore

Ore rich zone with conglomeratic - breccious appearence commence from 70 metres onwards. Red, localy green colored rock fragments are cemented by reddish clays in hand specimens. Magnetism is emphasized at greenish samples.

Polygenic rock fragments are cemented by limonite - goethite, clay and siderite according to petrographical investigations of compiled core samples. Features of rock fragments and matrix are presented below.

Sandstone fragments: Three kinds of quartz bearing sandstone are determined in the samples. First type contains rounded, locally angular quartz, chlorite, plagioclase, opaque minerals and trace amounts zirkon and turmaline. Small amount of chlorite as matrix can be observed in these grain supported sandstones. Opaque minerals fills cracks and fractures. Lineation of blurred character is sometimes seen at rock fragments.

Second type rounded, locally angular sandstone fragment consist of quartz opaque minerals, chloritized plagioclase and again trace amounts of zirkon and turmaline. These constituents are cemented by chlorite and clay. The most important features of this type which distinguish it from the others are intensive clay matrix and no lineation at the grains. In addition, various grain sized siderites in matrix and as fracture fillings in semirounded sandstones are observed (Plate I, Fig. 3).

On the other hand, third type sandstones are "cemented by very fine grained quartzs and ironoxide and hydroxides (Plate I; Fig. 4). Distinguishing feature at this type sandstones is intergrown textures of iron minerals and quartzs.

Metamorphic rock fragments: Transported and locally rounded various rock fragments such as slate and phyllites which are effected from low grade metamorphism contain very good schistosity and elongation along one axeis. The schistosity of the rock formed from these metamorphic rock fragments which are made up of fine grained quartz, chlorite, muscovite, graphite, coal like material and filled cracks and fractures and locally at matrix by siderite is weak.

Basic rock fragments: Basic rock fragments totally chloritized, silicified and kaolinized hornblend and biotite phenocrystals of angular rounded basic rocks are intensively altered. Rock fragments are rich in opaque minerals. Due to original rock textures, these rocks are considered as spitilized basalts and/or diabases (Plate I; Fig. 5).

Siderite Fragments: Grain sizes of siderite particles vary between very fine grained and up to 2.5 mm. Fine and medium grained siderites are euhedral to subhedral and contain opaque mineral inclusions. This appearance look like graphic texture (Plate I; Fig. 6). Colloform textured siderites are observed at the cracks and open spaces associated with quartz, chalcedony and locally euhedral zoned dolomites.

Fragments rich in opaque minerals: Local network like openspaces, observed in generally angular and rarely rounded opaque rich rock fragments, are filled by chlorite, quartz and siderite. Furthermore, euhedral to subhedral opaque minerals together with siderites do also exist.

Three types of matrix are seen from surface to deeper parts of ore dominant sections.

Ironoxide - hydroxide matrix: Quartz bearing sandstone of conglomerate apperance, slate, phylltes, basic volcanic rock fragments rich in siderite and opaque minerals and locally individual

minerals are cemented by limonite and goethite. This rock is again fractured and cemented again as angular rounded particles.

Green colored clay matrix: Mixed with ironoxide and hydroxide clay cement fillings of various kinds of rock fragments is colored to red. In addition, opaque minerals bearing clay cement occur in openspaces of quartzs in sandstones.

Siderite matrix: Fine to medium grained siderite cement among rock fragments and network like siderite veinlets again in cracks and fractures on the same are observed. Such particles are transported and cemented again by siderite.

In drill cores, green clay matrix gradually vertically and laterally pass to limonitized siderite rich matrix.

ORE MINERALOGY

36 polished section are prepared from surface, open pit and drill core samples of Otlukilise iron deposit and investigated by ore microscope. Gangue minerals are determined by means of polarizan microscope.

Surface samples: Some of the samples from Yanıktepe formation contain sandstone with quartz, carbonate and locally volcanic and metamorphic rock fragments. The features of these components are presented below.

Basic rock fragments: Subhedral to euhedral, fein grained cataclastic chromite crystalls are observed in silicified and carbonatized rock fragment with indications of ophitic texture. In addition, rutile, leucoxene, apatite, grains up to 280 micron and pyrite and hematite much smaller than those are found in these rock fragments.

Graphite bearing schist fragments: Transported graphite bearing schist fragments contain graphite, coal particles and locally rutile grains generally in accordance with schistosity.

Quartz fragments: Angular, locally euhedrat quartz up to 4 mm include transported hornblend grains.

All of above mentioned rock fragments are cemented by calcite and/or dolomite and sometimes by siderite.

The features of chromite and magnetite observed in highly serpentinized, silicified and carbonatized and locally aspestos bearing ultramafic rock fragments of Yanıktepe formation are as follows:

Euhedral to subhedral cataclastic chromites are replaced by chromspinell and magnetite at their edges and fractures (Plate II, Figure 1).

Magnetites reveal three types of formation. These are respectively; replacement production of chromites from it edges, skeletal shaped magnetites at the serpantinization and magnetites of euhedral shaped and in veinlets occurred hydrothermal emanations. All of these magnetites locally and sometimes completely replaced by hematite as result of martitization process.

Furthermore, small amount of heazlewoodite, millerite, pyrite, chalcopyrite are located in serpantinized, silicified and carbonatized ultramafic rock samples.

Open Pit Samples

Ore samples collected from open pit area are characterized by siderite, goethite, magnetite, quart, calcite, and/or dolomite, gypsum (?) and small amount of pyrolusite and psilomelane.

Siderite vary from generally anhedral fine grained to rarely subhedral medium grained crystalls at siderite dominat samples. Geothite replacements can be observed at fine grained, clamped siderites (Plate II; Figure 2). In addition, subhedral to euheral hydrothermal quartz and locally zoned magnetites replaced by siderites occur together with siderites.

These samples revealing party transportation features and conglomeratic apperance are cemented by calcite and/or dolomite, siderite, chalcedony and small amount of gypsum.

Drill Core Samples

Following rock fragments are observed in drill core samples:

Altered basic rock fragments: Highly chloritized, silicified and kaolinized basic rock fragments (Plate II; Fig. 3) contain chromite, siderite, magnetite, hematite and pyrite. Subhedral, fine to medium grained chromites are observed both within the basic rocks and at the matrix among basic rock fragments. Magnetites are generally fine grained, sub- to euhedral and partly replaced by hematite as result of martitization. Furthermore, lath like hematite occurrences of primary origin can also be seen.

Siderite fragments: Siderite fragments show anhedral very fine grained to euhedral fine grained features and concentric, zoned growth textures, in which magnetite, hematite, arsenopyrite, pyrite, chalcopyrite, fahlore (tetraedrite-tennantite) and enargite occur. Chalcopyrites are replaced by chalcosine an covellite, siderites by goethite, enargite and fahlores by Sb-As ochers. Five different type of magnetite formation are distinguished at siderites. First type is euhedral to subhedral, partly replaced by siderite and locally or totaly hematitized by martization (Plate II, Fig. 4-5). Second type magnetite reveals myrmekite like textures in siderites (Plate III; Fig. 1-2). Forth type magnetites are associated by lath like musketofite occurrences. Finally, the last one exhibit intergrown textures together with siderites (Plate III; Fig. 3). Arsenopyrites are fine- to medium grained, euhedral to subhedral and form twinnings of two and/or multiple inviduals. Melnikovite pyrites (Plate III, Fig. 4) and hematites are also observed as intergrown products with siderites. Fine grained siderites are replaced by goethite beginning from their edges. Small amount of chalcopyrite, covellite and goethite occur in siderite fragments.

Rock fragments: These are characterized by shale and sandstones. These rocks reveal well developed schistosity and consist of graphite, coal particles, hematite, siderite veinlets and pyrite framboides or pyrite bacteria stained by iron oxide and hydroxides. Rounded and partly grown together with hematite.

Concentric chamosite particles (?) and chalcedoy grown with siderite are also observed.

Two kinds of matrix cenient all rock particles. One is very fine grained matrix colored by ironoxide and hydroxides. These colored matrix composed of day minerals and different mineral (Plate III; Fig. 5-6) and rock fragments fill the open spaces between the coarse rock fragments of conglomerates. Second matrix is made up of fine grained siderite. All of these rock fragments are fractured by secondary processes and are cemented by calcite, dolomite, siderite and gypsum (?).

GEOCHEMISTRY

Sampling and Analytical Method

Mainly iron rich massive ore samples were compiled by second author of this paper from the operating time of mine of Otlukilise iron deposit in previous years. 13 samples are selected from these ores and detailed chemical analyses were carried out at Copenhagen University. Statistical data about these samples are presented by Ünlü and Stendal (1986). Because of expansiveness of such kind of chemical analyses, accuracy and to avoid from repetitation, the above mention data source will be used and so detailed interpretations and evaluations will be made.

Ten major and thirtyone trace element analyses had been conducted on 13 samples. W, B, Be, Mo, Li, Ag, As, Sb, Bi, Sn analyses were realized by Emmission Spectral Analyses (ESA) method. All other element analyses except Na and Mg been made by X-Ray Flourescence method.

Glass discette prepared by solvent of sodiumtetraborate were for major element analyses. Loss on ignition had been calculated by loss of other elements. Na and Mg analyses had been carried out by Atomic Absorbtion Spectrofotometer Analysis (AAS).

Trace element analyses have been conducted by X-Ray Flourescence method on powder pellets at PW 1400 Philips instrument using Norrish And Chappel (1977) technique. Interference of tube and sample spectral lines and major element per-

centages for matrix changes were used for some corrections on results. USGS standarts (G-2, GSP-1, AGV-1, W-1, BCR-1, PCC-1) were used for corrections (Gladney et al. 1983).

Results of Chemical Analyses

Chemical analyses of some samples collected from Otlukilise iron deposit are presented at Table 1. Maximum and minimum values, standart deviations and means for all samples will here only be referred since they are previously given by Ünlü and Stendal (1986).

40-90% Fe_2O_3, 1-35% SiO_2, up to 10% Al_2O_3 and up to 2.5% K_2O contents of massive ore samples of Otlukilise iron deposit indicate an iron-claystone formation at first galance. Reaching up to 3% MnO values derive from similar physicochemical behavior of Fe and Mn, MgO and CaO contents varying around 1% point out a small percentage of carbonate phase. Other associated oxides of ore are characterized by less than 5% Na_2O, TiO_2 and P_2O_5. Trend of major element values indicate an iron environment characterized by the dominance of carbonate, quartz and clay minerals (possibly clayey carbonate). The mean less than 10% varying within the limits of 5-20% of loss on ignition reflects that the recent character of ore is represented by oxide phase rather than carbonate phase.

Trace element values of Ba vary between 200-1800 ppm, Co, Cu and Zn between 2 -1225 ppm, Ni between 2 -50 ppm, S, Cl and As between 10 - 7000 ppm and all of these values suppose hydrothermal solutions. On the contrary, Pb contents are very low changing within 1 - 20 ppm values.

Ga contents vary between 20 - 30 ppm and Cr between 150 - 250 ppm which emphasize the role of ultramafic and mafic roks at ore formation. V values are relatively low varying from 10 to 125 ppm.

Rb, Zr, Sr with approximately 250 ppm, Ce with 150 ppm and La, Nd, Y, Nb, Sc with 50 ppm values probably indicate granitic effects on ore formation system. On the other hand, Th contents are less than 1%.

All of these geochemical values point out that a formation processed at a carbonate associated with clays deposition environment and ultramafic - mafic rocks are affected by hydrothermal solutions. Effects of granitic rocks to the system can also be slightly recognizable.

Geostatistics

Although sample number is relatively low, cluster and factor analyses are tired on linear regressions among elements pairs of 30 elements chemically analysed from 13 samples.

Correlation coefficients are determined on "In" base of element contents using computer programs. On the other hand, computer programs are not used to realize cluster and factor analyses. Results are obtained by trial and error method (Table 2). 435 correlation coefficients are grouped statistically and element associations are created taking into consideration of possive and negative relationships (for more detailed information see Çiftçi, 1994).

Three groups are determined with very high positive correlations ($r > + 0.85$) (Table 2). First group is represented by Fe, Zn, Cr and Co elements. In this element association, four element behave positively to each other. Second group can be classified into three subgroups namely a, b and c. Subgroup a consist of Ni, Cu, Cl and S, b of K, Al, Si, Na, and ti and c of Zr, Rb, Nd, ce, y, Nb and Sc. The elements of subgroup exhibit positive relationship to each other. When considering the statistical behaviors of these three subgroups, they also show relatively positive relationship. Because of only the relationship of subgroup c to other subgroups are relatively questionable the values at Table 2 are written in parenthesis. The group include P and V elements, therefore it is a relatively small group.

Two groups with high positive correlation coefficients ($+0.85 > r > +0.70$) are clearly to be seen in Table -2, First group is represented by Fe, Zn, Cr, Co and Mn elements. The only difference from the first group of very high positive correlation is presence of Mn. On the other hand second group is characterized by four subgroups a, b, c, d. First subgroup very high positive correlation. Second

Table 1- Result of chemical analyses of Otlukilise iron deposit. Areas without results mean any analyses performed. Total iron is given Fe_2O_3.

Sample Nr.	2	4	7	9	11	14	17	20	23	26	29	31	32
Main Element (%)													
SiO_2	0.84	1.14	1.57	4.99	56.04	33.84	3.61	4.14	2.16	36.45	26.74	25.83	13.15
TiO_2	0.00	0.00	0.01	0.02	0.63	0.58	0.04	0.00	0.00	0.60	0.42	0.41	0.17
Al_2O_3	0.00	0.01	0.47	0.56	9.47	8.87	0.83	0.17	0.00	9.26	7.04	6.60	2.83
Fe_2O_3	88.09	87.13	75.43	81.53	38.51	42.46	89.56	79.71	96.66	44.86	45.26	52.04	71.98
MnO	2.73	2.49	0.87	0.91	0.03	0.04	0.13	0.87	1.56	0.03	0.19	0.06	0.20
MgO	0.62	0.57	0.75	0.52	0.70	0.75	0.64	0.44	0.70	0.82	0.88	1.13	0.93
CaO	0.26	0.24	0.44	0.05	0.31	0.40	0.07	0.04	0.30	0.33	0.91	0.62	0.59
Na_2O	0.00	0.00	0.02	0.02	0.29	0.19	0.00	0.01	0.00	0.25	0.19	0.11	0.07
K_2O	0.00	0.00	0.09	0.11	2.53	2.23	0.09	0.00	0.00	2.34	1.79	2.06	0.80
P_2O_5	0.17	0.18	0.02	0.03	0.14	0.14	0.03	0.01	0.05	0.13	0.11	0.11	0.05
Loss on Ignition	7.29	8.24	20.33	11.27	11.35	10.39	5.00	14.91	8.35	5.89	16.46	11.01	9.36
Trace Element (ppm)													
S	390	50	1190	780	6820	9820	720	490	210	3150	3730	2470	1020
Cl	30	10	340	30	950	830	170	30	10	1780	320	1890	1660
Rb	< 0.5	1.0	5.9	12.0	171.0	172.0	20.0	5.6	< 0.5	214.0	142.0	267.0	101.0
Ba	2624	2930	2645	2985	17710	16173	1904	1163	2343	6362	6515	218	981
Pb	< 1	< 1	< 1	< 1	14	14	< 1	< 1	< 1	9	7	20	< 1
Sr	36.0	26.0	8.2	31.0	182.0	141.0	11.0	10.0	49.0	64.0	71.0	21.0	13.0
La	< 1	< 1	3	8	15	14	< 1	< 1	3	16	19	16	2
Ce	< 2	< 2	11	< 2	50	68	23	< 2	12	68	41	155	57
Nd	8	6	18	15	48	46	20	13	15	32	30	18	15
Y	< 1	< 1	7.4	5.4	27.0	26.0	13.0	2.2	4.6	25.0	18.0	18.0	11.0
Th	< 1	< 1	< 1	< 1	< 1	< 1	< 1	< 1	< 1	< 1	< 1	< 1	< 1
Zr	15	16	16	28	248	265	34	15	13	218	182	158	72
Nb	3.2	3.4	2.3	3.8	14.0	13.0	3.2	3.4	2.7	14.0	10.0	12.0	7.8
Zn	190	224	365	246	3	41	129	150	367	25	53	47	265
Cu	< 2	5	54	46	966	1216	436	< 2	< 2	836	1063	1225	617
Co	386	395	348	420	100	124	490	408	408	160	174	208	324
Ni	< 2	< 2	< 2	< 2	23	32	< 2	< 2	< 2	33	27	48	7
Sc	< 1	1	3	2	15	12	6	< 1	< 1	14	9	10	7
V	47	123	19	21	82	83	26	13	17	86	71	69	40
Cr	256	259	207	231	157	154	253	225	247	176	162	164	199
Ga	30	34	25	31	19	21	23	23	21	27	22	21	24
W	<30	136	125			66		163	215		170		300
B	<10	<10	90			180		<10	<10		180		175
Be	< 5	< 5	< 5			< 5		< 5	< 5		< 5		< 5
Mo	<10	<10	<10			<10		<10	<10		<10		<10
Li	0.1	0.1	3			18		0.1	0.1		14		5
Ag	5	10	11			76		8	2		11		11
As	62	76	790			1760		76	1850		650		4000
Sb	< 1	< 1	< 1			< 1		< 1	< 1		< 1		< 1
Bi	4.2	1.3	18			9.5		1.0	2.5		9.5		35
Sn	< 0.5	< 0.5	0.5			0.7		< 0.5	< 0.5		0.6		< 0.5

subgroup b is represented by K, Al, Si, Na and Ti elements which is also the same element association of subgroup b of second of very high positive correlation. Third subgroup c also exhibit similar features like a and b to very high positive correlation and include Zn, Rb, Nd, Ce, Y, Nb, Sc and La. The difference is existance of La in this subgroup. The last subgroup d, which does notexist very high positive correlation group, consist of Ca, Mg, Sr, Ba element association. Every element of each subgroup reveals high positive correlation coefficients among each other and each subgroup also is characterized by again same type of correlation coefficients as pairs with each other. Y, Nb, Sc and La elements of second group are shown by dashes on top of them. The reason why is that their minimum and maximum values vary within very close limits that is for Y: < 1-27 ppm, for Nb: < 2.3-14 ppm, for Sc: <1-15 ppm and for La :< 1-19 ppm, which can inevitably increase the correlation coefficients and this should be carefully taken into account during interpretation. It would be better if the results of

Neutron Activation Analyses (NAA) were used instead data could give more accurate values and so better correlation coefficients. Elements of subgroup c of second group are displayed within parenthesis, because three elements are relatively weak relationships when compared with elements of other group.

Two main group occur with very high negative coefficients (r < -0.83) at Table - 2. First group are represented by Fe, Zn, Cr, Co, while second group by three subgroups (a, b and c). The subgroup a consists of Ni, Cu, Cl, S and b of K, Al, Si, Na, Ti and c of Zr, Rb, Nd Y, Nb, Sc and La. The most important point is that elements of first and second group exhibit positive correlations to each other but as a group they represent very high negative correlations. It means that while the value of an element of first group is increasing, the value of an element of second group can decrease or vice versa.

High negative correlations (-0.65 > r > -0.83) are shown at the last row of Table -2. First group of the high negative correlations differ from very high negative correlations only with the presence of Mn and Ga. Subgroup a and b consist from the same elements when compared with again very high negative correlation subgroups. Subgroup c differ from those by the addition with Ca, Mg, Sr and Ba elements subgroup d with high negative correlations appear hear with Ca, Mg, Sr and Ba elements which do not exist in subgroups of very high negative correlations. Dash lines on top of some elements and paranthesis are put because of the same reasons mentioned above.

Table 2- Element groups and associations determined from Cluster and Factor analyses.

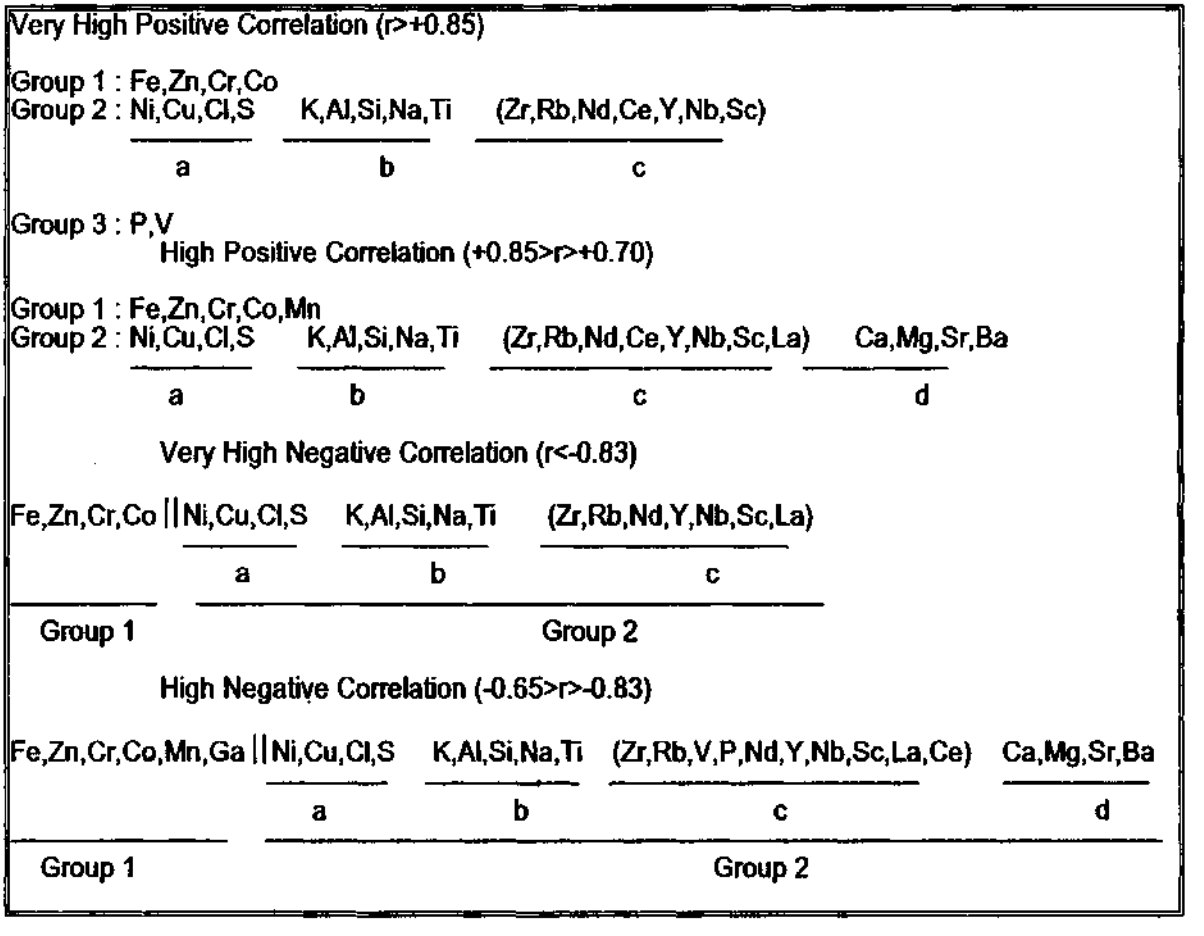

Element behaviors of each subgroups, groups and behaviors among groups are clarified by using cluster and factor analyses. Thus, element mobilities are statistically set from the geochemical point of view.

Interpretation of Geostatistical Results

Element groups and associations of Table -2 will be tried to be interpreted as follows:

Discussion of especially last associations creates the base of genetic evaluation. Group 1: Fe, Zn, Cr, Co, Mn, Ga elements (oxidic phase), Group 2: a) Ni, Cu, Cl, S (sulphidic phase), b) K, Al, Si, Na, Ti (silicate phase), c) Zr, Rb, V, P, Nd, Y, Nb, Sc, La, Ce (effects of granitic rocks(?) and d) Ca, Mg, Sr, Ba (carbonate phase) are represented by subgroups and element associations. Subgroup d that is Ca, Mg, Sr, Ba element association characterize carbonate depositions while subgroup a (Ni, Cu, Cl, S) sulphide phase resulted from the reactions between seewater and submarine volcanic rocks. On the other hand, subgroup b (K, Al, Si, Na, Ti) represents silicate phase (clay minerals and quartz). These subgroup is represented by clay constituents (clay minerals and quartz). But positive correlation relationship between the elements of this subgroup and subgroup d which consist of Ca, Mg, Sr, Ba elements, indicate same kind of mobility of these two groups. That is when carbonate phase increase, increase also the silicate phase. Geochemical studies carried out on common sedimentation environments characterized by carbonate and clayey level alternations reveal high negative correlation relationship between these constituents and while one is accumulating the other one is waiting to be deposited. As shown at Table -2, positive relationship between clay and carbonate components reveal at least that clay minerals transported to carbonate deposition environment are not deposited alternately as supposed above or silicate are derived from another soures and transported to the environment. This different source can be hydrothermal solutions associated submarine volcanism and penetraped using fractures at the bottom of the basin. These solutions following different processes and channels transported elements of silicate phase to the environment and represent positive correlation relationship between carbonate and silicate phase which are participated to carbonate environment during ore formation instead of negative correlation relationship which indicate a mathematical expression of "deposition of clay carbonate alternations is such in common deposition environments.

So, the positively related a, b and d subgroups, in other words carbonate, silicate and sulphide phases altogether characterize sulphide phase resulted from the reaction between seewater and submarine volcanites spreading out on a carbonate deposition environment and at the same time silicate formations mostly related with hydrothermal fluids associating the same volcanites. High positive correlation coefficients among these three shows this relationship extremely well.

Group 1, as earlier mentioned, forms from Fe, Zn, Cr, Co, Mn and Ga elements. This association symbolize most probably ultramafic and partly mafic rocks. The existence of iron in this group directly indicate that the source of iron of this ore deposit should be searched at this kind of rocks. However, very high negative correlation coefficients between Group 1 and Group 2 elements can be interpreted as that the source of Group 2 elements are more different that the ones Group 1. The mineral associations of Group 1 and 2 exhibit clearly sequential conjugateness. The interpretation of this statement point out an hypothesis that iron and associated elements are extracted from the country rocks by means of fluids heated by submarine volcanites and/or their porphyries (of granitic rocks ?). These fluids are transported into the deposition environment of submarine volcanism. Various iron mineral are formed due to the changes at Eh, pH and temperature factors controlled by physicochemical conditions created by basinal changes at the bottom. It should not be also ignored that the changes at unstable minerals and new stable minerals could also occur. This synthesis brings an explanation for the iron occur. This synthesis brings an explanation for the iron element source of exhalative sedimentary or synsedimentary volcanogenetic type of formation.

Geochemical interpretation represented until now, reflects a sedimentation basin in which iron and associated elements, which are leached from

serpentinites by direct or indirect effects of submarine volcanics spred on a carbonate deposition environment, are transported by hydrothermal exhalites which are associated with silicate phases of hydrothermal origin, associated sulphide phase resulted from same submarine volcanics and sea water reactions.

The most critical point at this model is that the questions of how, when and with kind of rocks are associated Zr, Rb, V, P, Nd, Y, Nb, Sc, La and Ce elements of subgroup c of second group. As mentioned above, there are some uncertanties at their interpretation because of their narrow variation limits. But some diagrams from Ünlü and Stendal (1989) are carried in order to discussion properly.

Sample number 14 at Figure 5 represents an ore sample comprised from quartz, hematite and magnetic characterizing the matrix of conglomeratic ore of Otlukilise iron deposit. On the other hand conglomeratic ore itself is represented by sample number 20 and goethite mineral. Sample number 32 is an ore sample consisted of siderite and ore sample consisted of siderite and magnetite in serpentinized ultramafic rocks around Divriği A- and B-Kafa is characterized by sample CS 1-10 and contains intensively serpentine and magnetite. Biotite-hornblend diorites of Divriği A- and B-Kafa are represented by CA-10 sample and biotite-hornblende (quartz) monzonites of Divriği A- and B-Kafa by AA-20 sample (for more information see Unlu ve Stendal, 1988).

The result from the distribution of rare earth elements Figure 5 is that goethite and magnetite with siderite bearing ores of sample 20 and 32 respectively, exhibit close similar characteristics with serpentinites of Divriği A- and B-Kafa. On the contrary, ore formed from quartz, hematite and magnetite constituents with sample number 14 is in accordance with diorites and monzonites of Divriği A- and B-Kafa region, when are element contents and distribution features are taken into consideration. Sample number 14 of Otlukilise iron deposit reveals a relationship and/or an effect from for example granitic rocks. With the careness of only. one sample used for the interpretation, it is avoided to generalize for granitic effects.

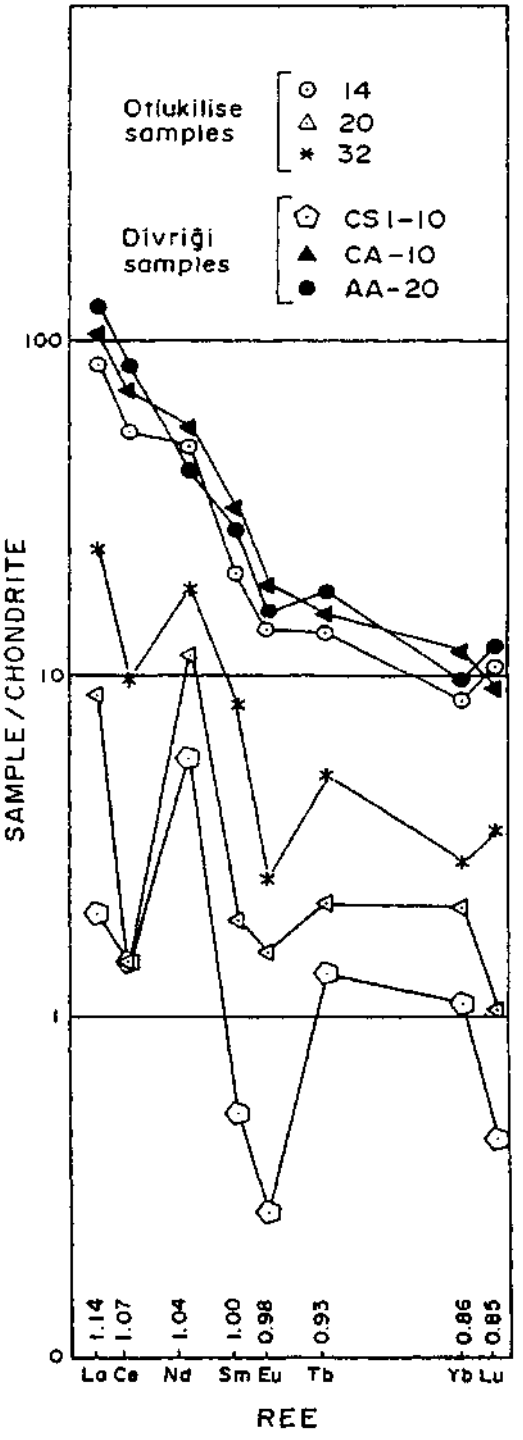

Fig. 5- Correlative REE distribution diagrammes between ore samples of Otlukilise iron deposit and the ones of Divriği A-B Kafa Iron Deposit.

Schematized model of Otlukilise iron deposit prepared from the geochemical data and basin evolution model is presented at Fig. 6. Syntectonic sediments of fault controlled basin which forms the basement under ophiolitic nappe overlying the limestones of Yüceyurt formations are rudist bearing limestone, shale, marl and sandstone alternation and limestone, clayey limestones of Yanıktepe and Akdere formations are subaerial to marine as well as submarine volcanics. Primary iron deposit exhibit concordance with contem-poraneous volcano-sedimentary sequence and is formed by metal mobilizaton created by hydrothermal convective systems of submarine volcanics.

XRD Studies

Sampling and Analytical Method

X-ray difractograms of whole rock are taken using XRD instrument and mineral associations are determined from 31 ore samples collected from O-42 drill hole (drilled by Gülibrahimoğlu, 1979) of Otlukilise iron deposit. XRD studies are carried out on samples conglomerate - breccia comprised from different rock particles which are cemented by siderite, clay, and/or clayey siderite, compiled between 80 and 290 metres, below weathering zone. These studies have been realized by Philips PW 3710 difractometer of MTA General Directorate at the conditions of 30 mA, 40 kv, 29 = 3°/dak. and 2°-70° and with Cu filter.

XRD Results

Sample numbers, depths of samples, minerals determined from difractograms and microscopic descriptions of samples are given at Çiftçi, (1994) in detail.

Determined minerals from all difragtograms are siderite, quartz, illite, magnetite, hematite and small amounts of albite, K-feldispar, amphibole, pyroxene, ankerite, baryt, sphene and opal (?). No zonal distribution of mineral associations with the depth have been found.

Percentage contents of quartz, siderite, clay, magnetite and hematite mineral constituents as major minerals are estimated from the intensities of each peak at XRD studies (Table - 3). From this table, it is clearly to see that first three samples (Z-35, 53 and 61) are quartz rich and poor in siderite, following nine samples (from Z-72 to Z-109) are generally rich in both quartz rich and siderite and fourteen samples from Z-110 to Z-131 except Z-112 without any quartz but rich in siderite (for example sample Z-131 is formed completely from siderite) and the last five samples contain partly quartz and partly siderite rich samples (from Z-132 to Z-138). It should be emphasized that a relative reverse relationship between siderite and quartz components is to take into consideration. Clay component at all samples vary between 1.12% and 40.29%. Theoritically siderite increase is paralell to clay increase but is reverse with quartz increase. Magnetite ratio vary from 2.56% to 27.99% and quartz and clay increase together. Hematite contents change between 2.05% and 13.25% and exhibit a slight parallelism with magnetite increase.

Quantitative vertical distribution graphic of 31 samples as a result of XRD studies are presented at Fig. 7. Quartz content vary between 40% and 85% from 81 to 170 metres of drill cores, siderite vary between 5% to 35% and increase with depth. Clay contents change from 2% to 9%. Hematite and magnetite reveal a parallel distribution though in various ratios. Quartz and siderite contents reflects an alternating sequence between 170 and 290 metres with approximately 90% for quartz and 100% for siderite. At least four levels for quartz and siderite repeat by clay contents of up to 40% at siderite levels. Magnetite together with hematite represented a parallel vertical distribution pattern with siderite.

Correlation coefficients of these constituent pairs are presented at Table - 4. High negative correlation relationship (r = 0.88) observed between quartz and siderite at this table is significant. A relatively high negative coefficient (r = -0.62) between quartz and clay components, a moderate negative coefficient (r = -0,45) between quartz and magnetite and a low negative coefficient (r = - 0.22) between quartz and hematite are clearly to observe. At the same table, a low positive correlation coefficient (r = 0.01) between siderite and clay, a very low (r = 0.12) between siderite and magnetite and noncorrelation (r = 0.30) between

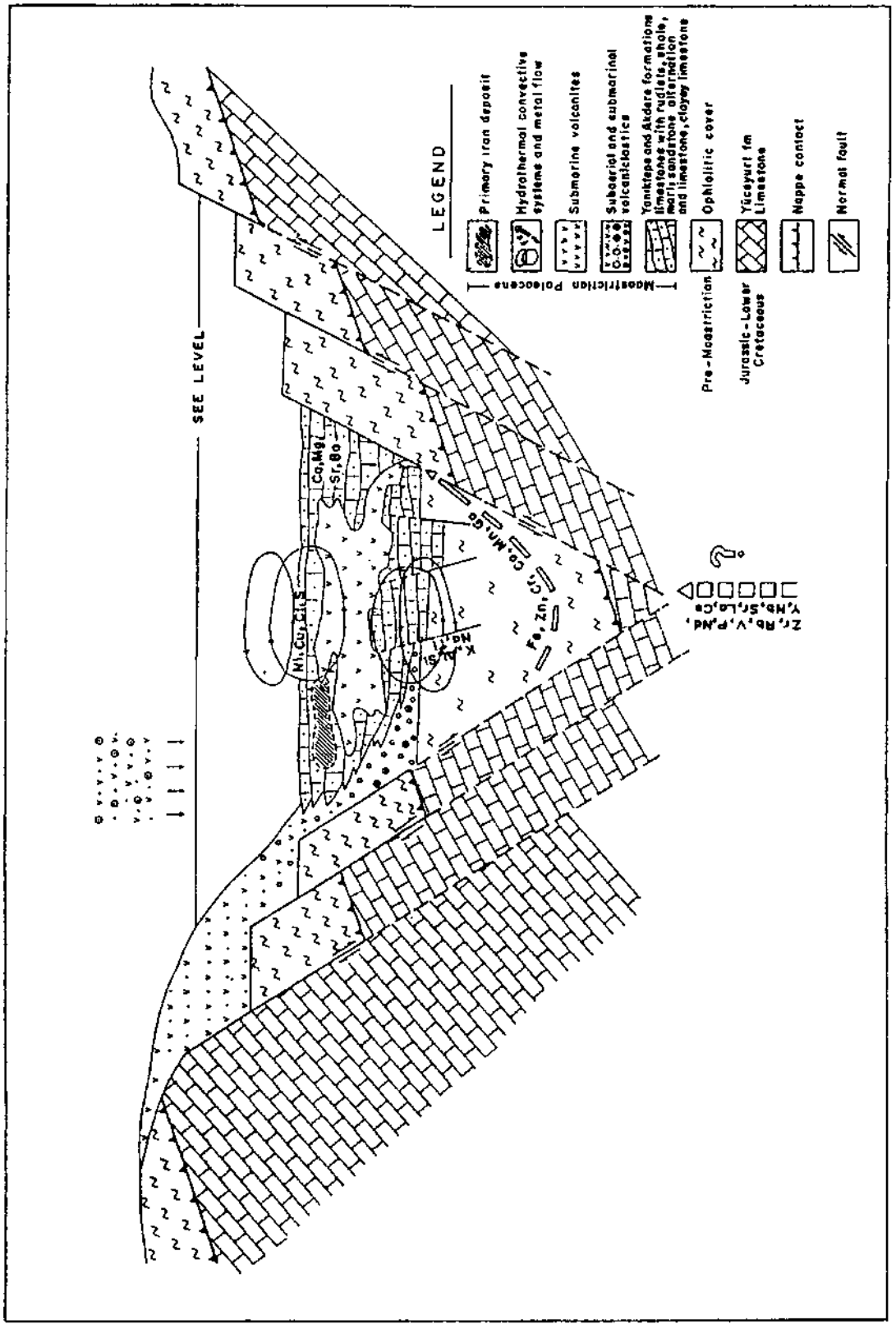

Figure 6- Schematized hypotetical generation model of Otlukilise Iron Deposit.

Sample Nr.	Z-35	Z-53	Z-61	Z-72	Z-81	Z-85	Z-89	Z-104	Z-105	Z-106	Z-107	Z-109
Components(%)												
Quartz	54.51	80.31	85.33	39.66	55.48	-	65.27	41.70	54.82	-	53,56	47.46
Siderite	10.28	9.28	7.56	25.78	36.41	80.94	26.62	50.88	44.06	68.24	44.70	41.31
Clay	4.82	2.25	2.30	9.25	2.13	11.10	3.29	2.56	1.12	19.39	1.74	5.32
Magnetite	17.14	5.59	2.65	12.25	-	-	-	2.56	-	-	-	3.07
Hematite	13.25	2.57	2.16	13.06	5.98	7.96	4.82	2.30	-	12.37	-	2.84
Total	100.00	100.00	100.00	100.00	100.00	100.00	100.00	100.00	100.00	100.00	100.00	100.00

Sample Nr.	Z-110	Z-111	Z-112	Z-113	Z-115	Z-117	Z-118	Z-119	Z-120	Z-121	Z-122	Z-126
Components(%)												
Quartz	-	-	52.41	-	-	-	-	-	-	-	-	-
Siderite	73.06	83.36	37.06	56.33	70.37	56.97	91.75	53.18	54.33	68.85	43.94	61.09
Clay	15.19	10.97	5.11	12.14	6.83	7.05	4.56	23.18	30.63	18.86	38.77	23.34
Magnetite	6.62	-	3.37	27.99	22.80	22.73	3.69	20.00	12.35	12.28	14.55	10.52
Hematite	5.13	5.67	2.05	3.54	-	13.25	-	3.64	2.69	-	2.74	5.05
Total	100.00	100.00	100.00	100.00	100.00	100.00	100.00	100.00	100.00	100.00	100.00	100.00

Sample Nr.	Z-129	Z-131	Z-132	Z-133	Z-134	Z-136	Z-138
Components(%)							
Quartz	-	-	92.03	89.39	-	-	94.54
Siderite	75.27	100.00	5.68	9.07	59.71	56.30	3.88
Clay	9.32	-	2.59	1.54	40.29	21.84	1.58
Magnetite	11.89	-	-	-	-	13.67	-
Hematite	3.52	-	-	-	-	8.18	-
Total	100.00	100.00	100.00	100.00	100.00	100.00	100.00

Table 3- Percentages of mineral componenets of O-42 drill cores samples.

siderite and hematite are also visible at the second vertical colomn. On the other hand, a low positive correlation coefficient (r = 0.32) between clay and magnetite, a very low (r = 0.09) between clay and hematite can easily be seen at the third vertical colomn. The last colomn points out a low positive correlation coefficient (r = 0.30) between magnetite and hematite.

Interpretation of XRD Results

Siderite, clay and quartz assemblage observed usually at particular sample difratograms suppose either intergrown textures developed among siderite and/or clayey siderite an quartz minerals or cementation of these minerals or rock fragments consisted from these minerals.

Siderite, clay and magnetite amounts decrease at the environment characterized by quartz in a wide ore horizon, but increase where clay exists at the environment. Furthermore, magnetite, hematite and siderite exhibit though weak but similar behavior features.

Quantitative distribution relationship of components of samples to the depth show an alternating association between quartz and siderite, clay and/or clayey siderite, magnetite and hematite. In other words, when one is decreasing the other increase. This event also points out an alternating deposition environment prior to deformation.

Amort silica observed in almost all the samples of conglomerate-breccia which consist of various kinds of rock fragments and siderite, clay and/or

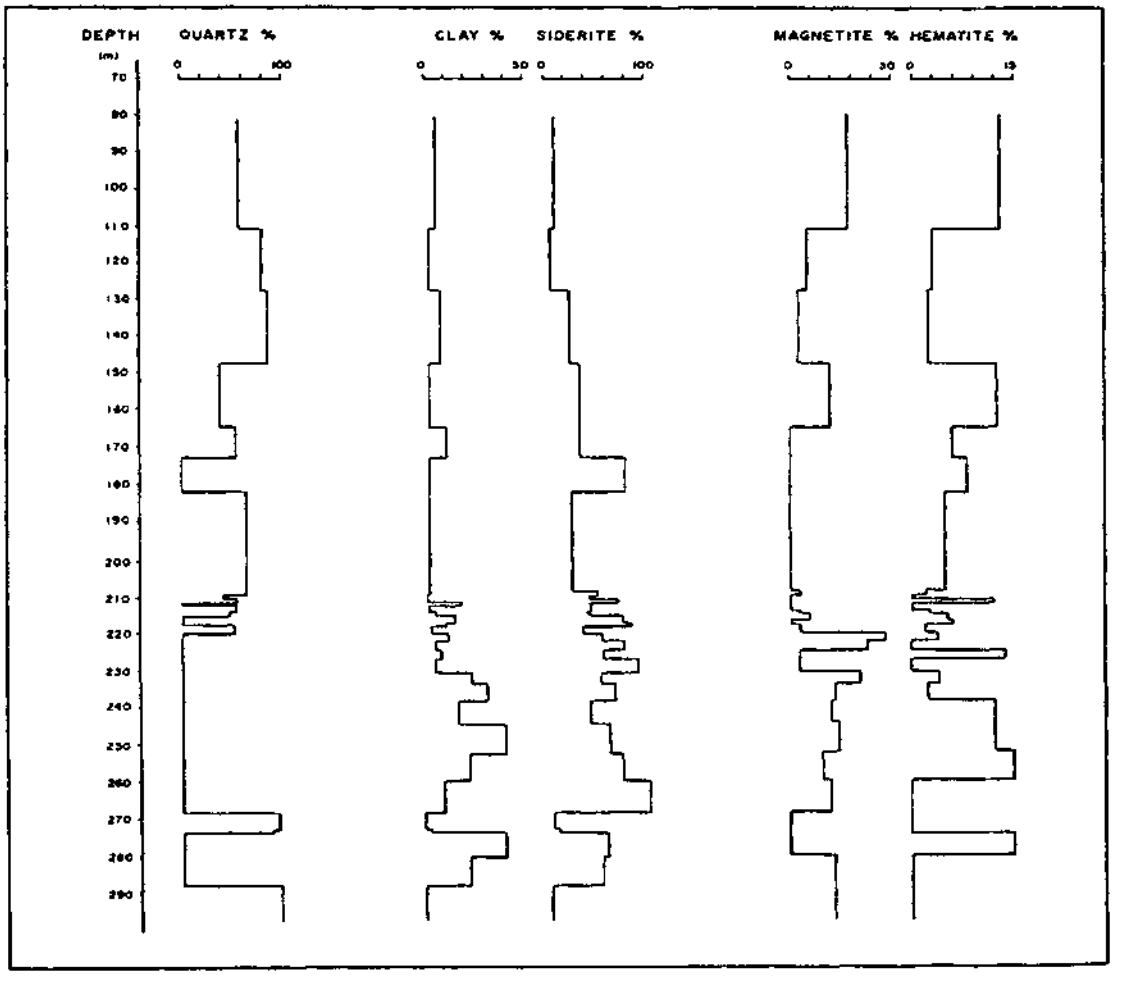

Figure 7- Quantitative vertical distribution graphic of constituents of samples.

clayey matrix and are called as "accumulated ore" according in previous studies (Gülibrahimoğlu, 1979) associates to ore as a significant component.

Positive correlation relationship among (K, Al, Si, Na, Ti group of massive ore samples were mentioned above (Table -2). In addition, a very high positive correlation coefficient (r = 0.99) was determined between Si and K and between Si and Al in massive ore samples (Çiftçi, 1994). So the mentioned elements could generally be symbolized as K-Al silicates. Under these circumstances, a

	Quartz	Siderite	Clay	Magnetite	Hematite
Quartz	1.00				
Siderite	-0.88	1.00			
Clay	-0.62	0.30	1.00		
Magnetite	-0.46	0.12	0.31	1.00	
Hematite	-0.22	0.01	0.09	0.30	1.00

Table 4- Correlation coefficients of componenet pairs of O-42 drill cores samples.

negative correlation relationship with r = -0.62 (Table - 4) observed between quartz and clay determined from XRD studies on conglomeratic-breccia samples gain importance. So, determined Si values from XRD studies indicate quartz besides clay. Conglomeratic-breccia samples are rich in quartz when compared with massive ore samples.

High negative correlation coefficient (r = -0.88) estimated between quartz and siderites of conglomeratic breccia samples point out that Si element associate ore as free quartz minerals besides as a clay component. This statement is meaningfull at genesis of ore formation.

Massive ore samples include 1-35% SiO_2 (Table - 1) and conglomeratic-breccia ore samples 1-95% SiO_2 (Table - 3). Massive ore samples are rich of these features, massive ore samples exhibit plastic behavior but conglomeratic breccia ore samples a brittle one. From all those characteristics, it can be concluded that partly fractured ores can occur at or during formation of an ore horizon which contains clay and quartz by the movements of the bottom of basin. This special result indicate the presence of massive and conglomeratic-breccia ores together at the same basin.

CONCLUSIONS

1- Jurassic - Lower Cretaceous aged limestones of Yüceyurt formation from the basement of the study area. Early sediments of a basin developed in relation to ophiolite emplacement and opened over a fault controlled basement in the region consist of reefal limestones of Upper Cretaceous age and shale, marl and sandstone alternation and locally volcanic rocks of both subaerial and marigin origin. All these units are called as Yanıktepe formation. Paleocene aged Akdere formation made up of pelagic sediments and volcanic intercalations reflects deeper parts of the basin. After the sedimentation of Akdere formation, basin is evolved to subaerial period and marinal Gövdelidağ and Plio-Quaternary aged Gürün formations and volcanites of subaerial character cover all other units.

2- The oldest volcanic rocks in the studied area are observed as chloritized, carbonatized volcanic rock fragments in Yanıktepe and Akdere formations. Hihgly altered chloritized, silicified and argillized angular and rounded basic rock fragments are called as spititicbasalts and/or diabases found in drill core samples accompanying to mineralization. These are accepted as contemporaneous volcanites in the above mentoned formations.

3- Main ore minerals are siderite, magnetite, hematite and minor amounts of pyrite, chalcopyrite and arsenopyrite. Secondary ore minerals are represented by goethite in addition to pyrolusite and psilomelane. Other associate minerals are dolomite/calcite, ankerite, ankeritized dolomite, graphite, gypsum, chamosite and chert. In addition to pyrite framboids, observation of existence of gell-colloform textures (colloform siderite, kidney-like siderite, gell magnetite, melnikovite pyrite and colloform quarz) and very fine grained textures (very fine grained siderite, hematite, quartz and chalcedony) and myrmekitic cloud like, skeletal megnetite bearing siderite, musketofite occurrences, zoned siderite and magnetite assemblage all represent ore characteristics.

4- Geochemical studies carried out on iron rich massive ore samples suppose a synsedimentary-volcanogenic mineralization past. Iron and associated elements are directly of indirectly derived from serpentinites by submarine volcanites extrude into carbonate depositions.

5- Mineralogical studies carried out on especially between quartz and siderite, and clay and/or clayey siderite levels in iron poor conglomerate-breccia ore samples indicate a sedimentary relationship prior to deformation. Thus, an ore horizon characterized by interference of clay and quartz rich sediments can form during the formation processes of locally massive and fragmented ores in the same basin even in small distances by the movements at the basement during or just after the ore formation.

6- Karst evolution and sedimentation controlled by fracture systems can run with ore development mechanism and retransport and redeposit it in proper places. These places can be the basement limestones like Otlukilise iron deposit. The last period of ore deposit evolution is the oxidation under surfical conditions and thus enrichment of ore by

Gülibrahimoğlu, İ. 1979, Sivas - Gürün - Otlukilise demir yatağının jeolojisi ve sondajları: M.T.A. Gen. Müd., Derleme Rapor No: 6613 (Unpublished).

Gümüş, A., 1962, 1961 yılı çalışmaları neticesine gore Sivas İli, Kangal ve Gürün ilçeleri dahilinde teklif edilen demir eksplorasyon programı (Pınargözü, Davutoğlu, Elkondu, Otlukilise): M.T.A. Gen. Müd., Derleme Rapor No: 3371 (Unpublished).

———; 1964, Otlukilise (Sivas - Gürün) Demir Yatağı (55 / 334 ruhsat no'lu) hakkında nihai jeolojik rapor: M.T.A. Gen., Müd. Derleme Rapor No: 3376 (Unpublished).

Kormalı, R., 1972, Sivas İli Gürün ilçesi Otlukilise Demir Madeni çevresinin 1/10.000 ölçekli jeoloji raporu: M.T.A. Gen. Müd., Derleme Rapor No: 1901 (Unpublished).

Kozlu, H., Günay, Y., Dercourt, P., Cross, P., Cross, P. and Bellier, J.P., 1990, Doğu Toros bölgesinde, Neo - Tetis'in konumu: Turkiye 8. Petrol Kong., 387 - 403.

Kurtman, F., 1978, Gürün Bölgesinin jeolojisi ve tektonik özellikleri: Maden Tetkik ve Arama Derg., 91, 1 - 12.

Laznicka, P., 1985, Empirical Metallogeny: Developments in Economic Geology, 19, 1758 s., Elsevier, Amsterdam.

Lehmann, E., 1972, On the source of the iron in the Lahn ore deposits: Mineral. Deposita, 7, 247-270.

Metin, S., 1982, Doğu Toroslarda Derebaşı (Develi), Armutalan ve Gedikli (Saimbeyli) köyleri arasının Jeolojisi: İ.Ü. Müh. Fak., Jeo. Müh. Bölümü, Doktora tezi, 134 s.; (Unpublished), Istanbul.

. . . . . .; Ayhan, A. and Papak, İ., 1986, 1/100 000 ölçekli açınsama nitelikli Türkiye Jeolojik Haritalan Serisi: Elbistan I - 22 paftası, M.T.A. Yayınları.

———; . . . . . .; -. . . . . .; 1987, Doğu Torosların batı kesiminin jeolojisi (GGD TÜRKİYE): Maden Tetkik ve Arama Derg., 107, 1-12.

Norrish, K. and Chappel, B.W., 1977, X - ray fluorescence spectrometry: Zussman, J., (ed.), Physical Methods in Determinative Mineralogy, 2nd ed. Academic Press, 201 - 272, London.

Özer, S., Terlemez, İ., Sümengen, M. and Erkan, E., 1984, Pınarbaşı (Kayseri) çevresindeki allokton birimlerin stratigrafisi ve yapısal konumları: Türkiye Jeol. Kur. Bült, 27, 61-69.

Özgül, N., 1976, Torosların bazı temel jeoloji özellikleri: Türkiye Jeol. Kur. Bült., 19 (1), 65 - 78.

. . . . . .; Metin, S., Göğer, E., Bingöl, İ, Baydar, O. and Erdoğan, B., 1973, Tufanbeyli dolayının Kambriyen ve Tersiyer kayaları: Türkiye Jeol. Kur. Bült, 16 (1), 82-100.

Quade, H., 1970, Der Bildungsraum und die genetische Problematik der vulkono - sedimentaren Eisenerze: Clausthaler Hefte, Heft 9, 27 - 65, Berlin.

. . . . . .; 1976, Genetic problems and environmental features of volcano-sedimentary iron-ore deposits of the Lahn - Dill - Type: Wafl, K.H., ed., Handbook of Strata - Bound and Stratiform Ore Deposits, 255 - 294.

Stendal, H., Ünlü, T. And Konnerup - Madsen, J., 1995, Geological setting of iron deposits of Hekimhan Province, Malatya, central Anatolia, Turkey: Trans: Instn. Min. Metall. (sect. B. Appl. Earth sci.), 104, 46 - 54, London.

Unlu, T., 1983, Die Genesse der Siderit Lagerstatte Deveci in der Hekimhan - Provinz Malatya/Turkei und ihre wirtschafftliche Bewertung: Doktora gahsmasi, Berlin Teknik Üniversitesi, 84 s., Berlin.

———; and Stendal, H., 1986, Divriği Bölgesi demir yataklarının element korelasyonu ve jeokimyası (Orta Anadolu - Türkiye): Jeoloji Mühendisliği, 28, 5 -19.

-----,-;———; 1989, Divriği Bölgesi demir cevheri yataklarının nadir toprak element (REE) jeokimyası. Orta Anadolu, Türkiye: Türkiye Jeol.Kur. Bull., 32 (1-2), 21-38.

PLATES

PLATE-I

Fig. 1. Volcanic rock fragment (upper left) in rudist bearing limestone. Crossed polar (XPL), magnification x16.

Fig. 2. Volcanic rock fragment showing flow texture cemented by micritic and locally sparitic matrix (in the middle) surrounded by micritic and sparitic rock fragments and some quartz grains (at upper, lower and right edges). XPL, magnification x16.

Fig. 3. Coarse grained (gray - dark gray) siderites (at right side) and fine grained (gray) siderites in rounded sandstone. XPL, magnification x16.

Fig. 4. Very fine grained quartzs cemented by iron oxides. Plane polarized light (PPL), magnification x16.

Fig. 5. Rounded basic volcanic rock fragment (from mid lower to upper part) filled by siderites at amygdules (light gray - white in the middle). XPL, x40.

Fig. 6. Siderite rock fragment including euhedral to subhedral opague minerals (black) and subhedral zoned dolomites (white - light gray). PPL, x16.

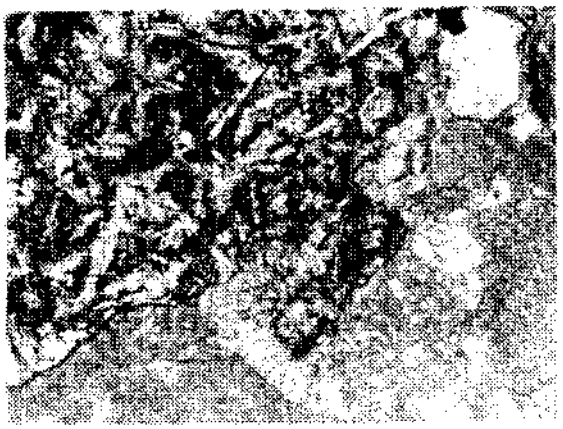

1

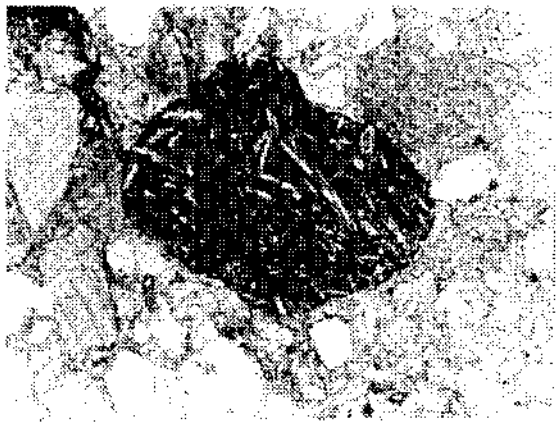

2

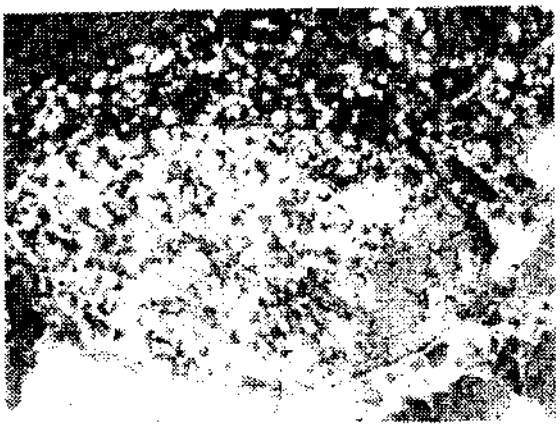

3

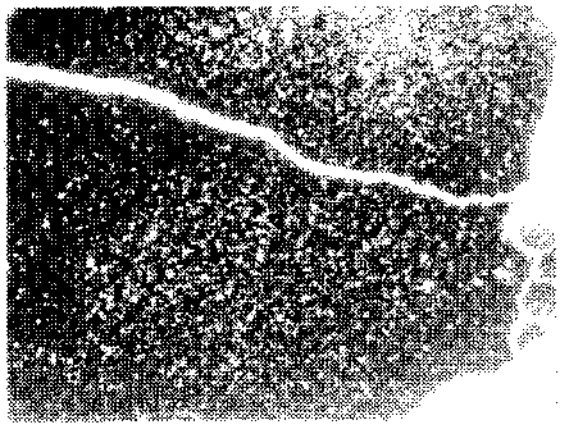

4

5

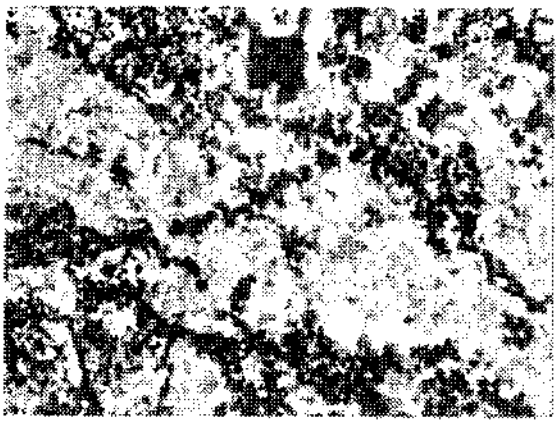

6

PLATE-II

Figure 1. Chromite (dark gray) replaced by chromspinel (gray) and magnetite (light gray). In Oil, x200.

Figure 2. Very fine grained siderites (dark gray) replaced by goethite (light gray) from their edges. in oil, x200.

Figure 3. Volcanic rock fragments (midright and midleft, light gray) cemented by siderite (gray - light gray) and small amount of hematite laths (white). In oil, x200.

Figure 4. Partly martitized, zoned magnetite (white - light gray) replaced by siderite (dark gray). In oil, x200.

Figure 5. Limonitized and chloritized basic volcanic rock fragment (at left edge, dark gray) and magnetite (in the middle, gray) and chalcopyrite (to right side, light gray) in concentric siderite (in the middle and lower part, pale gray). In oil, x200.

Figure 6. Siderite (dark gray) and magnetite (gray) association exhibiting myrmekitic like textures. In oil, x200.

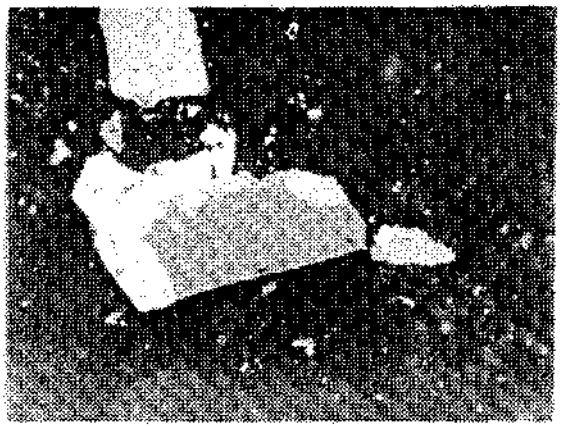

1

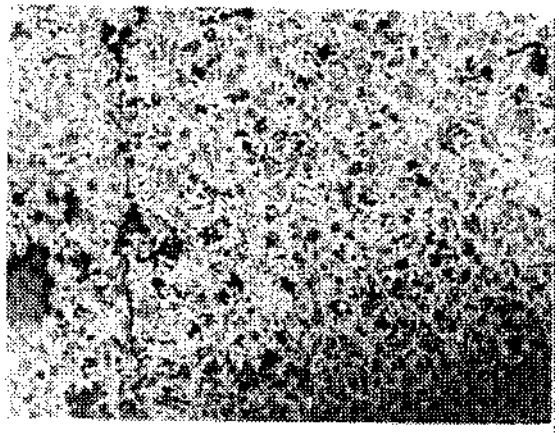

2

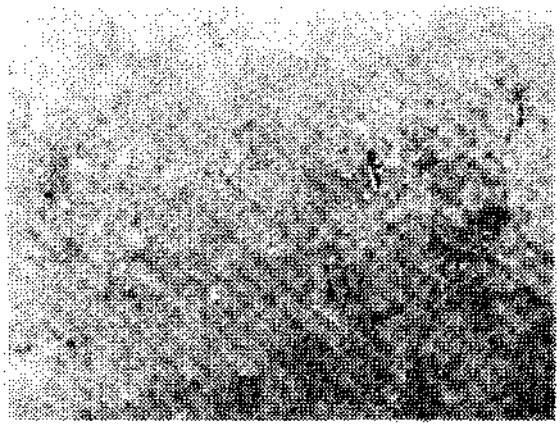

3

4

5

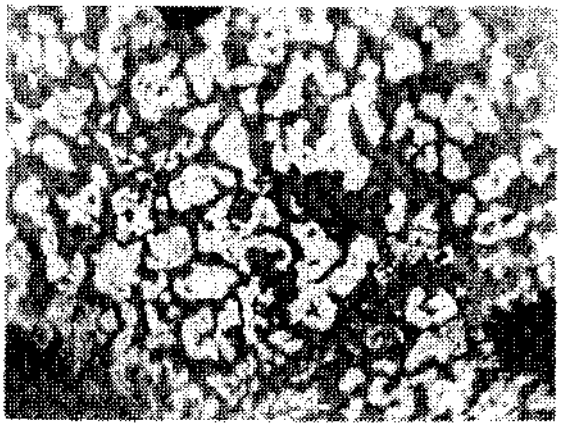

6

PLATE-III

Figure 1. Cloud like magnetites (in the middle and to lower and right sides, light gray fine spots) and hematite laths white and chalcopyrite grains (midright and lower side, rounded and white) in siderites (light gray, gray). In oil, x200.

Figure 2. Magnetites (light gray fine spots) in euhedral siderites (gray). In oil, x200.

Figure 3. Euhedral to subhedral magnetites (gray) grown together with siderites (dark gray). In oil, x200.

Figure 4. Gell textured melnipovite pyrites (light gray) intergrown with siderites (dark gray). In oil, x200.

Figure 5. Transported chromite (triangles, gray) in clay matrix, fractured siderite vein (midupper and right side, gray), gell textured magnetite (in the middle and lower parts, pale white) and arsenopyrite grains (shiny white). In oil, x200.

Figure 6. Completely martitized magnetites grains (white) and limonitized pyrite framboid (midlower and lower left sides, rounded, pale white) in clay matrix stained by lirhonite. In oil, X200.

iron element. This represents the actual ores of Otlukilise iron deposit.

DISCUSSION AND CONCLUSION

Genetical discussions of Lahn-Dill type deposits focus on syngenetical or epigenitical type of formations (Quade, 1976). These two types exhibit differences both for their relationships to wall rocks and deposition characteristics.

According to some authors, Otlukilise iron deposit has been interpreted as an epigenetic type of formation being formed as open space fillings in limestones of the basement and metasomatic replacements in them by ore fluids.

Most of karstification events observed often in the region, developed upon fracture systems after mineralizations make the ore minerals unstable and alter also the other components of ore deposit. Thus, the interpretation of the events becomes more difficult. As complementary supplements to the offered, model, fracture zones being served as ore bringing channels and the ones occurred by new tectonic movements helping the ores to reach the actuel surface are filled by silicious ore bearing hydrothermal fluids. The movements at these fractures after all these events can cause to some of conglomerate-breccia ores. On the other hand, in some stable areas in the basin, clay rich and quartz poor massive ores (rich in siderite component) can form. However, remembering that the basin is opened over a basement, new views can be added to the synthesis of ore genesis. Mineralizations can not be limited by ore bringing channels (i.e. fractures) but ore formations with synsedimentary characters in sedimentary basin may reach up to huge sizes and losing their original positions by later on tectonic events, they can evolve actuel sites. Some characteristics of these secondary appearances present some clues on the primary position of ores.

Otlukilise iron deposit exhibits similar features to Hekimhan-Deveci Siderite Deposit by geographical positions, wall rock relations and age of formations. Deveci Siderite Deposit represent a typical case for synsedimentary-volcanogenic of exhalative-sedimentary type of formation in Turkey (Ünlü, 1983). This deposit is indicated as an example of Lahn-Dill type ore deposit (Lehmann, 1972) in Turkey by the same author. Although main ore mineral of Lahn-Dill Deposit is hematite with a small amount of siderite, principal ore mineral in Deveci and Otlukilise Deposits is siderite. MnO contents of Deveci and Lahn-Dill Deposits reach up to 5%. Nonexistance of manganese in Otlukilise iron deposit can be explained by mobile character of Mn during the replacement of siderite to goethite. While silica component of Deveci Siderite Deposit is lower than 8% (see in Ünlü, 1983), this ratio is much greater in Otlukilise and Lahn-Dill deposits. Lahn-Dill deposit is characterized by silica centers where many submarine volcanic piles present. Deveci Siderite Deposit is accepted as a similar occurrence of Vares (Crotia) Iron Deposit where siderite orebody is described (Quade, 1970) by Unlu (1983).

Otlukilise iron deposit involves chromite bearing highly altered basic volcanic rocks. The typical observed in the deposit are gell colloform textures indicating rapid cooling, very fine grained, myrmekitic and contemporaneous growing textures siderite (together with clay) and quartz. This deposit is also characterized by silica rich fluids like Lahn-Dill Deposit. Magnetite and hematite are often replaced by siderite. In addition to these replacement textures, contemporaneous growing of magnetite and siderite are often observed. Fe^{+3} ions are depleted by the minerals formed earlier and so relative Fe^{+2} enrichment of the environment is occurred. Silica and iron elements are the components brought out to the environment from the deeper parts of basin being understood from textural relationships. Due to the Eh and pH conditions of the environment, these components are stabilized as iron and silica bearing minerals. Under these circumstances, it is impossible from the physiochemical point of view that iron has been transported circumstances, it is impossible from the physiochemical point of view that iron has been transported from the continent. Because during the transportation from continent resembling an oxygen rich environment to the basin. Fe^{+2} would be oxidized and precipitated as Fe^{+3} and so no siderite would have been occurred in the basin.

Within the limitations of the data and observations in this study, this paper tries to give the mes-

sage that whether a source of oceanic lithosphere or ophiolitic rocks lying on the basement can be supposed for iron element origin of exhalative-sedimentary or synsedimentary-volcanogenic iron deposits (Stendal et al. 1995) developed in volcanosedimentary sequences of basins opened over a platform characterized by a geotectonic environment of ophiolitic cover on the basement.

ACKNOWLEDGEMENT

This paper is prepared basing on Master's Thesis of first author at the Department of Geological Engineering of Faculty of Science at Ankara University under supervision of second and third authors. We want thank Prof. Dr. Ayhan Erler, Prof. Dr. Baki Varol, Assoc. Prof. Dr. Okan Tekeli and Dr. Ahmet Çağatay for their constructive critism. We also express our thanks to University af Kopenhagen for laboratory facilities at geochemical studies. Rock samples, thin sections and whole representative material with this paper have been saving at the Department of Geological Engineering of Ankara University.

REFERENCES

Akkuş, M, F., 1971, Darende - Balaban Havzasının (Malatya, ESE Anadolu) jeolojik ve stratigrafik incelenmesi: Maden Tetkik ve Arama Derg., 76, 1 - 60.

Alkan, M. and Türkmen, H., 1987, Sivas - Kangal - Gürün (Uzunyayla - Otlukilise) yöresi demir prospeksiyonu jeoloji raporu: M.T.A. Gen. Müd., Derleme Rapor No: 8200 (Unpublished).

Atabey, E., 1993a, Doğu Toros karbonat platformunda Önülke Dağarası havza gelişimine bir örnek: Akdere Havzası, Gürün - GB Sivas (Türkiye). Türkiye Jeol. Kur. Bült., 36 (1), 51 -61.

———;1993b, Gürün Otoktonu'nun stratigrafisi (Gürün-Sarız arası), Doğu Toroslar -GB Sivas (Türkiye): Türkiye Jeol. Kur. Bult., 36 (2), 99-113.

. . . . . .; 1993c, Akdere Basin: An example for the foreland - intermontane basin eastern Tauride carbonate platform, Gürün SW Sivas - Turkey: Geologica Romana, 29, 401 - 409, Roma.

Aziz, A. and Erakman, B., 1980, Tufanbeyli (Adana) - Sarız (Kayseri) - Gürün (Sivas) ilçeleri arasında kalan alanın jeolojisi ve hidrokarbon olanakları: T.P.A.O. Rapor No: 1526 (Unpublished).

. . . . . .,. . . . . .; Kurt, G. and Meşhur, M., 1981, Pınarbaşı, Sarız (Kayseri), Gürün (Sivas) ve Darende (Malatya) ilçeleri kalan alanın jeoloji raporu: T.P.A.O. Rapor No: 1601 (Unpublished).

Barosh, P.J., 1971, Geology of the Otlukilise iron mine, Sivas Province Turkey: M.T.A. Gen.Müd., Maden Etüt Arş., No: 4814 (Unpublished).

Bottke, H., 1981 Lagerstattenkunde des Eisens: Verlag Gluckauf GmbH, 202 s., Essen.

Çiftçi, D., 1994, Otlukilise (Gürün - Sivas) Demir Yatağı'nın maden jeolojisinin incelenmesi: A.Ü.F.F. Jeo. Müh. Bölümü, Yüksek Lisans Tezi, 195 s. (Unpublished), Ankara.

Demirtaşlı, E., 1967, Pınarbaşı - Sarız - Mağara ilçeleri arasındaki sahanın litostratigrafik birimleri ve petrol imkanları: M.T.A. Gen., Müd. Derleme Rapor No: 3489 (Unpublished).

Gladney E.S., Burns, C.E. and Roelandts, I., 1983, 1982 compilation of elemental concentrations is eleven United Stages Geological Survey rock standarts: Geostandards Newsletter 7, 3 - 226.

1

2

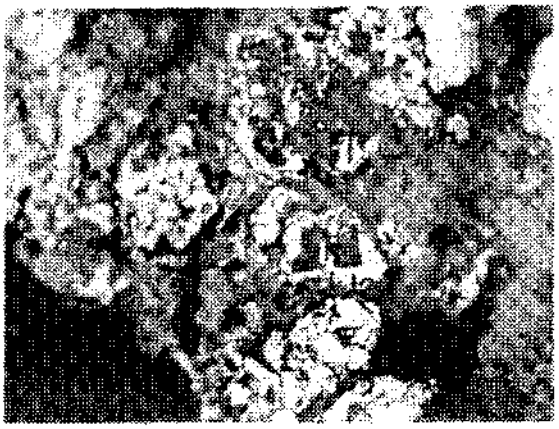

3

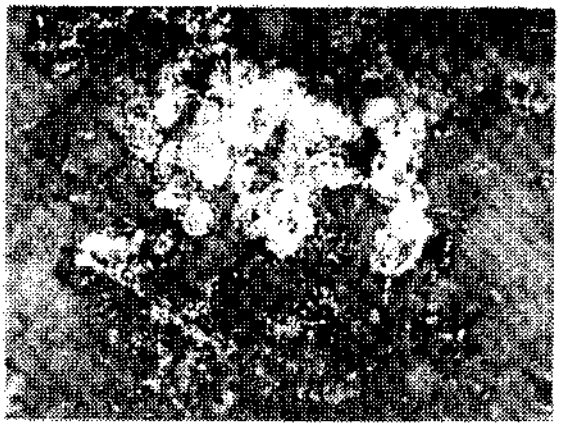

4

5

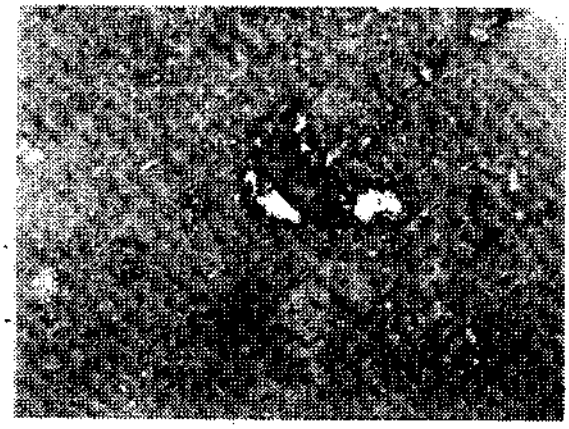

6

Mineral Res. Expl. Bull., 118, 51-66, 1996

DISTRIBUTION AND GENESIS OF NEOFORMED MINERALS IN KOYUNAĞILI (MIHALIÇÇIK-ESKİŞEHİR) AREA

Selahattin KADiR* and Halil BAŞ**

ABSTRACT.- The study area is located at the Southwest of Koyunağılı village situated in the south margin of the Beypazarı-Qayirhan basin which is in the Middle Sakarya Massif. The Neogene units in the investigated area are Çoraklar, Hırka, Karadoruk, Akpınar, Bozçayır, Acısu and Kırmızıtepe Formations. The mineralogic features of the clay minerals and tha host rock samples were studied by means of petrographic, XRD, DTA-TG, SEM-EDX and IR Spectra techniques. Various effects of pH values of the environment related to evaporation and feeding of the basin from several areas, cause the formation of different mineral paragenesis. The main mineral paragenesis are; loughlinite + analcime + calcite + dolomite + feldspar, sepiolite + analcime + dolomite + illite, sepiolite + analcime + dolomite + opal-CT + feldspar, montmorillonite + analcime + dolomit + illite + feldspar + quartz + opal-CT, montmorillonite + analcime + calcite + felspar + illite and montmorillonite + dolomite + calcite + analcime + quartz + Feldspar. Montmorillonite is formed at the margin of the basin, derived from freswater and detritic materials which contain Al and Mg. Aluminum ions are generally dominant in the shallow part of the basin facies of the Bozçayır and Acısu Formations. In the Akpınar Formation, sepiolite is formed at a non-acidic environment, which is rich in Mg and Si, but poor in Al. At the center of the area (around Ocak), loughlinite is formed in a way similar to that of sepiolite by combining of Na, originated from the alteration of tuff, to the Si and Mg. As a result of the alteration, especially after the formation of montmorillonite the proportion of (Na+K)/H increases and finally analcime and feldspar are formed. At the south of the area magnesite is formed at the bottom part of the Hırka Formation, due to the high Mg and pH and low Si values. To the north, some dolomite, depending on the decreasing of Mg content, is observed. At the north, dolomite and calcite are formed interbededly, due to changes in the pH conditions controlled by evaporation and freshwater participations. Sepiolite, loughlinite, analcime, feldspar, opal-CT and a small amount of quartz are formed authigenically, in and around the altered glass pores as a result of alteration of volcanic glasses.

1. INTRODUCTION

The study area is located in the southwest of the Koyanağılı village in the southern margin of the Beypazarı-Çayırhan of the Central of Sakarya Massive (Fig. 1).

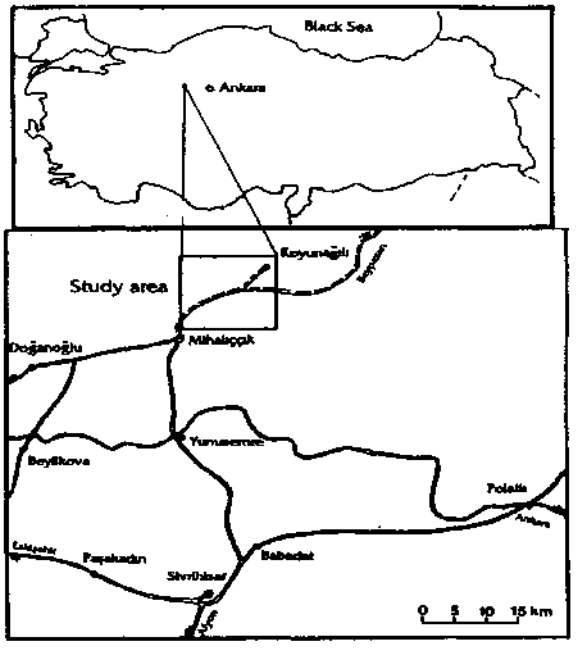

Fig. 1- Location map of study area.

Metamorphic rocks of Paleozoic age and Mesozoic serpantinites form the basement (Fig. 2). The unconformably overlying Middle-Upper Miocene units are spreaded widely and they comprise of the comformable units of the Çoraklar Formation (conglomerate, sandstone, mudstone, siltstone and tuff), the Hırka Formation (tuff), the Karadoruk Formation (dolomite), the Akpınar Formation (silicified tuff, crystal tuff and carbonate interbedded clay and claystone alternotions), the Bozçayır Formation (clay) and the Acısu Formation (claystone-limestone alternations) from the bottom to the top respectively. The Acısu Formation is uncomformably overlain by the Kırmızıtepe Formation (conglomerate, sandstone, mudstorre

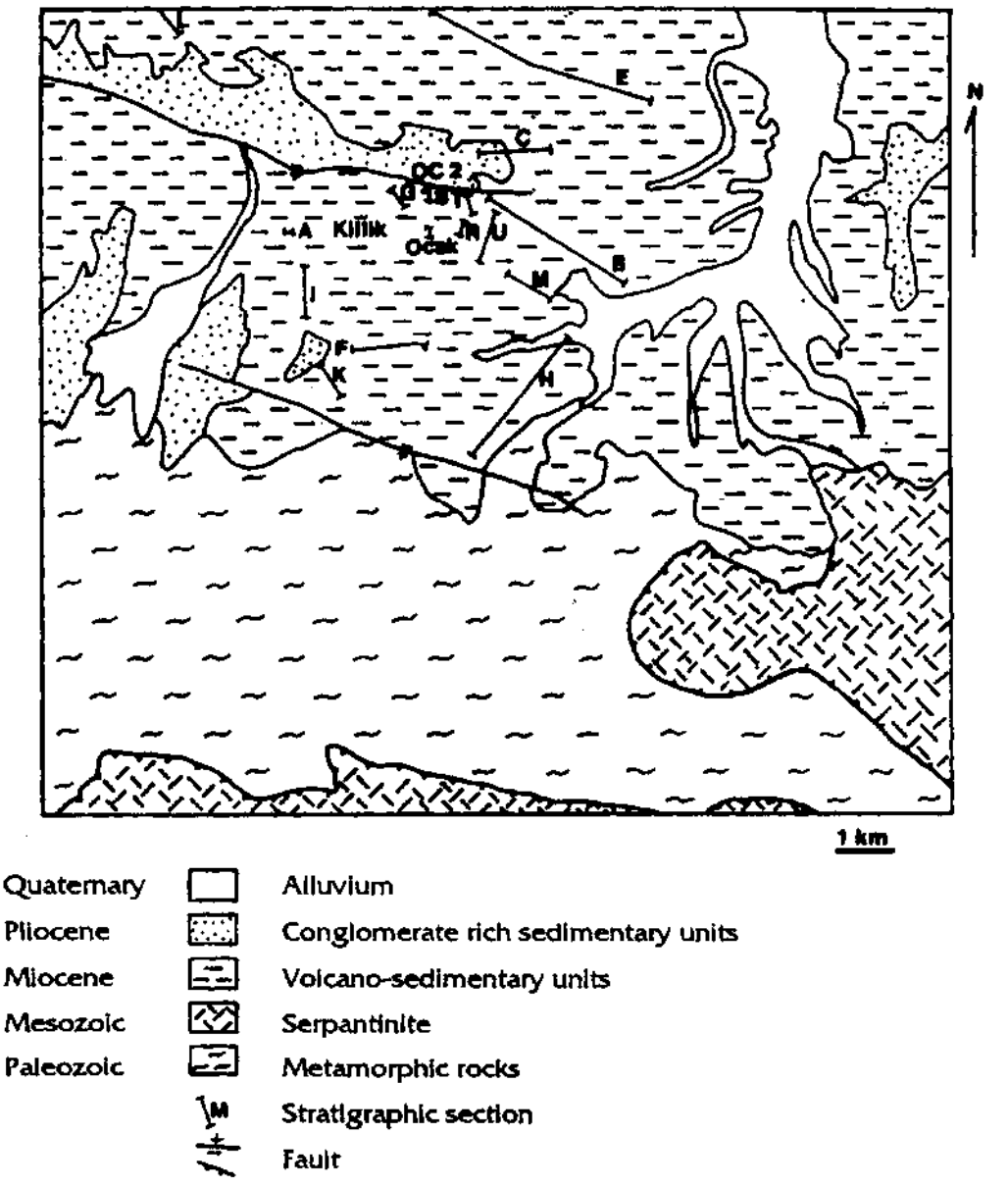

Fig. 2- Generalized stratigraphic section of study area.

and claystone alternation) of Pliocene age. Quaternary alluvium deposits are the youngest units of the study area (Fig. 3). The clays of Akpınar Formation contain sepiolite, loughlinite (Na-sepiolite), analcime, montmorillonite, feldspar, dolomite, calcite, opal-CT and quartz minerals. Loughlinite deposit seems to be economic at the Ocak area. However, at the other areas, sepiolite is in mineral paragenesis of minerals such as dolomite, magnesite, calcite, montmorillonite, analcime, felspar, quartz and opal-CT within the tuffs.

In the study area, several geological studies were carried out for different purposes. Bituminous schists and trona investigations were studied by Siyako (1982, 1983), Şener (1981), Tenekeci et al. (1983), Kayakıran and Çelik (1986), Helvacı et al. (1988, 1989), Gündoğdu et al. (1985).

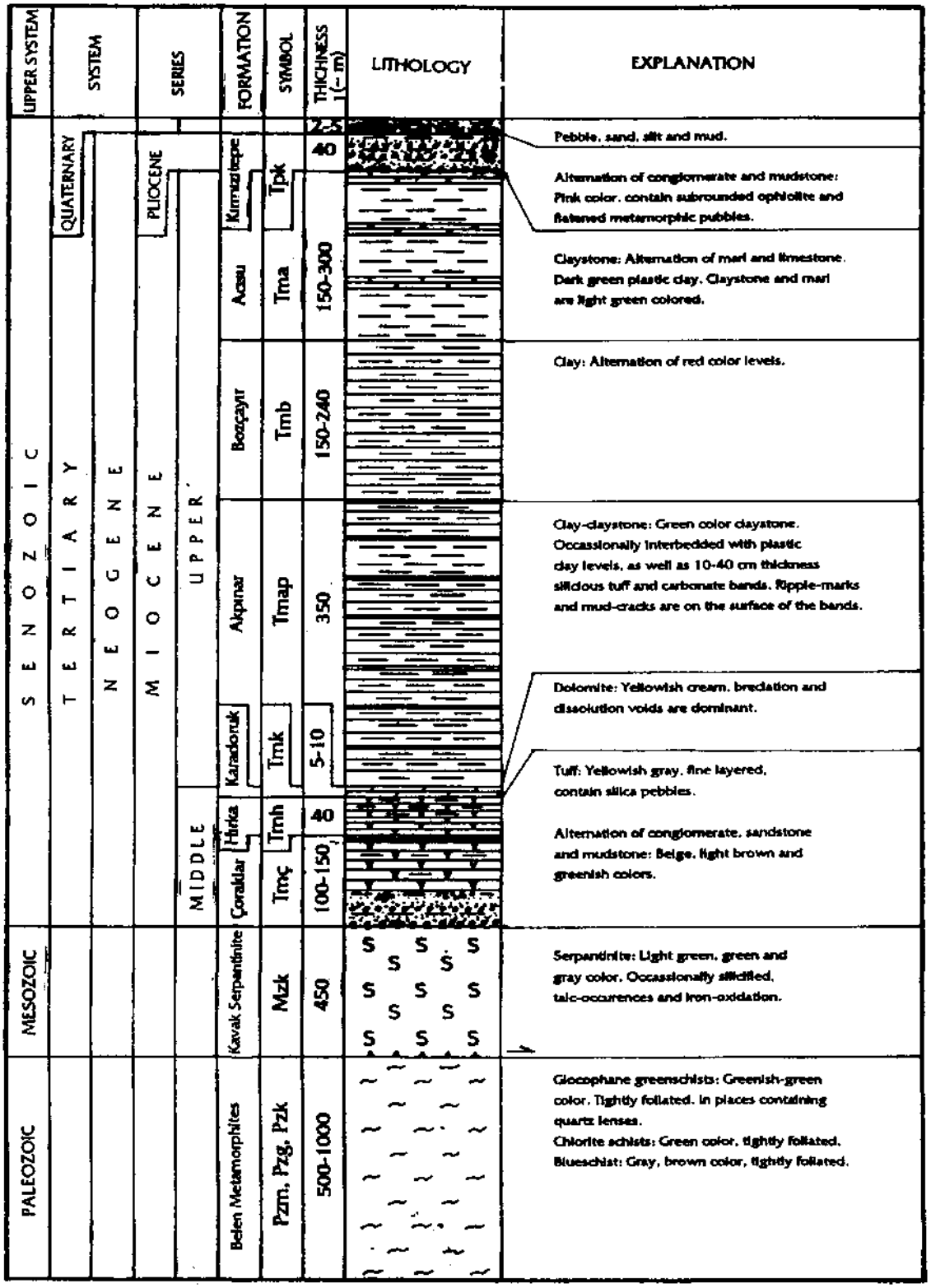

Fig. 3- Generalized geologic map of study area.

The mineralogical investigation was firstly performed by Echle (1967, 1974, 1978). He studied the sedimentology of the area as well as the formation of sepiolite-loughlinite and transformation of these minerals.

Ataman (1976) studies the Beypazarı basin, which contains analcime, dolomite, K-feldspar, searlesite, loughlinite, sepiolite, palygorskite and smectite minerals.

The purpose of this study is to determine the vertical and horizontal distribution of volcanic sepiolite-loughlinite bearing neoformed minerals in the Koyunağılı area.

2. MATERIAL AND METHODS

The mineralogy of the samples were determined by using of petrographic, XRD, DTA-TG, SEM-EDX and IR-spectrum techniques.

Petrographic, XRD, DTA-TG and SEM studies were performed in the laboratories of General Directorate of Mineral Research and Exploration of Turkey (MTA), EDX works were conducted in the General Directorate of Turkish Petroleum (TPAO).

During the field work, 20 stratigraphic sections were studied in detail and 310 samples were collected for mineralogical investigation These sections were named as A, B, C, E, F, G, H, I, L, M, R, Q, Ocak, R, S, T, U (Fig. 2). The distance between the stratigraphic sections at the center of the area is about 500-1000 m and the distance between the sections of the margin is about 1500 m.

3. RESULTS

Mineral paragenesis of each formation in the investigation area is as follows:

3.1. Hırka Formation: The Hırka Formation (M) is the oldest unit in the study area. The mineral distribution in the stratigraphic section H from relatively high to low amounts are: magnesite, dolomite, montmorillonite and illite (Fig. 4a). F sections contain montmorillonite, sepiolite, analcime and feldspar minerals (Fig. 4b). Towards the north, in the section M, dolomite and trace amount of kaolinite, illite, felspar and quartz are present. In section E, dolomite, illite, montmorillonite and analcime with a small amount of feldspar and calcite are present (Fig. 4c, 5). The southern margin of the area (section H), magnesite mineralization is relatively dominant because of high Mg and low Si and also of the short distance to the basement. Since the proportion of Mg and pH values are much lower towards the north, the dolomite becomes more dominant mineral, but montmorillonite and analcime seem to abundant at the presence of Al. Hırka Formation contains of green colored opal-CT nodules (3-10 cm).

3.2. Karadoruk Formation: This formation is generally composed of dolomite, quartz and small amount of feldspar.

3.3. Akpınar Formation: Akpınar Formation is cropped out in the most of the units within the stratigraphic section (Fig. 4a, b, c, 5, 6a, b, c, 7b). Sepiolite and montmorillonite are dominant in the Akpınar Formation. At the southern part of the area (section H), dolomite and sepiolite are dominant and small amount of analcime, illite, feldspar, amphibole, quartz and opal-CT are also present. At section F, montmorillonite, dolomite, illite and small amount of feldspar, talc and amphibole minerals were recognized. Dolomite and opal-CT were determined in section M. The bottom part of the section B is dominated by dolomite, montmorillonite, and illite, while its upper part is dominated by sepiolite, montmorillonite and analcime. Sepiolite, dolomite and analcime are dominant in the section E at the north. Loughlinitization is present in the Ocak section. Therefore, the mineral distribution of formations in the south close to the basement is montmorillonite, dolomite and sepiolite; towards the north, dolomite + opal-CT, dolomite + montmorillonite + sepiolite + analcime; sepiolite + dolomite + analcime become dominant minerals. This shows that sepiolite increases from south to north direction of the region.

The south, the west and center of the investigation area contain 0.5-1 m thick opal-CT beds and 3-10 cm opal-CT nodules.

3.4. Bozçayır Formation: Montmorillonite and mixed-layer clays (montmorillonite + sepiolite) are

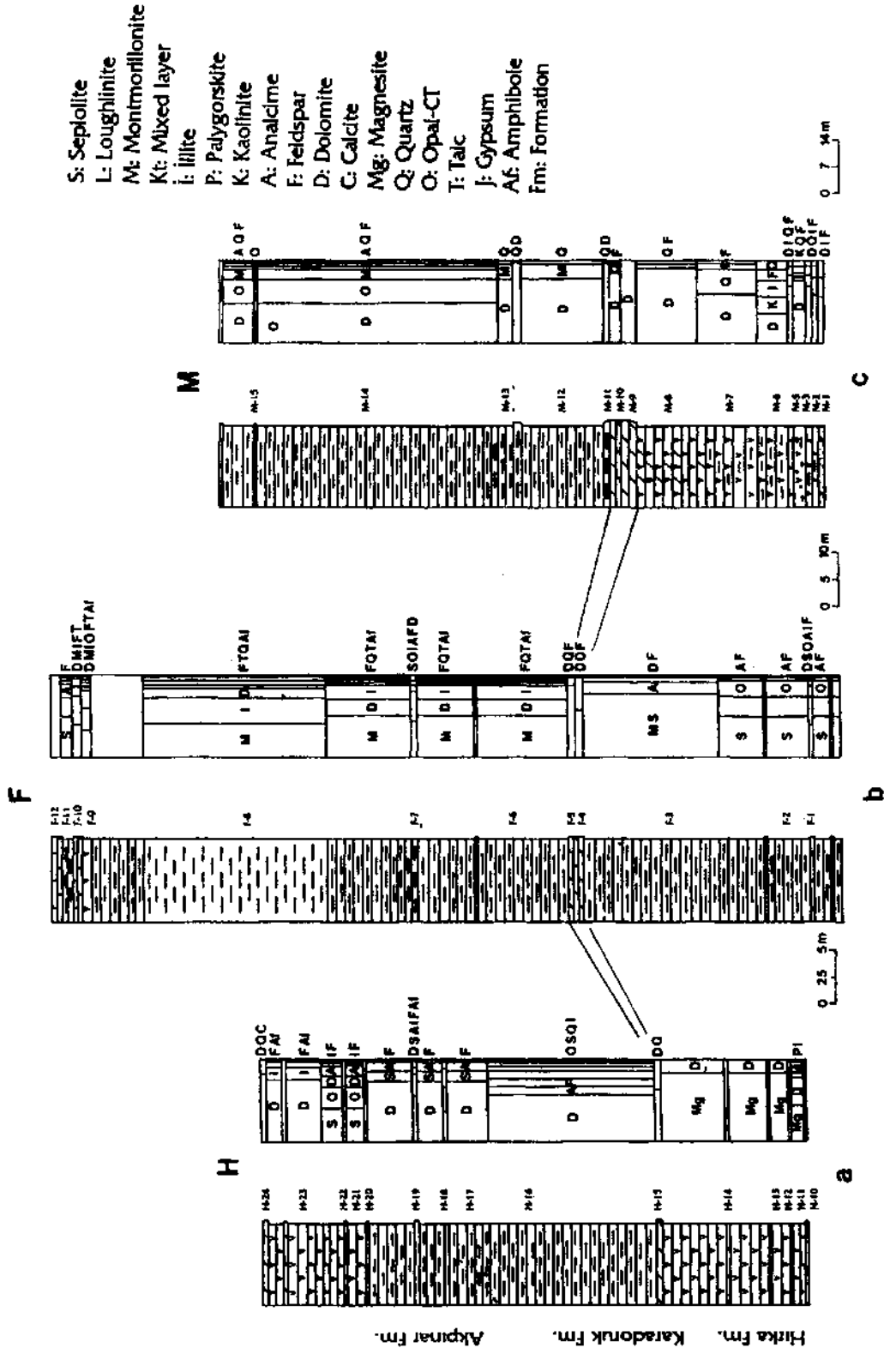

Fig. 4- Mineral distribution in Hırka, Karadoruk and Akpınar, Formations in the Southern part of the study area (See Fig. 2, for section locations and Fig. 4, for symbol explanations).

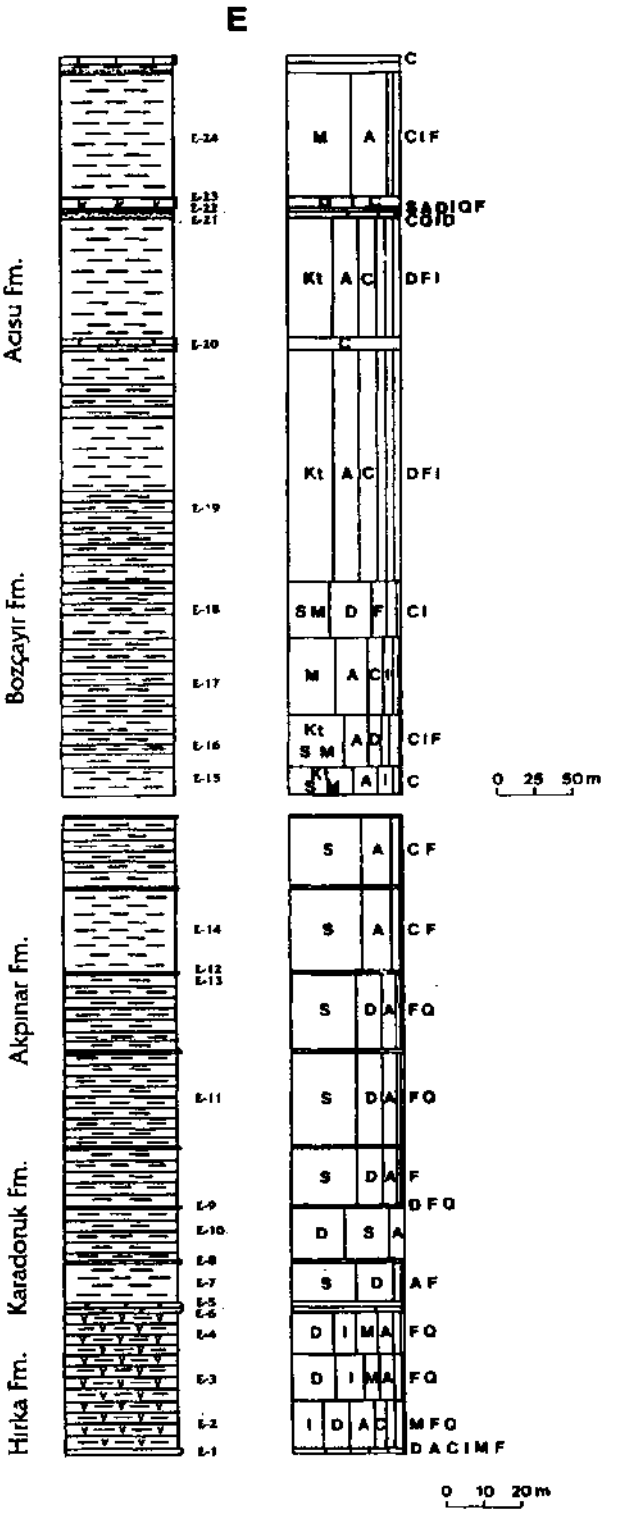

Fig. 5- Mineral distribution in Hırka, Karadoruk, Akpınar, Bozçayır and Acısu Formations in the northern part of the study area (See Fig. 2, for section locations and Fig. 4, for symbol explanations).

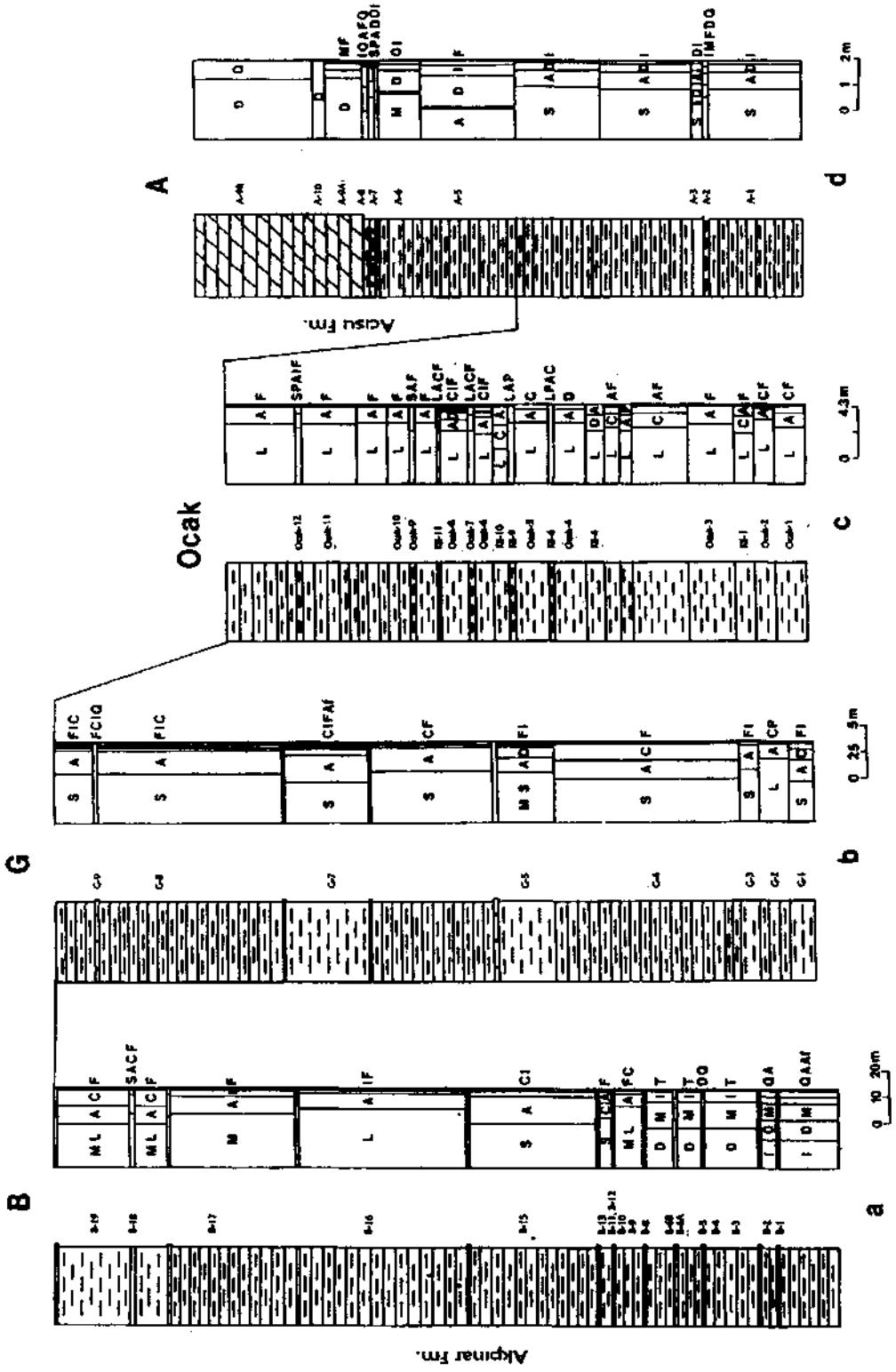

Fig. 6- Mineral distribution in Akpınar and Acısu Formations in the center of the study area (See Fig. 2, for section locations and Fig. 4, for symbol explanations).

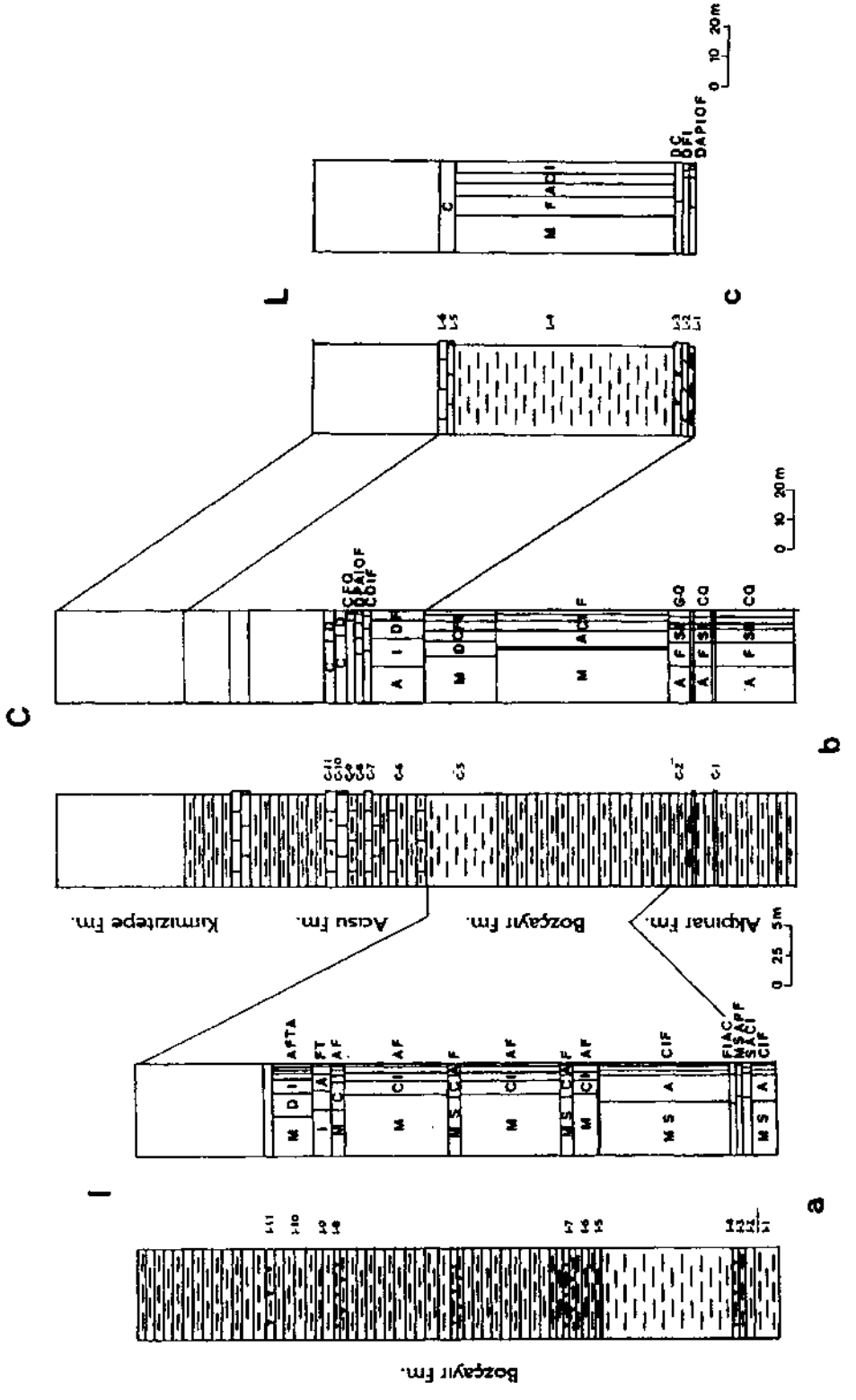

Fig. 7- Mineral distribution in Akpınar, Bozçayır, Acısu and Kırmızıtepe Formations (See Fig. 2, for section locations and Fig. 4, for symbol explanations).

dominant and a small amount of analcime, dolomite, calcite, felspar and illite are also determined (Fig. 5, 7a, b).

3.5. Acısu Formation: Montmorillonite, mixed-layer clays and analcime are dominant in this formation.

4. DISCUSSION

Sepiolite forms in basic environments (pH 8-9) when SiO_2 and MgO proportions are high (Caillere, 1951, Milton and Eugster, 1959; İsphording, 1973; Starkey and Blackmon, 1979; Singer and Galan, 1984; Velde, 1985; Weaver and Beck, 1977). The formation of sepiolite was examined experimentally by many workers. Mumpton and Roy (1958) prepared composition of 38.1 % MgO, 59.6% SiO_2, 2.3% Al_2O_3 and observed that montmorillonite, talc, silica and chlorite phases were formed rather than sepiolite at different heat and water vapor pressures. Hast (1956), Wollast et al. (1968), Mumpton and Roy (1958) formed sepiolite without adding Al_2O_3 to the mixture. This shows that Al_2O_3 seems to prevent the formation of sepiolite.

Wollast et al. (1968) found out that the reaction of sea water with the silica had caused the formation of hydro-magnesium silicate. The composition and structure of this formation is similar to that of sepiolite. These authors state that sepiolite is precipitated in environments which the pH value is higher than 8, high MgO and low or zero Al_2O_3. When pH value is less than 8, sepiolite does not form but the environment becomes saturated with amorph silica. Sepiolite does not form if the silica concentration is high and pH as well as magnesium values are low.

The fault, dip and strikes of the beddings show that the center of investigation area seem to be a depression zone. The source of MgO of the formation of sepiolite is probably derived from the alteration of basic, ultrabasic and metamormophic rocks which are cropped out at the south and east of the investigation area. Sepiolite-dolomite, sepiolite-montmorillonite-talc, magnesite-dolomite, magnesite-dolomite-montmorillonite-illite mineral paragenesis support the idea of the source of magnesium (Fig. 8). In addition; smecite (montmorillonite) and montmorillonide-sepiolite mineral paragenesis in Hırka and Akpınar formations were determined (Fig. 8). Generally mixed-layer montmorillonite are formed at the environment which comprise of high amount of fresh water influx (Fig. 9).

Starkey and Blackmon (1979, 1984) found that the reaction of aluminum with silica and magnesium in a pH > 9 environment forms montmorillonite, chlorite and talc rather than sepiolite.

Cheminal analyses show that sepiolite contain high MgO and low Al_2O_3 (Fig. 10). The proportion of Al_2O_3/MgO decreases from the margin toward the center of the investigated area (Killik). This means that the amount of the aluminum in the horizontally distributed minerals of the same formation decreases from the margin towards the center (Fig. 10). At the south, low Mg causes the formation of dioctahedral smectite (montmorillonite) and at the central area, that is more stable, high Mg and Si and low Al content cause to form the sepiolite minerals. The mineral distribution of the study area is agree with in the mineral distribution of that of Northwest African Lake which tends to contain montmorillonite-illite-chlorite-kaolinite, montmorillonite-palygorskite, palygorskite-sepiolite, sepiolite paragenesis from the margins towards the center (Millot, 1964). The region is devoid of palygorskite mineral in nature, probably due to the most of the aluminum being used in the occurrence of aluminum silicate and zeolite.

illite is very low in the studied area because of the mobility of K in the solution. The same condition was mentioned by Fontes et al. (1967), Galan and Ferro(1982).

Vertical mineral distribution of the investigated area is as follows; montmorillonite, in Hırka Formation, sepiolite, in Akpınar Formation, montmorillonite and mixed-layer clay (montmorillonite dominant) in Bozçayır and Acısu Formations and the upper part of the Akpınar Formation at the center of the investigated area (around Ocak).

The source of silica for the formation of sepiolite is probably the alteration of volcanic tuff and/or Si^{+4} of the sorrounding litnologies. Amorphous material and opal-CT were also determined in the

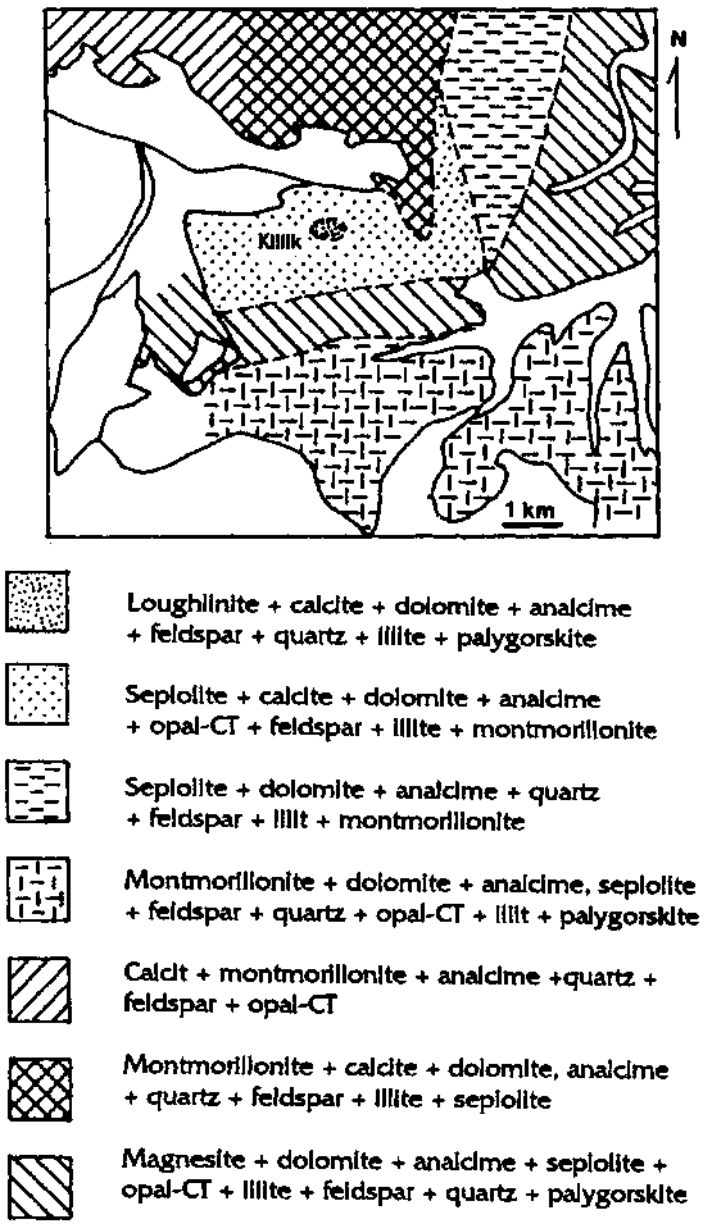

Fig. 8. Neoformed mineral distributions in the Neogene age units.

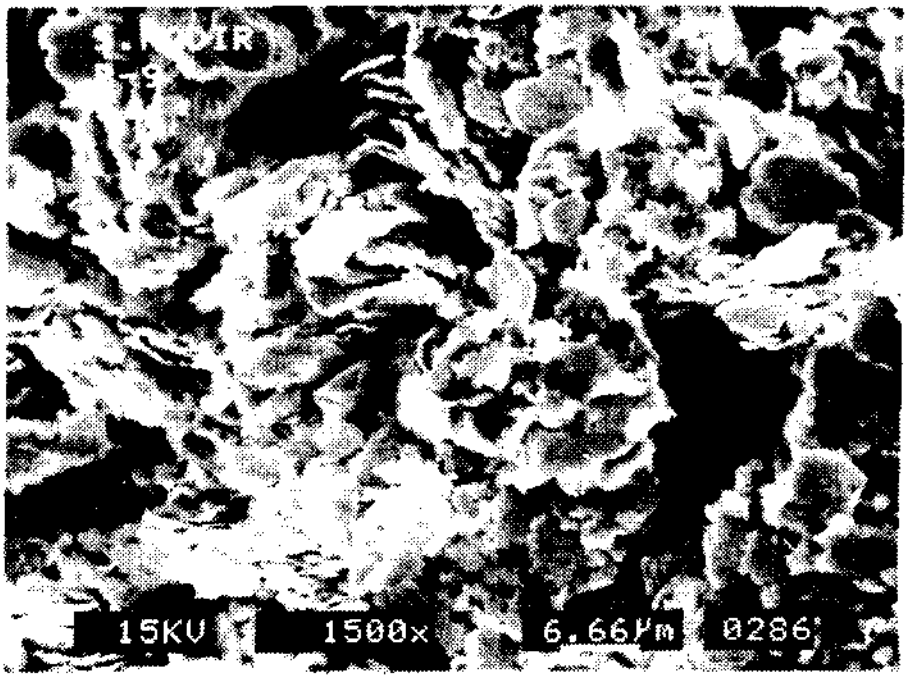

Figure 9. SEM view of authigenic montmorillonite showing cornflakes structure.

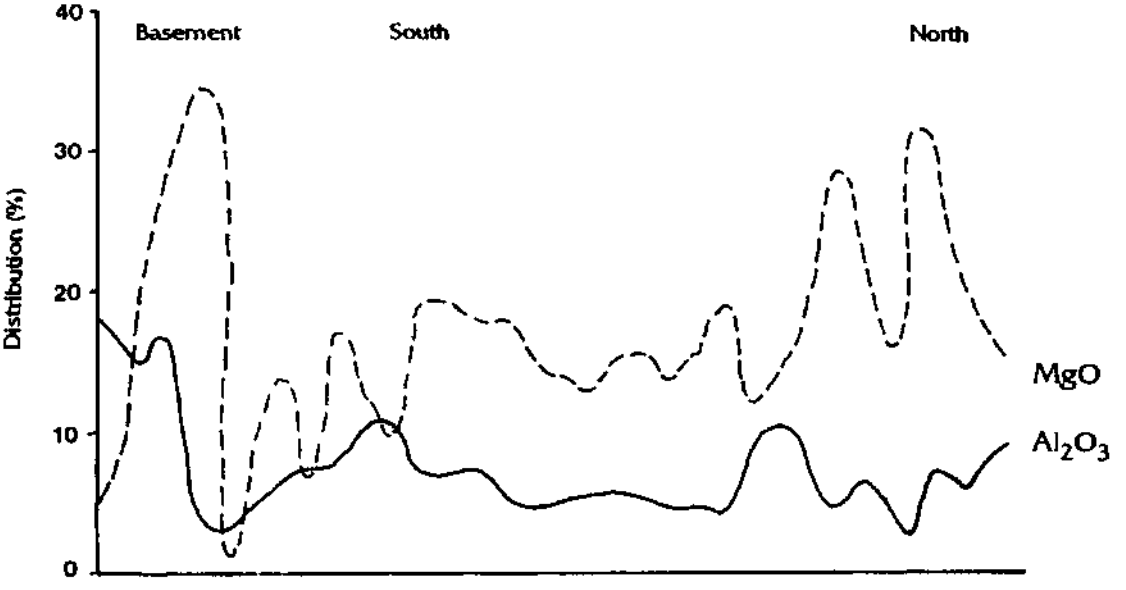

Fig. 10- MgO and Al_2O_3 distribution curves of the investigation area (From south to north).

taken samples of the region (Kadir and Baş, 1995). It was observed that (001) peak of the clay minerals are relatively sharp and strong. This shows that the alteration is very strong (Jones, 1986). The argilization degree of the area is controlled by pH value and the diagenesis period (Hardie et al., 1978). Scanning Electron Microscope studies showed that sepiolite and loughlinite fibrous were formed authigenically in and around the altered pores as a result of alteration of the volcanic glass (Fig. 11) (Kadir and Baş,1995).

At Killik area, loughlinite seems to be a small lens inside of the sepiolite zone (Fig. 8). Loughlinite is formed in the same way with that of sepiolite by combining of Na, probably originated from the alterated tuffs to the Si and Mg.

The formation of montmorillonite causes the concentration of alkaline ions in the rest material which is suitable to form zeolite minerals (Sheppard and Gude, 1969, Moiola, 1970). By the hydrolization of volcanic glasses, pH value increases and the concentration of alkaline ion causes to form montmorillonite (Hay, 1963). The (Na+K)/H activity ratio of pore waters increases and the environment become suitable for the zeolite to form.

In the study area the evolution of more saline alkaline pore waters becomes a favoured environment for the precipitation of analcime. The geochemical change in pore-water is thought to be influenced by probably;

1. Mineralogy and geochemistry of tuffs, igneous, metamorphic and ophiolitic sorunding rocks.
2. The climatic condition of the evaporates.
3. The accumulation of the sediments within a closed hydrographic basin.
4. A higher than normal geothermal gradient due to the magnetic activity.

However, the diagenesis of tuff of the area seems very complicated. Due to the mineralization period of analcime, carbonate and small amount of feldspar neoformed with the clay minerals.

Preburial diagenesis of the tuff under an oxidation regime at near neutral pH, conditions favour the precipitation of quartz and K-felspar (Walker et al., 1978). Evaporation of pore-water causes to increase of pH value, the alteration of felspars probably provide a source of Na^{+} and Al^{+3} for analcime precipitation.

$$NaAlSi_3O_8 + 6H_2O + 2H^{+} \rightarrow 3Si(OH)_4 + Na^{+} + Al(OH)^{+}_2$$

$$CaAl_2Si_2O_8 + 4H_2O \rightarrow 2Si(OH)_4 + Ca^{+} + Al(OH)^{+}_2$$

Following the above alteration, interstratal solutions would evolve the saline, alkaline brines and increase the amount of the fluid, basinward. With further concentration and temperature increase (due to burial) calcite would be precipitated as following;

$$Ca^{+2} + HCO_3 \rightarrow CaCO_3 + H^{+}$$

Calcite

As a result when conditions were sufficient with alkaline, analcime would be precipitated (below 100°C) as in the following reaction:

$$2Si(OH)_4 + Na^{+} + Al(OH)^{+}_2 \rightarrow NaAlSiO_6.H_2O + 3H_2O + 2H^{+}$$

Analcime

In the studied area some small amount of albite and sanidine were found to be associated with zeolite. Hay (1966), İijima and Hay (1968), Sheppard and Gude (1968, 1969, 1973), Hay (1970), Eugster (1970), Surdam and Parker (1972), Surdam (1981) reported that there is a relationship between the authigenic mineralizetoin and the deposition. In high saline and alkaline environment, the volcanic glasses dissolve and analcime neoforms and analcime is transformed to feldspars as showed in the following reactions:

$$NaAlSi_2O_6.H_2O + SiO_2 + K^{+} \rightarrow KAlSi_3O_8 + H_2O + Na$$

Analcime K-feldspar

$$NaAlSi_2O_6.H_2O + SiO_2 \rightarrow NaAlSi_3O_8 + H_2O$$

Analcime Albite

The presence of loughlinite and Na-feldspar in the Killik area indicates the Na enrichement. SEM investigation shows that analcime, albite and sani-

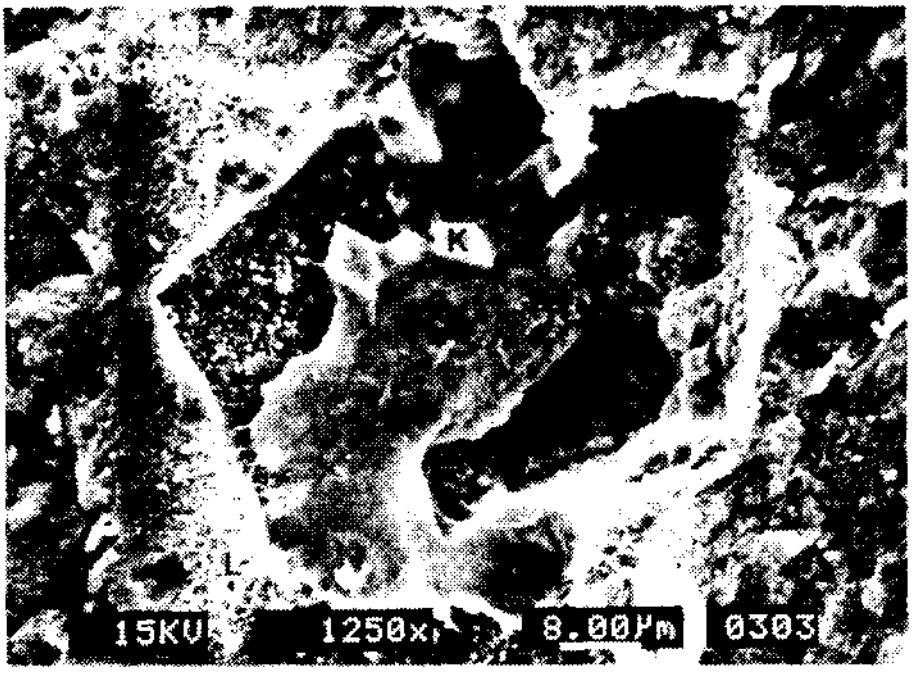

Fig.11- Neoformation of loughlinite and feldspar in and around of dissolution voids of altered volcanic glasses in Sample Ocak-10.
C: Volcanic glass, L. Loughlinite, K: K-feldspar, A: Analcime.

dine minerals authigenically to be neoformed and seem to own automorphic crystal structures.

Generally amorphous materials, authigenic opal-CT and small amount of quartz were determined in the study area. The amount of silica decreases as feldspar forms from the silicious analcime. Very small amount of silica left behind, is crystallized as quartz. Therefore, the amount of quartz is expected very low. Similar condition could be seen in the Green River formation where small amount of silica is also found together with the analcime and K-feldspar (Ijima and Hay, 1968).

Mineralogic and geochemical studies showed that magnesite + dolomite, dolomite, dolomite + calcite and calcite mineral zones were determined vertically and horizontally (Fig. 8).

Magnesite formation in the Hırka formation at the south and the bottom part of Akpınar at the Killik area show that Mg and pH values are considerably high and probably indicate the lowest level of the stratigraphic section of the study area. Following the formation of magnesite, the amount of Mg decreases and with the presence of Ca, dolomite precipitated. At the north, the change of Mg and Ca proportions cause the precipitation of dolomites and calcites.

5. RESULTS

1. The study area is comprised of the Middle-Upper Miocene aged volcano-sedimentary rocks which are composed of 6 main formations (Çoraklar, Hırka, Karadoruk, Akpınar, Bozçayır and Acısu Formations).

2. Sepiolite, loughlinite, analcime, montmorillonite, feldspar, magnesite, dolomite, calcite, illite, quartz and opal-CT are neoformed minerals and they are discerned within these formations.

3. Sepiolite is formed in the condition of basic pH value, which is rich in Mg and Si and poor in Al

at the center and northern parts of the study area within the Akpınar Formation.

4. At the center of study area (Killik), loughlinite is formed by combining of Si and Mg and Na originated from the alteration of tuffs.

5. Montmorillonite is formed within shallow margin facies at high pH conditions and in the presence of Al.

6. After montmorillonite forms, the analcime is formed from the remnant Na.

7. Magnesite and dolomite are dominant in the lower part of the sequence (Hırka Formation), while dolomite, calcite or the repitition of these minerals are dominant at the upper part (Akpınar, Bozçayır and Acısu Formation).

8. The source of Mg for the neoformation of the minerals seem to be basic, ultrabasic and ophiolitic rocks which are cropped out at the south and the east of the investigated area. Na and K were probably derived from tuffs. On the other hand Si and Al were probably derived from the both sources.

6. REFERENCES

ATAMAN, G., 1976. Türkiye'de yeni bir analsim oluşuğu ve zeolitli serilerle plaka tektoniği arasında muhtemel ilişkiler. H.Ü., Yerbilimleri (2), 9-23, Ankara.

CAILLERE, S., 1951, Sepiolite. in: G. W. Brindley, X-ray identification and structures of clay minerals: Mineral Soc., London, 224-233.

CAMPBELL, A. S. and FYFE, W. S., 1965, Analcime-albite equilibria: American Jour. Sci. 263, 807-816.

ECHLE, W., 1967, Loughlinite (Na-sepiolith) und Analcim in Neogenen sedimenten Anatoliens: Contr. Mineral. Petrol. 14, 86-101.

.....--, 1974, Zur mineralogie und petrogeneses jungtertiarer tuffitischer sedimente im Neogen-Backen nördlich Mihalıççık (Westanatolien, Turkei): N. Jb. Miner. Abh. 121,43-84.

—....., 1978, The transformations sepiolite <=>loughlinite experiments and field observations: N. Jb. Miner. Abh. 133 (3), 303-321.

EUGSTER, H. P., 1970, Chemistry and origin of the brines of lake Magada, Kenya: Mineralog Soc. America Spec. Pub. 3, 215-235.

FONTES, J. C.; FRITZ P.; GAUTHİER, J. and KULBİCKİ, G.; 1967, Mineraux argileux, elements traces et compositions isotopiques ($^{18}O/^{16}O$-et$^{13}C/^{12}C$) dans les formations gypsiferes de l'Eocene Superieur et dans l'Oligocene de Cormeilles-en Parisis: Bull. Cent. Rech. Pau.-SNPA, 1,315-366.

GALAN, E. and FERROS, A., 1982, Playgorskite-sepiolite clays bf Lebrija. Southern Spain: Clays and Clay Minerals, 30, 191-199.

GÜNDOĞDU, M. N., TENEKEÇİ, O.; ÖNDER, R; DÜNDAR, A. and KAYAKIRAN, S., 1985 Beypazarı trona yatağının kil mineralojisi, on çalışma sonuçları: II. Ulusal Kil Sempozyumu Bildirileri, H. Ü. (Eds: M. Niyazi Gündoğdu ve Hüsnü Aksoy), 141-153, Ankara.

HARDİE, L. A.; SMOOTH, J. P. and EUGESTER, H. P., 1978, Saline lakes and their deposits. A sedimentological approach: In modern and ancient lake sediments: A. Matter, M, E Tucker (Eds.) Blackwell Sci. Publ. Oxford, 7-24.

HAST, N., 1956, Low-tempreture synthesis of sepiolite: Arkiv Mineral Geol., 9, 313-360.

HAY, R. L., 1963, Stratigraphic and zeolitic diagenesis of the John Day Formation of Oregon: California University. Pubs. Geol. Sci., 42, 199-262.

....., 1965, Pattern of silicate authigenesis in the Green River Formation of Wyoming (abstr.): Geol. Soc. Amer. Spec. Pap. 82, 88 s.

, 1966, Zeolites and zeolotic reactions in sedimentary rocks: Geol. Soc. Amer. Spec. Paper, 85, 130 s.

. . . . .--, 1970, Silicate reactions in three lithofacies of a semi-arid basin, Olduvai George Tanznia: Mineral. Soc. Amer. Spec. Paper, 3, 237-255.

HELVACI, C.; İNCİ, U.; YAĞMURLU, F. and YILMAZ, H., 1989, Geologic and Neogene trona deposit of the Beypazarı region: Doğa Bilim Dergisi, 13(2), 245-256.

. . . . . --, YILMAZ, H and İNCİ, U., 1988, Beypazarı (Ankara) yöresi Neojen tortularının kil mineralleri ve bunların dikey ve yanal dağılımı: Jeoloji Mühendisliği, no. 32-33, 33-42.

İİJİMA, A. and HAY, R. L, 1968, Analcime composition in the Green River Formation of Wyoming: American Mineralogist, 53 (1-2), 184-200.

İSPHORDİNG, W. C., 1973, Discussion of the occurrence and origin of sedimentary palygirskite-sepiolite deposits: Clays and Clay Minerals, 21, 391-401.

JONES, B, F., 1986, Clay mineral diagenesis in lacustrine sediments. In Diagenesis Workshop: U. S. Geol. Survey Bull., 1578, 18s.

KADİR, S. and BAŞ, H., 1995, Koyunağılı (Mihalıççık-Eskişehir) sepiyolit oluşumlarının mineralojisi, VII. Ulusal Kil Sempozyumu, Kill 95 Bildiriler Kitabı (Eds: Mehmet Şener, Ferda Öner ve Erdal Koşun), 19-31, Ankara.

KAYAKIRAN, S. and ÇELİK, E., 1986, Beypazarı trona (doğal soda) yatağının maden jeolojisi raporu: M.T.A. report No. 8079, Ankara.

MİLTON, C. and EUGSTER, H. P., 1959, Mineral assemblages of the Green River Formation. In P. H. Abelson, Ed., Research in Geochemistry, Vol. 1, John Wiley and Sons, New York, 118-150.

MİLLOT, G., 1964, Geologie des Argiles. Masson and Cie, Paris, 510 s.

MOİOLA, R. J., 1970, Authigenic zeolites and K-feldspars in the Esmeralda Formation, Nevada: American Mineralogist, 55, 1681-1691.

MUMPTON, F. A. and ROY, R., 1958, New data on sepiolite and attapulgite: Clays and Clay minerals 5, 136-143. Nat. Acad. Sci. Natl. Res. Con. Rub. 566 s.

SHEPPARD, R. A., and GUDE, A. J., 3rd, 1968, Distribution and genesis of authigenic silicate minerals in tuffs of Pleistocene lake Tacopa, Inyo Country, California: U. S. Geol. Survey Prof. Paper, 597, 38 s.

. . . . . , ... , 1969, Diegenesis of tuffs in the Barstow formation, Mud Hills, San Sarnardino Country, California: U. S. Geol. Survey Prof, Paper, 634, 35 s.

. . . . . , ———— , 1973, Zeolites and associated authigenic silicate minerals in tuffaceous rocks of the Big Sandy Formation, Mohave Country. Arizona: U. S. Geol. Survey Prof. Paper, 830, 36 s.

SİNGER, A. and GALAN, E., 1984, Palygorskite-Sepiyolite Occurences, Genesis and Uses. Developments in Sedimentology, 352 s.

SİYAKO, F., 1982, Eskişehir-Mihalıççık-Koyunağılı linyit kömürü sahasının jeoloji raporu: M.T.A., Report No. 7111, Ankara.

. . . . . , 1983, Beypazarı (Ankara) kömürlü Neojen havzası ve çevresinin jeoloji raporu. M. T. A., Report No., 7431, Ankara.

STARKEY, H. C. and BLACKMON, P. D., 1979, Clay mineralogy of Pleistocene lake Tacopa, Inyo County, California: Paligoskite-Sepiyolite Occurrence, Genesis and Uses, A. Singer and E. Galan (Ed.), 137-147.

SURDAM, R.C. and PARKER, R.B., 1972, Authigenic aluminosilicate minerals in the

STRATIGRAPHY OF THE AUTOCHTHONOUS AND ALLOCHTHONOUS UNITS AT THE EASTERN PART OF THE ISPARTA ANGEL, WESTERN TAURIDES-TURKEY

Mustafa ŞENEL*; İbrahim GEDİK*; Halil DALKILIÇ*; Mualla SERDAROĞLU*; Ali Zafer BİLGİN*; M. Fuat UĞUZ; A. Sait BÖLÜKBAŞI; Metin KORUCU** and Necdet ÖZGÜL*"

ABSTRACT.- The investigation area which located at the eastern part of "Isparta Angle" of Taurus mountain, includes Beydağları-Karacahisar autochthonous, Anamas-Akseki autochthonous and Antalya nappes. Beydağları-Karacahisar autochthonous which is cropped out below the Antalya nappes as tectonic windows is represented by from bottom to top Precambrian, Cambrian, Carboniferous and Middle Triassic-Danian sedimentary deposits. Anamas-Akseki autochthonous represented by Upper Triassic-Middle Eosen rock units is over thrusted to Antalya nappes and Beydağları-Karacahisar autochthonous at the north and is seperated from Beydağları-Karacahisar autochthonous by Kırkkavak fault at the eastern part of the investigation area. During the Mesozoic period Anamas-Akseki and Beydağları-Karacahisar autochthonouses were developed as different platforms. In the Antalya nappe which composed of offshore platforms, slope, basin and fragments of oceanic crust, from bottom to top Çaltepe, Alakırçay, Tahtalıdağ and Tekirova ophiolitic nappes are distinguished on the basis of their structural and stratigraphical properties. Çaltepe nappe includes Şeyhdere, Sofular, Zindan, Yaka, Yılanlı and Kocaoluk sequences, Alakırçay nappe, Alakırçay, Koçular, Sülekler sequences, Tahtalıdağ nappe, Yumaklar, Erenler, Dutdibi, Ovacık, Güme and Dulup sequences. Akpınar sequence which is composed of Middle-Upper Triassic basic volcanic and through the upper part Jurassic-Cretaceous platform carbonates structurally conformable to Alakırçay nappe. Also, Tekirova ophiolitic nappe is composed of Ayvalı peridotite and Kırkdirek melange.